Montanuniversität Leoben - University of Leoben
Department Metallurgie - Department of Metallurgy
Nichteisenmetallurgie - Nonferrous Metallurgy

Implementation of Alternative Reducing Agents in Metallurgical Operations

Dipl.-Ing. Gernot Rösler

Christian Doppler Laboratory for Optimization and Biomass Utilization in Heavy Metal Recycling

A thesis submitted in partial fulfilment of the requirements for the degree of a Doctor of Metallurgical and Mining Sciences at the University of Leoben

Leoben, February 2015

STATUTORY DECLARATION

I declare in lieu of oath that I wrote this thesis and performed the associated research myself, using only literature cited in this volume.

_____

Dipl.-Ing. Gernot Rösler

Leoben, February 2015

Acknowledgments

First of all I would like to thank the head of the Christian Doppler Laboratory for Optimization and Biomass Utilization at the Recycling of Heavy Metals, Dr. Jürgen Antrekowitsch, for the possibility to be part of his research group. Furthermore, many thanks to Prof. Helmut Antrekowitsch as head of the Chair of Nonferrous Metallurgy at the Montanuniversitaet Leoben.

Moreover, a huge thank you to Dipl.-Ing. Alois Unger and Dipl.-Ing. Christoph Pichler for the fruitful technical discussions as well as their great support and friendship during my time at the CD Laboratory.

A big thank you to my colleagues Dr. Stefan Steinlechner, Dr. Holger Schnideritsch, Dipl.-Ing. Stephan Steinacker and my former graduate student and present working mate Dipl.-Ing. Stefan Wegscheider for the contributions to this thesis, as well as to my former colleagues who are no longer at the Montanuniversitaet, Dr. Rene Rumpold, Dr. Gerald Schneeberger, Dr. Ion Agirre Arisketa and Dr. Thomas Griessacher.

Without any technical assistance, the present thesis wouldn´t been possible; thanks to Luigi Cattini, Andreas Sprung, Erich Troger and Thomas Link for their help in the laboratories as well as for all the analytics.

I would like to thank my parents, Sylvia and Karl Rösler, for their support in the past, which made it possible for me to get a university education that is culminating with this thesis.

Last but not least, I would like to thank my soulmate Caterina for her never-ending encouragement and showing patience while writing these lines, by dedicating this thesis to her.

Acronyms

2sDR	Two step Dust Recycling
ASTM	American Society for Testing and Materials
B.E.T.	Brunauer, Emmett and Teller
BOF	Basic Oxygen Furnace
CFC	Chlorofluorocarbon
CRI	Coke Reactivity Index
CSR	Coke Strength after Reaction
DBFZ	Deutsches Biomasse Forschungszentrum
DIN	Deutsche Institut für Normung e. V.
EAF(D)	Electric Arc Furnace (Dust)
EEX	European Energy Exchange
EFTA	European Free Trade Association
equ.	Equation
EU-ETS	European Union - Emission Trading System
GHG	Greenhouse Gas
ISO	International Organization for Standardization
MSW	Municipal Solid Waste
NEM	Chair of Nonferrous Metallurgy
PAH	Polycyclic Aromatic Hydrocarbons
PCI	Powder Coal Injection
SDHL	Saage, Dittrich, Hasche and Langbein
SPA	Solid Phase Adsorption
SX	Solvent Extraction
TBRC	Top Blown Rotary Converter
UNFCCC	United Nations Framework Convention on Climate Change
WOX	Waelz Oxide

Kurzfassung

Aufgrund des Anstieges der anthropogenen Treibhausgasemissionen führte die Europäische Kommission das sogenannte Emissionshandelssystem ein. Die bei der verarbeitenden Industrie anfallenden CO_2-Emissionen sind somit meldepflichtig und mittels erworbener Emissionsrechtzertifikate auszugleichen, weshalb natürlich eine Reduktion der Emissionen aufgrund einer Prozessoptimierung erstrebenswert ist. Die ebenso betroffene metallurgische Industrie ist nun auf der Suche nach Alternativen, da deren Prozesse hauptsächlich auf den Einsatz von fossilen Kohlenstoffträgern und somit einer anrechenbaren CO_2-Emission basieren.

Die vorliegende Arbeit versucht über die Implementierung von alternativen und CO_2 neutralen Reduktionsmitteln in metallurgischen Recyclingprozessen eine Emissionsminimierung herbeizuführen. Das Hauptziel stellt dabei die Herstellung sowie die anschließende Charakterisierung von Holzkohle und Pyrolysegas aus Biomasseabfällen dar. Im Anschluss dessen erfolgt eine Evaluierung des Kohlenstoffträgers im entsprechenden metallurgischen Prozess.

Speziell der entwickelte „2sDR“ (Two step dust recycling)-Prozess wurde dahingehend adaptiert, um mittels Holzkohle als Reduktionsmittel Schwermetalle simultan aus Stahlwerksstäuben rückzuführen und dabei die CO_2-Emissionen gering zu halten. Dieses Verfahren wurde speziell entwickelt, um jeden Elektrolichtbogenstaub ohne Limitierung in Bezug auf Materialqualität aufzuarbeiten und dabei entsprechend dem „Zero Waste“ Gedanken keine neuen Abfälle zu generieren.

Die zweite Einsatzmöglichkeit von Holzkohle und Pyrolysegas, die in dieser Arbeit beleuchtet wird, ist die notwendige Nachbehandlung von Wälzoxid sowie Wälzschlacke, um deren Produktqualität zu erhöhen. Damit Wälzoxid in der primären Zinkindustrie einsetzbar wird, muss ein Reinigungsschritt erfolgen, da es verschiedenste Verunreinigungen enthält. Die einfache Deponierung von Wälzschlacke ist wiederum aufgrund einer geänderten Gesetzgebung verboten, weshalb eine Aufarbeitung unumgänglich ist. Beide Produkte wurden mit Pyrolysegas bzw. Holzkohle nachbehandelt, wobei vielversprechende Ergebnisse das Resultat waren.

Neben den bereits erwähnten Vorzügen beim Einsatz durch erneuerbare Rohstoffe in der Metallurgie, stellt auch der sehr niedrige Schwefelgehalt einen klaren Vorteil dar. Die angewandten Verfahren resultieren somit in schwefelfreien Produkten, womit kein Zwischenschritt notwendig ist, um diese direkt ihrer weiteren Verwertung zuzuführen.

Abstract

Since the anthropogenic greenhouse gas emissions are increasing more and more, the European Commission introduced the so-called emission trading system. With this, the CO_2 emissions evolved by the manufacturing industry based in Europe have to be reported and balanced by acquired emission allowances. The main focus now is to lower the emissions by process optimization. It is well-known that the metallurgical industry is a big polluter, and now searching for alternatives. Since this industry is mostly based on the utilization of fossil carbon carrier, CO_2 emissions have to be accounted and paid.

The present thesis focuses on the implementation of alternative reducing agents in metallurgical recycling processes to induce a minimization of the accountable emissions. The main goal is the conversion and subsequent characterization of waste biomass into a renewable charcoal and pyrolysis gas. The produced alternative reducing agent is forwarded to the desired metallurgical process with a subsequent evaluation.

Especially the developed “2sDR” (Two step dust recycling)-process is adapted to run by charcoal to minimize the CO_2 emission at the simultaneous recovery of heavy metals from EAFD´s. This new recycling process was developed to treat EAF-dusts during melting of steel scrap without any limitation regarding material properties. A main goal of this recycling process was to generate no new wastes, according to the Zero Waste principles.

The second utilization possibility of charcoal and pyrolysis gas considered in this thesis is the product upgrade of Waelz oxide as well as Waelz slag. Waelz oxide has to be treated in advance to the recycling in the primary zinc industry since it contains several impurities. The treatment of Waelz slag has become mandatory because of the change in the legal requirements, since Waelz slag is classified as hazardous waste. Both species were treated using pyrolysis gas respectively charcoal achieving very promising results.

Beside the already mentioned benefits due to the utilization of renewable resource in metallurgical processes, a further advantage could be seen in the low quantity of sulphur. The applied processes using renewable resources generates in products which do not require intermediate treatment and can therefore directly be forwarded to their final application.

Table of contents

1 INTRODUCTION 1

1.1 The European emission trading system 2

1.2 Metallurgy and its contribution to global climate change 5

1.3 Approach of this thesis 7

2 SOLID REDUCING AGENTS 8

2.1 Characterization of solid fossil carbons 9
2.1.1 Ultimate analysis (CHNS) 12
2.1.2 Proximate analysis 13
2.1.3 Determination of the specific surface area 13
2.1.4 Reactivity tests 17

2.2 Brown coal 21

2.3 Stone coal 22

2.4 Anthracite 24

2.5 Coke 24

2.6 Petroleum coke 26

2.7 Desulco® 27

3 ALTERNATIVE REDUCING AGENTS 30

3.1 Charcoal 32

3.2 Pyrolysis gas 40
3.2.1 Characterization of the gas fraction 40
3.2.1.1 Permanent gas 41
3.2.1.2 Tars 44
3.2.2 Results 51
3.2.3 Interpretation of the results 55

3.3 Utilization possibilities 55
3.3.1 Charcoal 55
3.3.2 Pyrolysis gas 57
3.3.2.1 Steam reforming 58
3.3.2.2 Catalytic upgrade 59
3.3.2.3 Thermal cracking 59

3.4 Overview of utilization possibilities 59

4 CARBURIZATION OF IRON 61

4.1 Theoretical background – carbonization 62

4.2 Experimental procedure 66
4.2.1 Hot stage microscope 66
4.2.2 High temperature chamber furnace 69
4.2.3 Induction furnace 73
4.2.3.1 Charcoal “Eucalyptus No.4” 77
4.2.3.2 Charcoal “Eucalyptus No.6” 78
4.2.3.3 Charcoal “olive tree cuttings” 79
4.2.3.4 Reference fossil coke “petroleum coke” 80

4.3 Conclusion and further processing 81

5 THE “2SDR” PROCESS 84

5.1 Overview of the recycling of EAFDs 84

5.2 Set-up of the “2sDR” process 88
5.2.1 Clinkering 88
5.2.2 Reducing step 91

5.3 Utilization of charcoal in the iron bath process 98

6 PRODUCT OPTIMIZATION OF THE WAELZ PROCESS 104

6.1 Clinkering of Waelz oxide 106
6.1.1 Experimental set-up of the clinkering trials 107
6.1.2 Results of the alternative cleaning step 110
6.1.2.1 First trial; 100 % CH_4 110
6.1.2.2 Second trial; 100 % pyrolysis gas 112
6.1.2.3 Third trial; pyrolysis gas / CH_4 gas mixture 114

6.2 Treatment of Waelz slag 118
6.2.1 Experimental procedure 120
6.2.2 Results 122

6.3 Conclusion of the optimization possibilities 124

7 CONCLUSIONS 126

8 OUTLOOK 128

9 BIBLIOGRAPHY 129

10 LIST OF FIGURES 142

11 LIST OF TABLES 147

1 Introduction

In times of changing climate and limited resources, sustainability, especially in the metallurgical industry, is getting more and more important in Europe. Furthermore, due to this, an entire recycling of all wastes occurring should be considered in order to fulfil the above-stated goal. Since these residues contain various heavy metals, primary resources are saved. Huge amounts of dusts, slags and sludges are generated during metallurgical processes, which have to be further processed or in the worst case forwarded to landfilling, often causing an enormous financial effort. Several recycling possibilities were invented in the past to treat these “wastes” to recover some quantities of heavy metals, leaving a new residue behind, which is – depending on the country – utilized, for example, for construction purposes. With a future change in the legal requirements, which has already been done in several communities – a simple use of slags out of recycling processes might not be allowed anymore, due to the fact that other heavy metals are still present in the slag. Often, these species are associated with highly leachable chemical bonds, and if the mentioned residue out of a recycling process were utilized near the soil, a contamination of ground water could not be avoided.

Therefore, considerable efforts have been made in the recent years to develop or redesign metallurgical processes which have the aim to be specified as “zero waste” technology. That means all various phases obtained in a process can be forwarded to a defined purpose without the necessity to operate a landfill. In the present thesis, some of these processes will be described with a special focus on the production of the generated CO_2 emissions in the field of electric arc furnace dust recycling.

Since carbon dioxide can be associated with the global climate change, the European Union introduced the emission trading system that forces companies to lower their emissions, which will be described in detail in the following subchapter. With an increase of anthropogenic CO_2 emissions, the natural greenhouse gas effect gets intensified, which leads to a possible change in the global climate. A representative picture of the basic principle of the greenhouse gas effect as well as its influencing factors can be found in Figure 1-1.

Moreover, the present thesis will put its focus on the metallurgical recycling industry that is highly linked to fossil carbons and therefore a big polluter with respect to the overall CO_2 emissions.

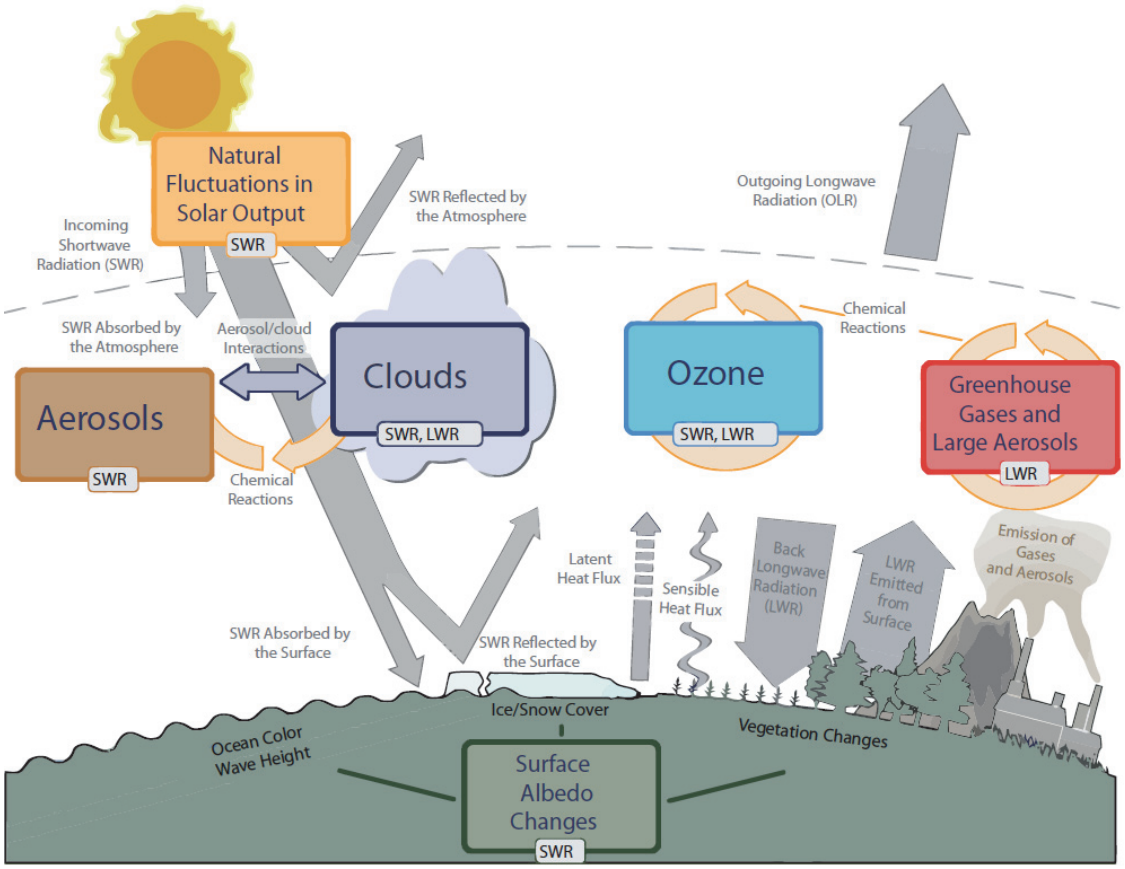

Figure 1-1: Schematic drawing of the basic principle of the greenhouse effect and the influencing parameters [1]

1.1 The European emission trading system

The European emission trading system (EU-ETS) is the strongest tool for fighting global climate change at the moment. It covers 11,000 power plants as well as huge production facilities in 31 countries within Europe. With this it is planned to decrease the annual CO_2 emissions in Europe significantly in the coming years. The key data of this enormous trading system
are [2; 3]:

- This system includes 28 EU countries as well as three EFTA countries (Iceland, Liechtenstein and Norway).
- Approximately 45 % of the overall GHG emissions in the EU are covered.
- Limitation of emissions of 11,000 power plants and production facilities as well as flights to / from EU / EFTA countries.

The basic principle works according to the “cap and trade” system. The overall emissions produced by power plants and other emissions are “capped” by EU legislation. The maximum amounts of emission allowances (certificates) are regulated by the government and equal a specific number of certificates which have to be used by these companies. Each certificate

allows its owner to exhaust one ton of CO_2 and an equal amount of N_2O and CFC (chlorofluorocarbons), respectively [4]. Every allowance can be only used once, whereby at the end of each year all the owned allowances have to cap the produced emissions of a company; in case of noncompliance, penalty fees will be charged [5]. Furthermore, these companies are published, so-called “named and shamed.” However, environmentally friendly companies which own too many certificates are allowed to “trade” – to sell the CO_2 emissions on the market. Further possibilities are the purchase of credits generated by emission saving projects, such as reforestation in a third world country. But these concepts have to be accepted by the “Kyoto Protocol´s Clean Development Mechanism.” The EU-ETS is responsible for a lot of projects carried out in developing countries to invest in low carbon-consuming technology [2].

Concluding, it can be said that this very flexible system allows the industry to decide between several ways how to deal with their emissions [2; 6]:

- Decrease in the emission by investing in new technologies or / and change the type of carbon carrier (e.g. to renewable ones).
- Purchase (to cover the emissions) or sale (if there are too many) of allowances.
- A combination of the presented alternatives.

The ramp up of the emission trading system takes several years; therefore, it was divided into four structured phases [2]:

- 2005-2007: The emission trading system was introduced as the biggest trader worldwide. Due to the fact that the estimated amount of allowances was too high, the price of the certificates decreased to 0 €.
- 2008-2012: Similar to the beginning of the second period, Iceland, Norway and Liechtenstein as well as the air traffic joined the ETS. The number of certificates decreased by 6.5 %, but the emissions actually released were much lower since the economic crisis reached Europe in 2008. Therefore, a lot of certificates were not used with a subsequent decline in their price.
- 2013-2020: The third part of the emission trading system started with important changes. The EU decided to introduce a maximum of emissions, which is an annual decrease of 1.74 %. Moreover, the number of traded certificates should increase with a simultaneous decrease in the national allocation of allowances.
- 2021-2028: This time period will be the future trading era.

The focus of the European community lies on gases where an exact determination is possible. Usually, every company listed in this trading system has to participate in the ETS. Exceptions

are allowed if the size/output is very that small. The following list gives an overview of companies and industrial branches where participation is mandatory [2; 7]:

- Carbon dioxide (CO_2) from power generation, aviation, oil refineries, steel mills as well as nonferrous smelters, lime, ceramics and the refractories industry, and many more
- Nitrous oxide (N_2O) exhausted by nitric, aldipic, glyoxal and glyoxylic acid producers
- Perfluorocarbons (CFCs) used in the production of aluminium

Unfortunately, the disadvantage of the ETS is that huge producing companies in Europe have their main competitors somewhere abroad. Especially the metallurgical industry as well as supporting companies (e.g. refractory production) are suffering, since they are losing their competitiveness due to the additional financial efforts, as mentioned initially. Thus, they are supported by their home countries with free allocations to prevent the upcoming “carbon leakage.” This term means that because of the ETS, companies move their production facilities to nations with lower or no emission legislation. In doing so, they escape the ETS, but it may cause an increase in global anthropogenic CO_2 production. Therefore, the allocation of certificates leads to a benchmarking of companies in the same branch with regards to their technology and emissions, respectively. This means that only high technologized industries get 100 % free certificates, and the remaining producers of the branch correspondingly less [2]. Finally, Figure 1-2 will show the evolution of the price of one ton of CO_2 in the recent years.

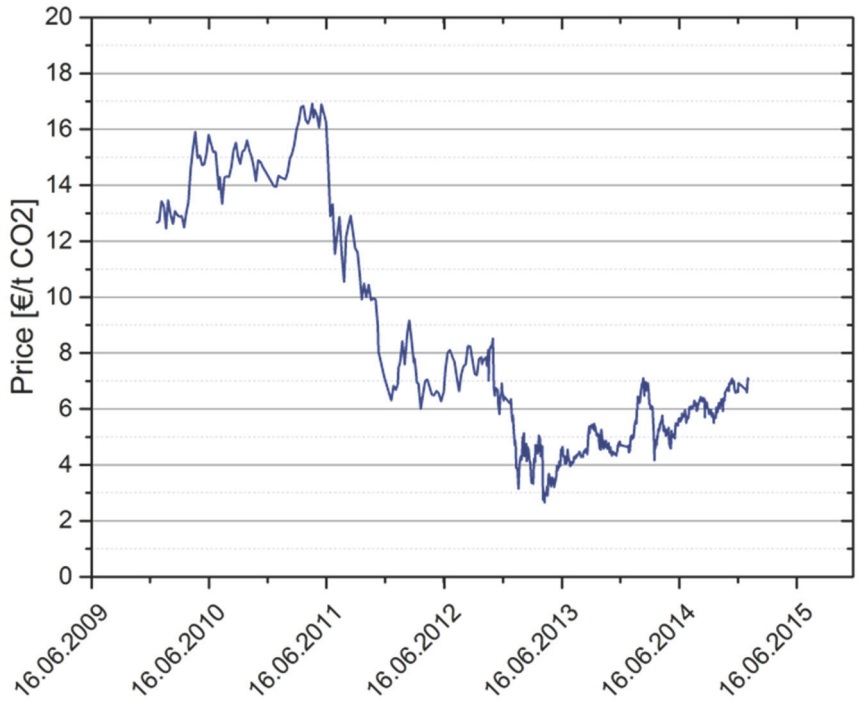

Figure 1-2: Price development of the CO_2 taxes over the last years according to the EEX [8]

1.2 Metallurgy and its contribution to global climate change

The global climate change led to a transformation in legal requirements which force a country or a community of countries to lower their greenhouse gas emissions. The most common example is the Kyoto Protocol. By signing this type of declaration, a decrease of the greenhouse gas emissions of 5.2 % (based on the emissions in 1990) is required [9]. The most harmful gas is, according to the protocol, CO_2, since it is the one which is produced the most. Taking a closer look at the European Community, the biggest emitter is the energy sector, producing 1.3 billion t CO_2 in 2012. The only way to lower this amount is by an additional input of energy originated from hydroelectric, wind and solar power plants. Furthermore, some of the caloric power plants that are operated by coal, coke and oil have to be shut down. The second biggest polluter in the EU is the industrial sector, producing 0.5 billion t of CO_2 in 2012 [10]. A part of this amount is contributed by metallurgical companies [11; 12].

Due to the highly technologized industry, especially in Western Europe, a reduction of greenhouse gas emission by process optimization is hardly possible. As a consequence, new technologies have to be applied with lower energy demand as well as low amounts of off-gas and a minimum of newly generated residues. Another very smart way to save CO_2 certificates is to use renewable resources that produce – as per definition – no CO_2 when they are combusted or used for reducing purposes in the field of metallurgy. Renewable reducing agents produce no harmful CO_2 since it was used and implemented in its growing phase as a plant. With this definition, no certificates would be spent for e. g. the recycling process of residues, which means these redundant certificates can be traded on the EEX. Some perfect examples for such a type of renewable carbon is biomass or its conversion to charcoal, bio-oil and pyrolysis gas [11; 12]. Basically the term “biomass” is defined by the UNFCCC (United Nations Framework Convention on Climate Change). It says biomass is renewable if *“the biomass is originating from land areas that are forests,”* if it is *“woody as well as non-woody biomass and originates from croplands and/or grasslands.”* Furthermore, the term biomass also includes its products as by-products as well as residues and wastes originated by the agricultural and forestry industry. Moreover, biodegradable and non-fossil waste produced during industrial processes and within municipal solid waste (MSW) can be classified as renewable biomass [13].

Back to the main topic, it can be concluded that the driving force to lower the emissions in metallurgical facilities is not negligible, since their emissions make a remarkable contribution to the overall emissions. According to Table 1-1, the average specific CO_2 emissions from the production of selected metals can be found according to their production routes. It can be

observed that significant differences exist between primary and secondary metallurgy. Considering the emissions of each metal as well as its production route, an enormous amount of CO_2 is emitted into the earth´s atmosphere. Fortunately, the recycling of metals and the recovery of metals from metallurgical residues, respectively, offer a potential economic advantage. First of all, primary resources can be saved when recycling wastes. Secondly, heavy-metal-containing residues cause a lot of problems when trying to use e. g. slags for construction purposes. Just small amounts of heavy metals within the slag are necessary to label the residue as hazardous waste, depending on the country of origin. The reason is the leachability of heavy metals in combination with the Group 7 elements in the periodic table. Table 1-2 shows the limiting values of various heavy metals at landfills in different countries and communities [14]. As the demand of metals is still high and the waste deposit demands a high financial effort, a recovery of the heavy metals is definitely reasonable.

Table 1-1: Tabulation of selected metals in connection with their production ways and produced emissions [15–17]

Metal	Production process	Emission (kg CO_2/t Metal)
Steel	EAF route	400
	Integrated blast furnace / basic oxygen furnace route	1,700-1,800
	Direct reduced iron route	2,500
Aluminium	Primary[1]	2,290-4,155
	Secondary, Remelting	150-350
	Secondary, Refining	250-390
Copper cathodes	Primary	1,140
	Secondary	310
RLE[2] Zink	Hydrometallurgical pre-treatment	43
	Pyrometallurgical pre-treatment	1,425
Zink Imperial Smelting furnace		4,325
Lead	Primary	1,459
	Secondary	383
Nickel		1,640
Tin		16,200

[1] including alumina and electrode production, melting and casting
[2] Roasting-Leaching-Electrolysis

Table 1-2: Limiting values of heavy metals in landfills in selected countries and communities [18–20]

Element	Limits in Austria [mg/kg]	Limits in the EU [mg/l]	Limits in US [mg/l]
Zn	200	60	-
Pb	50	15	5
Cd	5	1.7	1
As	25	3	5
Cr	70	15	5
F	500	120	-
Cl	-	15,000	-

1.3 Approach of this thesis

This thesis will investigate the possible utilization of alternative reducing agents in metallurgical facilities with a main focus on the recycling of steel mill dust. This includes solid as well as gaseous materials such as charcoal and pyrolysis gas, respectively, which are both originated by biomass. Unfortunately, biomass is very high in volatile matter and therefore not suitable for direct usage in the field of metallurgy, which is why a conversion process seems to be mandatory, since it does not make any sense to change an existing process concept.

The main task of the renewable carbonaceous material and gas is to reduce the oxidic compounds within the residue and to recover metals. With this, CO_2 gas is produced which cannot be attributed to the anthropogenic greenhouse gas emission, because the gas originates from a renewable resource.

However, the initial research focuses on the production as well as the characterization of renewable fuels, since the achieved data serves as basis for a comparison with fossil fuels. The target is to produce high quality charcoal where the main characteristic will be the final carbon content in the future reducing agent. Further steps are trials in small scale using charcoal to show if a substitution of a fossil carbon based metallurgical process is possible. After a successful evaluation, scaling up to a bigger experimental set-up takes place, where a slight process optimization will lead to a potential utilization for charcoal in the field of metallurgy.

2 Solid reducing agents

Fossil solid carbonaceous material plays an essential role in the generation of electrical power as well as in other industrial utilizations, which means, for example, the whole metallurgical industry. Widely known typical solid fuels are, among others, coal and coke. However, in the field of utilization of solid carbons as reducing or carburization agents, greater distinctions have to be made. Depending on the country of origin, there is a big variety of different carbonaceous material. This means there is no unique or defined chemical composition of the carbons mentioned above; only a data range of each type of coal can be given. Even charcoal would be a possibility. Recent scientific theses have pointed out the advances of renewable resources compared with fossil ones [21]. Whichever its structure, the application of carbons is widespread, and its main tasks are – depending on the metallurgical process [22]:

- Delivery of heat energy by combustion
- Reducing agent
- Carburization agent
- Dust filter
- Support function (especially in shaft furnaces to ensure the gas permeability)

Various carbon carriers are available which can be found in or next (i.e. power plants) to metallurgical operations. Information regarding typical values of the carbonaceous material listed will be given in Chapter 2.2.

This section describes the various types of fossil carbons in detail to get an idea about their characteristics, advantages and disadvantages. Furthermore, the following chapter will go into detail in the field of alternative carbon carriers originating from the conversion of waste biomass.

Basically, fossil fuels are produced by the conversion of prehistoric plants and animals and are obtained as coal, crude oil and natural gas. Figure 2-1 shows the evolution of coal, which takes several million years. A very slow carbonization process (coalification) converts the biomass (for the definition see Chapter 1.2) by the absence of air to different products depending on the retention time. Generally, it can be stated that the longer the time, the higher the carbon content in the organic product [23]. In the following section, a short overview of the characterization of coal will be given along with some influencing parameters on its reactivity as well as analysis methods.

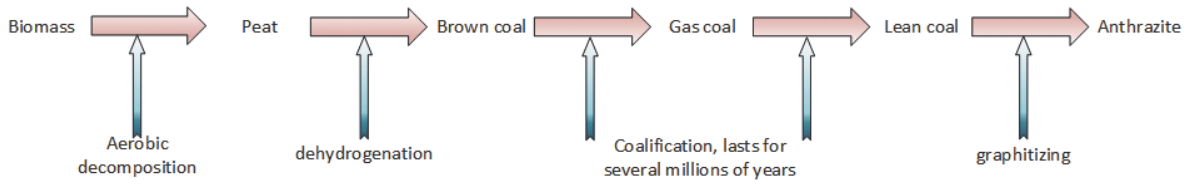

Figure 2-1: Schematic drawing of the evolution of coal, a process that needs several million years [23]

2.1 Characterization of solid fossil carbons

Fossil solid carbons can be defined as heterogeneous composite material, since it consists of mainly organic carbon, inorganic matter as well as porosity. Macroscopic views of coal show that the material seems to be a rugged and porous black material. Taking a closer look, microscopically it is made of the main part, carbonaceous matrix. Furthermore, huge amounts of micropores as well as microfissures along with inorganic matter of any size and shape are present. Coal is basically made of carbon, but distinctions have to be made with regards to its bonding hybridization. Especially carbon is well known for its allotropy, which means it can be found in a cubic structure (diamond), hexagonal structure (graphite), fullerene as well as carbyne. Moreover, a second possibility for a division might be given; graphitizing carbons (soft, non-porous, high density) and non-graphitizing carbons (hard, micro-porous, low density). An illustration of these two types is provided in Figure 2-2 [24].

Usually metallurgical coke is produced out of graphitizing coal. The average structure of coke can be described as a huge amount of small hexagonal crystals along with some quantities of mineral matter that equals the ash content after a total combustion. These non-organics typically have an amount of less than 15 % within the coke. Characteristic values of ash as well as average contents of minerals in the mineral matter can be seen in Table 2-1. However, although this species shows a low quantity in the carbonaceous material, it might have an important influence on the reaction of the carbon with gases, metals or slags. Elements like iron, calcium or magnesium as well as alkalis may have an influence at higher temperatures and can affect the reactivity of carbon positively or negatively. One possibility is the covering of the pores with a subsequent decreasing of the reactive surface by low melting particles. Increasing basicity of the ash may have a catalytic effect on the reaction behaviour of carbon with other species [24].

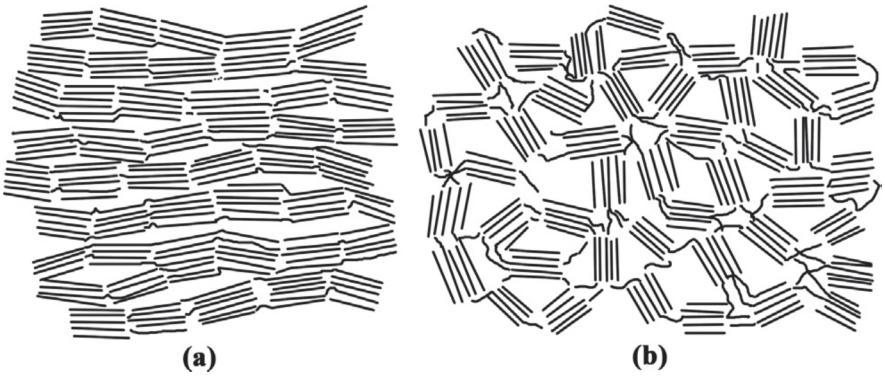

Figure 2-2: Illustration of graphitizing (a) and non-graphitizing carbons (b) [24]

Investigations in the field of mineral matter within carbonaceous material show that the main phases among others are represented by alumosilicates, as can be observed in Table 2-1 [24].

Determining the chemical analysis is the major part in the characterization of carbons. Therefore, different methods and standards are in use to test carbon carriers in an efficient way. The most common ones are those from the American Society for Testing and Materials (ASTM), the “Deutsche Industrie Norm” (DIN) and the International Organization for Standards (ISO). Since the results of all analysis standards contain the same parameters, a very clear explanation is pictured in Figure 2-3 [25].

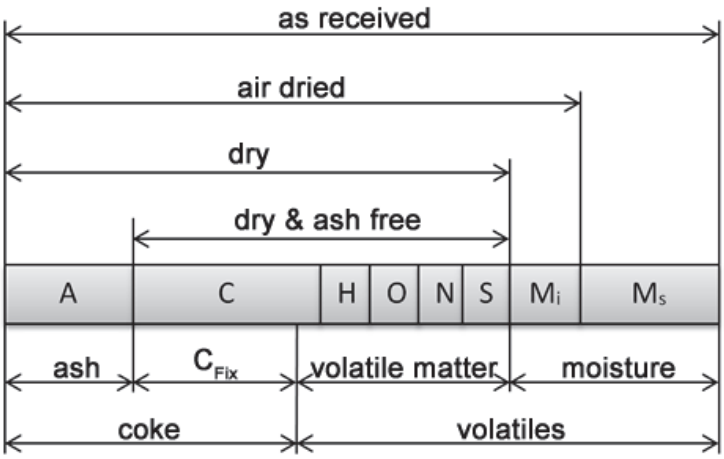

Figure 2-3: Basis for the characterization of solid carbon carriers [25]

Table 2-1: Max. / Min. values of mineral matter (wt-%) in different coke samples according to [24]

Mineralogy of cokes	Formula	Minimum [wt-%]	Maximum [wt-%]
LTI		9.6	19.9
Crystal : (Mainly anisotropic)			
Akermanite	$Ca_2MgSi_2O_7$	0.1	0.5
Anatase	TiO_2	0.3	0.9
Anorthite	$(Ca,Na)(Si,Al)_4O_8$	0.8	1.0
Bassanite	$CaSO_4.0.5H_2O$	0.3	1.6
Boehmite	$AlO(OH)$		0.4
Calcite	$CaCO_3$	0.2	0.8
Calcium iron oxide	$CaFe_2O_4$		0.2
Cristobalite	SiO_2	0.1	1.8
Diopside	$CaMgSi_2O_6$	0.4	1.6
Fluorapatite	$Ca_5(PO_4)_3F$	0.3	2.9
Gehlenite	$Ca_2Al_2SiO_7$	0.1	0.4
Grossular	$Ca_3Al_2(SiO_4)_3$	0.3	0.5
Hedenbergite	$CaFeSi_2O_6$		0.1
Hematite	Fe_2O_3		0.6
Illite	$(K,H_3O)(Al,Mg,Fe)_2(Al,Si)_4O_{10}[(OH)_2,H_2O]$	0.3	2.8
Iron	Fe	0.2	1.0
Jarosite	$(K,H_3O)Fe_3(SO_4)_2(OH)_6$	0.2	1.4
Lime	CaO		0.1
Magnetite	Fe_3O_4		0.4
Mullite	$Al_6Si_2O_{13}$	9.1	29.0
Oldhamite	CaS	0.1	0.2
Pyrrhotite	$Fe_{1-x}S$	0.1	3.4
Quartz	SiO_2	4.1	20.0
Rutile	TiO_2	0.1	1.2
Spinel	$MgAl_2O_4$		0.2
Troilite	FeS	0.1	0.6
Wustite	FeO	0.1	0.2
Amorphous (Mainly isotropic)		51.7	67.4

Slight differences in the analysis methods can be found in the sample treatment like it is explained in Table 2-2 for the so-called proximate analysis (moisture, volatiles, ash, C_{Fix}). According to these variations, the results obtained might vary, as seen in Figure 2-4. Here, several charcoals were investigated concerning their chemical (proximate) composition. As it is shown below, the fixed carbon content is slightly higher when using the DIN/ISO standards

or lower when applying the ASTM. In both cases, the fixed carbon (C_{Fix}) is calculated by the difference to 100.

Table 2-2: Test parameters for the determination of moisture, volatiles as well as the ash content of solid fuels [26–28] for ASTM; [29–31] for DIN

Parameter	Final Temp [°C]		Atmosphere		TGA type	Time / deviation	
	ASTM	DIN/ISO	ASTM	DIN/ISO		ASTM	DIN/ISO
Moisture	105 °C	105 °C	N_2	air	Constant weight	00.050 %	±5 °C
Volatiles	950 °C	900 °C	N_2	-	Fixed time	7 min	7 min
Ash	750 °C	815 °C	O_2	air	Constant weight	00.050 %	±10 °C

Since this thesis applies the standards according to DIN/ISO, a short overview of the parameters is given in the following section.

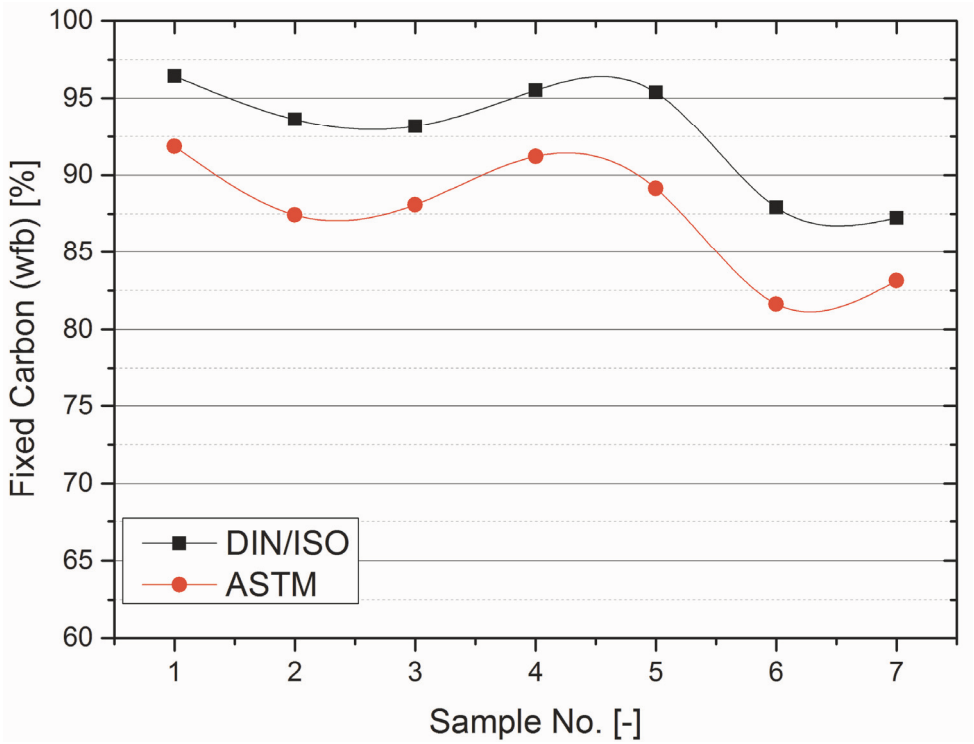

Figure 2-4: Differences in the fixed carbon content (water free base) of seven charcoal samples according to the analysis standard (DIN/ISO. or ASTM)

2.1.1 Ultimate analysis (CHNS)

The determination of carbon, hydrogen and nitrogen in carbonaceous material is carried out in accordance with DIN 51732. Further, DIN EN ISO 15350 can be used to estimate the sulphur content within the solid “fuel.” Usually, manufacturers of CHNS measurement devices provide units which measure CHN and S at the same time using the same sample. The sample is combusted using oxygen or an oxygen-containing atmosphere in both standardized tests. The products can be divided into gases (mainly carbon dioxide, water moisture, elementary

nitrogen and/or nitrous oxides as well as sulphur oxides and hydrogen halides) and the remaining ash. For this type of analysis, the volatile fraction is forwarded to the measurement units. In the case of CHS, the measurement principle is based on infrared spectroscopy and nitrogen can be analysed with thermal conductivity detectors. The obtained values are equal to the mass fraction (water free base) of the carbon and with this, the amount of oxygen is calculated by the difference to 100. Unfortunately, both standards don´t give any information regarding flow rate of the oxidation agent as well as the maximum temperature during the combustion [32; 33].

2.1.2 Proximate analysis

To get information about the amounts of ash, moisture, volatiles and the fixed carbon, the following standards can be applied [29–31]:

- DIN 51720 for volatile matter
- DIN 51719 for ash content
- DIN ISO 11465 for moisture
- C_{Fix} by the difference to 100

The testing parameters can be observed in Table 2-2. For the determination of volatile matter (DIN 51720), some information about the applied furnace, the crucible and the arrangement of the thermocouple in the furnace is given. Furthermore, the sample is kept in the furnace for 7 minutes in a closed system. Afterwards, it is removed from the furnace and cooled down.

With the application of DIN 51719, the ash content can be observed. In comparison to the previous analysis method, a special focus must be on the final temperature and the residence time. After the treatment, the sample is cooled down and weighted. Sometimes, a second incineration has to be performed if there are some remaining organic compounds visible.

Finally, the analysis of the moisture is carried out using the parameters given in Table 2-2.

Also for the proximate analysis, no special requirements are necessary regarding furnace type (except volatile matter) and sample size. The fixed carbon is calculated by difference.

2.1.3 Determination of the specific surface area

This chapter should explain the basic principles in the field of specific surface measurement, since this method is applied as the characterization method of various carbonaceous material. Along with this method, modern measurement units allow the simultaneous estimation of the pore size distribution.

The physical basis for this type of measurement is the adsorption of gases on solid surfaces at varying pressures and temperatures. The variation of these parameters leads to an increasing or decreasing layer build-up of gases on a solid. Usually the temperature is kept constant (isothermal), which means there is only one parameter which changes – the pressure. For the sake of completeness, it has to be mentioned that actually the thermodynamic equilibrium between adsorption and desorption of the gas is the target of the analysis. As already mentioned, a typical procedure for determining the specific surface area is starting at low pressures. Narrow pores like micro and mesopores are filled by the adsorptive as well as the free surface of the solid. Rising pressure leads to a further filling of macropores and the formation of multi-layer adsorption. The well-known B.E.T. equation can be applied to calculate the specific surface area based on the previously mentioned theory by drawing an adsorption isotherm according to equ. 2-1 [34; 35]:

$$\frac{\frac{p}{p_0}}{V_a \cdot \left(1 - \frac{p}{p_0}\right)} = \frac{1}{V_m \cdot C} + \frac{C-1}{V_m \cdot C} \cdot \frac{p}{p_0} \qquad \text{equ. 2-1}$$

- V_a: adsorbed gas volume
- V_m: equal value of a monolayer volume
- p: pressure that is kept variable
- p_0: saturation pressure of the applied gas (760 torr at -193 °C)
- C: B.E.T. constant

The given equ. 2-1 corresponds to the linear equation “y=d+kx.” It can be applied using the following requirements [34; 35]:

- localized adsorption
- multi-layer adsorption
- homogeneous sample
- neglected adsorption heat in the first layer
- adsorption heats are equal to the condensation heat of the adsorptive as well as all subsequent layers
- interactions of the adsorbate molecules can be neglected

“C” in equ. 2-1 is called the B.E.T. constant, which depends on the applied measurement gas only. Theoretically, it can be calculated by applying equ. 2-2

$$C = \exp\frac{E_1 - E_L}{R \cdot T} \qquad \text{equ. 2-2}$$

whereby the variables are [34; 35]:

- E_1: adsorption enthalpy of one layer
- E_L: adsorption enthalpy of further layers (equal to the condensation enthalpy of the gas on a solid surface)

Figure 2-5 shows an adsorption isotherm of a carbonaceous sample exemplarily. The experimentally determined adsorption isotherm (red dots) is limited to the evaluation range. The calculated BET line in red is overlaid to serve as a basis for the further calculation of the specific surface area [34; 35].

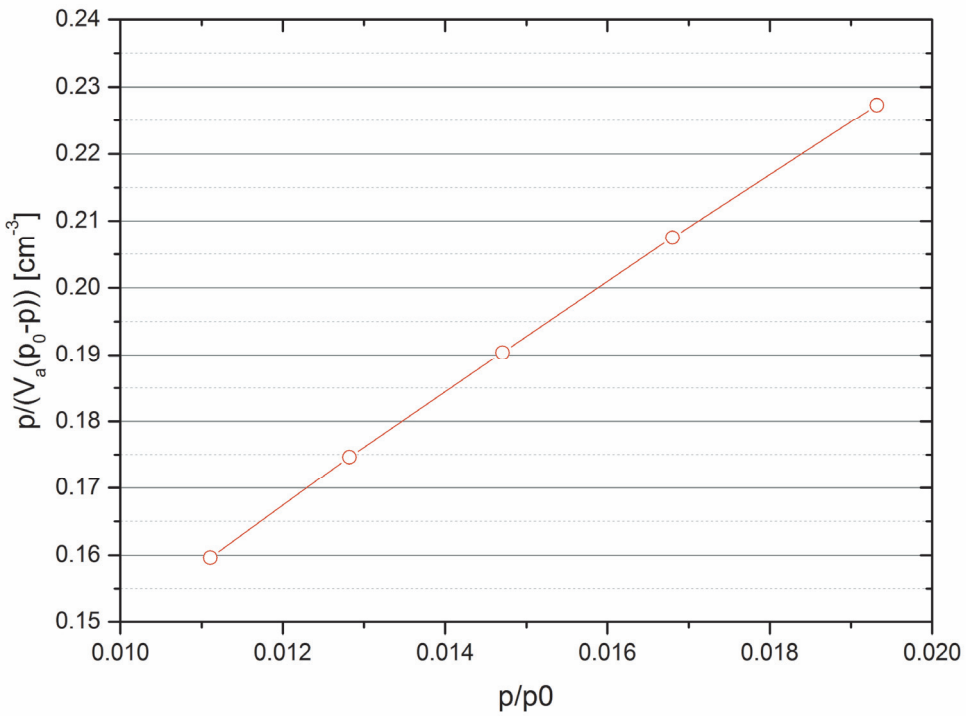

Figure 2-5: Extract from an adsorption isotherm with the calculated B.E.T. line [34; 35]

With this result, the slope “k” as well as the ordinate interception “d” can be calculated according to equ. 2-3 and equ. 2-4. Further calculations lead to the determination of the adsorbed volume and finally to the specific surface area (in m²/g) [34; 35]:

$$V_m = \frac{1}{d + k} \qquad \text{equ. 2-3}$$

$$C = \frac{k}{d} + 1 \qquad \text{equ. 2-4}$$

Finally, the space requirement of the applied adsorbate at the desired temperature is needed to calculate the specific surface area. The surface can be calculated using equ. 2-5 [34; 35]:

$$O_{SP} = V_m \cdot N_A \cdot a_m \qquad \text{equ. 2-5}$$

- O_{SP}: specific surface area [m²/g]
- N_A: Avogadro constant
- a_m: specific space of the applied gas molecule (N_2, CO_2, Kr, etc.)

As described previously, new measurement devices have the possibility to estimate the pore size as well as the pore size distribution by mathematical and statistical models. A short introduction of this topic should be mentioned here. Basically, the type of pores should be divided by their size [36; 37]:

- Nanopores (< 0.9 nm)
- Micropores (0.9-2 nm)
- Mesopores (2-50 nm)
- Macropores (> 50 nm)

For the determination of nano and mesopores or the pore size distribution, the use of CO_2 is recommended. The reason for this is the relatively high diffusion speed of the adsorbate molecules at 0 °C in comparison to temperatures of liquid nitrogen (-193 °C). This leads to a faster filling of the pores and a decreasing possibility for the measurement of incorrect values [37].

For the porosity and surface area measurements in this thesis, the gas adsorption device “NOVA 2000e” from “Quantachrome Instruments” was in use. It consists of two heating (sample preparation) and two measurement stations. The usable adsorption gases are N_2 for fossil carbons and CO_2 for charcoals (because of the high porosity, as mentioned before). Additionally, helium is needed as a purging gas as well as for the determination of the dead volume of the sample holders due to the negligible adsorption rate of He. To keep the sample at a constant temperature during the measurement, a Dewar vessel is used. This Dewar is filled with liquid nitrogen (-193 °C) in the case of N_2 adsorption measurements and filled with a cooling liquid at 0 °C in the case of CO_2 adsorption measurements. For the second type of measurement, a pump with an integrated cooler is used to keep the temperature constant. Additionally, a vacuum pump is applied to adjust the required pressure inside the sample holder.

Figure 2-6: “Quantachrome Instruments NOVA 2000e” for the measurement of the specific surface area and pore size distribution

2.1.4 Reactivity tests

Reactivity plays an important role in the characterization of carbon when it should be utilized in metallurgical furnaces. A huge variety of different methods is available; a few of them are described in the next section. Some of them are based on the weight loss during a thermal treatment in a special atmosphere like CO_2, while others count the ratio of the CO or CO_2 produced subsequent to the thermal treatment. Due to the fact that all the test parameters like temperature, residence time, gas composition, sample and grain size are related to metallurgical (fossil) coke, some of them had to be adopted to make the measurement possible. The grain size is the major problem because the shape of some biomasses is quite different to the crushed and sieved fossil coals.

Basically, the types of reactivity measurement can be divided into those which are related to a mass loss during a treatment with oxidizing agents (H_2O or CO_2) and those that measure the quality and quantity of the oxidizing products (CO, H_2) after this treatment. A very popular method which can be related to the first group is the standardized determination of the CRI (Coke Reactivity Index) according to ASTM D 5341 [38]. This method is very important for blast furnace operators since for this type of furnace, low reactivity coke is recommended. Furthermore, this standard includes a tumbling test to measure the coke strength after this

treatment (Coke Strength after Reaction - CSR). A second well-known test is the reactivity measurement according to Koppers, but this test is not standardized [39]. Here, the so-called R value is the result of the examination, which is based on the ratio of the amount of CO and CO_2 in the off- gas, according to equ. 2-6:

$$R = \frac{100\ CO}{CO_2 + {}^1/_2\ CO} \qquad \text{equ. 2-6}$$

It has to be mentioned that several other or newer standards are available, but these two are still the common ones, which is why they will be used for the comparison between the applied carbonaceous materials in this thesis.

The reactivity test based on Koppers allowed a clear distinction between the reactivities of the charcoal from different feed materials as well as a differentiation concerning charcoals from various carbonization temperatures. Additionally, the determination of the reactivity with the standardized CRI method (ASTM D 5341) was carried out, to also get a distinction of all charcoals concerning their weight loss during this heat treatment. Both methods are based on the Boudouard equation (C + CO_2 ↔ 2 CO), where the carbon from the charcoal reacts with the CO_2 from the supplied gas stream. On the one hand, the Koppers test calculates an R factor by the CO/CO_2 ration in the off-gas. On the other hand, the ASTM test results in the CRI factor (coke reactivity index), which represents the weight loss after the reaction time. Figure 2-7 shows the experimental set-up for reactivity measurement at the Chair of Nonferrous Metallurgy.

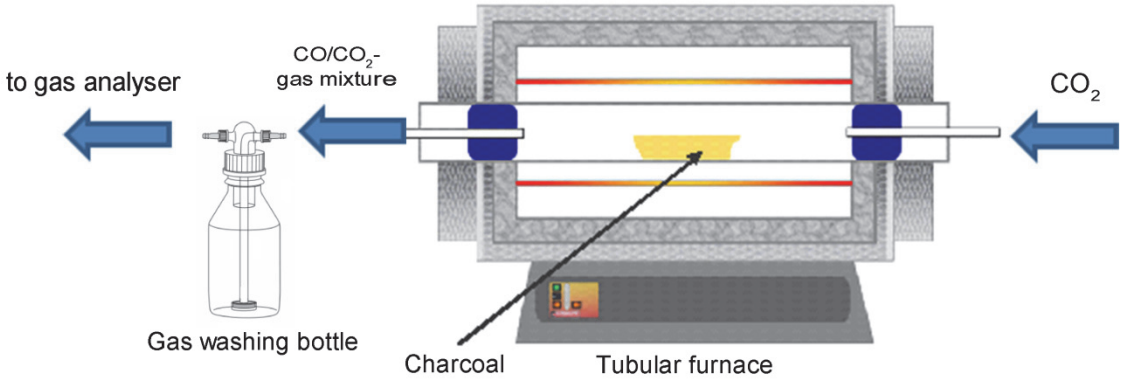

Figure 2-7: Test equipment for the measurement of the reactivity from charcoals

As it was already mentioned previously, it is mandatory to place a special focus on the adopted parameters which are different to the values that can be found in the recommendations or in the standards. But it was necessary to combine the two experiments as well as possible, which led to the following adjustments:

Table 2-3: Comparison of the different characterization methods and the applied reactivity measurement [38, 39]

	ASTM	Koppers	NEM
Furnace	Reaction furnace vessel made of heat-resistant steel	Quartz tube in an Ubbelode furnace [39] or similar	Tubular furnace, Alsint tube
Temperature	1,100 °C	950 °C	1,000 °C
Residence time	120 min	5 x 15 min	15 min
CO_2 purging	5 l/min	0.18 l/min	0.5 l/min
Sample size	200 g	34 cm³	32 cm³
Grain size	19-22.4 mm	0.5 – 1.0 mm	as delivered

Figure 2-8 shows the set-up for the CRI measurement. Due to the fact that relatively big Al_2O_3 spheres are used for preheating the gas, this type of set-up would not be possible for small or unshaped samples since they would fall beneath the spheres and block the pores. Although the time is the major difference between ASTM and NEM, they can be compared like it is pictured in Figure 2-10. Exemplarily, four different cokes were analyzed, using the ASTM or NEM method, respectively. Of course, the CRI at NEM is far too small, but the tendency of the results obtained in the standardized test and the optimized experiment are very similar.

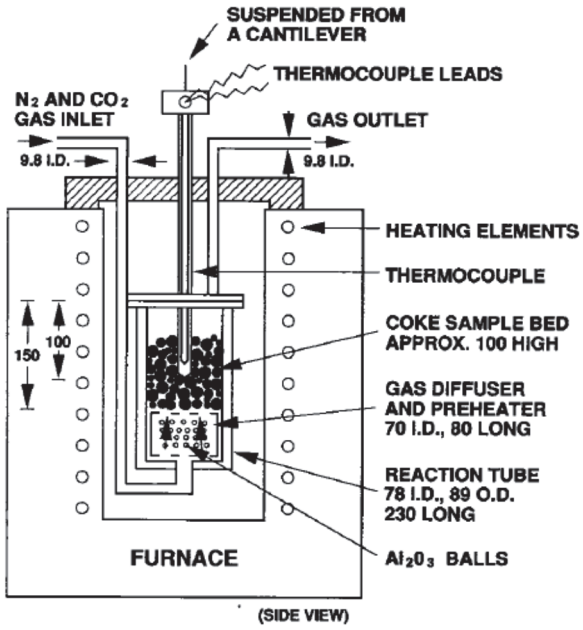

Figure 2-8: Standardized furnace with attached N_2/CO_2 purging and thermocouples according to ASTM D 5341 [38]

Figure 2-9 and Figure 2-10 compare values obtained by the application of the standardized ASTM method with the ones achieved at the Chair of Nonferrous Metallurgy as well as some regression lines.

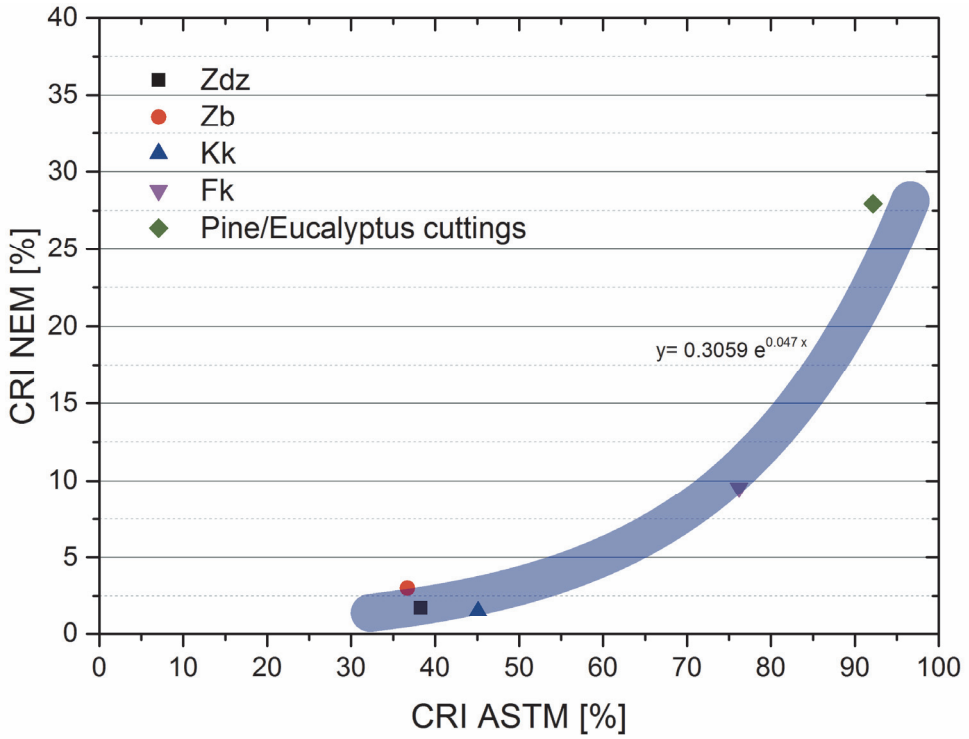

Figure 2-9: Comparison of the standardized CRI value with those from the set-up available at the Chair of Nonferrous Metallurgy

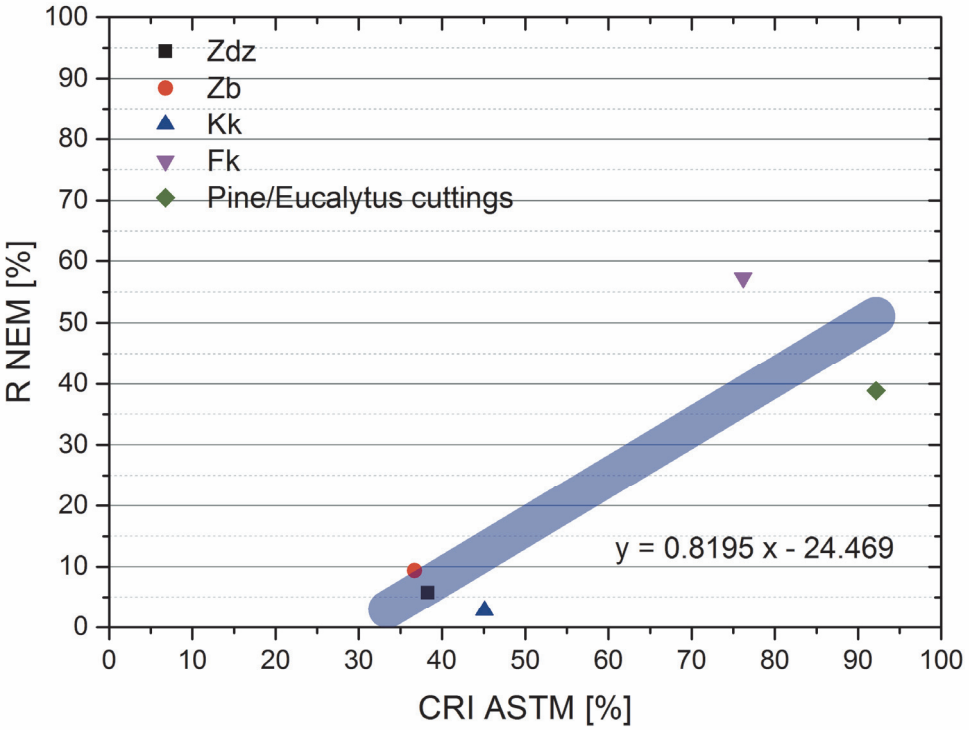

Figure 2-10: Comparison of the obtained CRI values from the ASTM with the R-value from the NEM testing unit

Figure 2-11 gives an overview of the reactivity measurement according to Koppers. It is clear that this experimental set-up is not possible or necessary anymore. State of the art technology allows the use of infrared spectroscopy, heat conductivity as well as paramagnetism-based measurement units (cf. Chapter 3.2.1) to analyse the obtained gas fraction. Therefore, it is not

required to do these trials at least five times, as it is recommended in the publication of Koppers [39] to get information about the formation of the CO/CO_2 ratio.

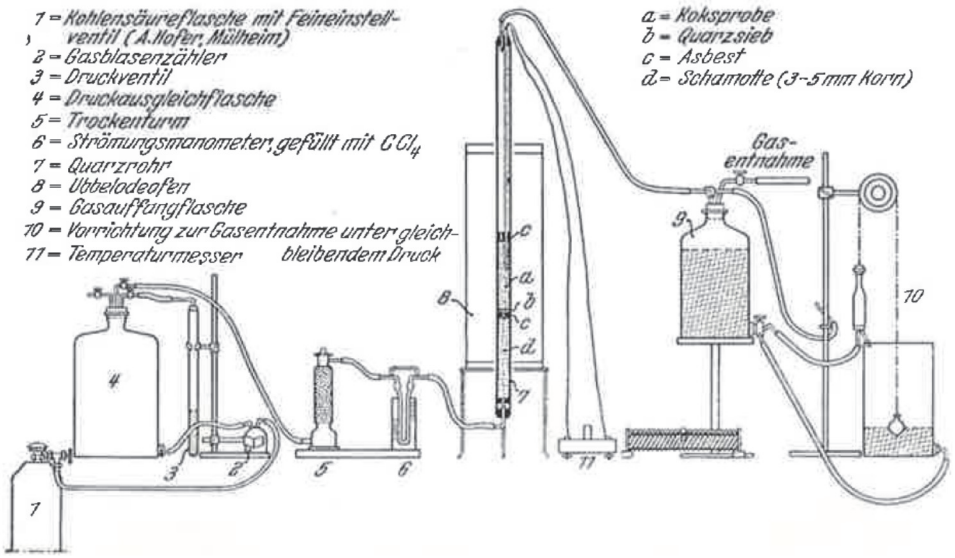

Figure 2-11: Experimental set-up for the determination of the coke reactivity according to Koppers; 1: CO_2 bottle; 2: gas bubble counter; 3: pressure valve; 4: pressure balance bottle; 5: drying tower; 6: pressure gauge; 7: quartz tube; 8: Ubbelode-furnace; 9: gas receiver bottle; 10: gas extraction; 11: thermometer; a: coke sample; b: quartz sieve; c: asbestos; d: fireclay [39]

In the following subchapters, several types of coke will be explained (according to Figure 2-1), starting with brown coal, since peat is not used in metallurgy because of its low quality. Moreover, an overview of the production of purified coal (coke) as well as artificial carbon carrier (Desulco® and petroleum coke) is given.

2.2 Brown coal

Brown coal, sometimes labelled as lignin in literature, is the lowest grade of solid fossil carbons, except peat. As an example, the maximum carbon content of Victorian brown coal from Australia is roughly 70 %. From this value, around 50 % is classified as hydrocarbons, which leads to the conclusion that approximately 35 % of the brown coal can be defined as fixed carbon (and therefore available for metallurgical purposes). Moreover, this type of carbon carrier shows a high concentration of oxygen and relatively low amounts of sulphur. Finally, based on the origin of this type of coal, it can be stated that brown coal is high in moisture but low in ash. Typical values of the chemical composition can be found in Table 2-4. Compared to other types, brown coal shows the lowest values of C_{Fix}, mostly because of its low age compared to other carbons [40].

Table 2-4: Proximate analysis [wt-%] of selected brown coals from Indonesia (col. 1-3) [41] and China (col. 4 and 5) [42]

	Taban	Berau	Samaranggau	Xiaolongtan	Huolinguole
Moisture	15.35	16.13	22.33	17.45	15.80
Ash	4.42	6.36	2.15	6.66	11.67
Volatiles	40.68	37.20	38.05	41.66	34.69
C_{Fix}	39.55	40.31	37.47	34.23	37.84

Although this type of carbon has very unfortunate characteristics, only one utilization possibility of lignin for metallurgical purposes is actually known. Particularly in some blast furnaces, this types of coal is used in the tuyeres, where it is injected into the hearth of the furnace. Therefore, the coal has to be grinded and pneumatically forwarded to the injection holes. The powdered coal injection (PCI) leads to a dramatic increase in the coke amount and an increase in the throughput of a blast furnace, respectively; details will be given in the next chapter since the operation of PCIs using stone coal is more common [43; 44].

2.3 Stone coal

In general, different names are known for stone coal; they might be labelled as hard coal, (sub) bituminous coal or black coal, but it always means the third oldest type of coal, after peat and brown coal. After hundreds of years in use in different kilns, furnaces, stoves, etc. it is definitely not possible to give a defined chemical composition since the analysis depends on the geographical origin of the carbonaceous material. Table 2-5 is a summary of the proximate analysis of 34 Chinese stone coals to get an overview of the range of the components within this type of carbon. In principle, stone coal can be divided into two substantial different types: the humic coals, which are originated by wood and/or grass residues and the sapropelic ones, which are made of all the other biomass sources (including algae, spores, plant residues, etc.) [45; 46].

Table 2-5: Range of the proximate analysis [wt-%] of 34 selected stone coals [45]

	Proximate analysis	
	Min.	Max
Moisture	3.40	1.14
Ash	8.55	11.11
Volatiles	6.67	7.30
C_{Fix}	81.38	80.45

Basically for metallurgical operations, stone coal is the preferred carbon for producing metallurgical coke. With this, a wide utilization could be realized, in ferrous as well as in nonferrous metallurgy. Several products can be obtained from the carbonization of stone coal,

depending on the parameter. Chapter 2.5 will give detailed information about the production of coke as well as its application fields [47].

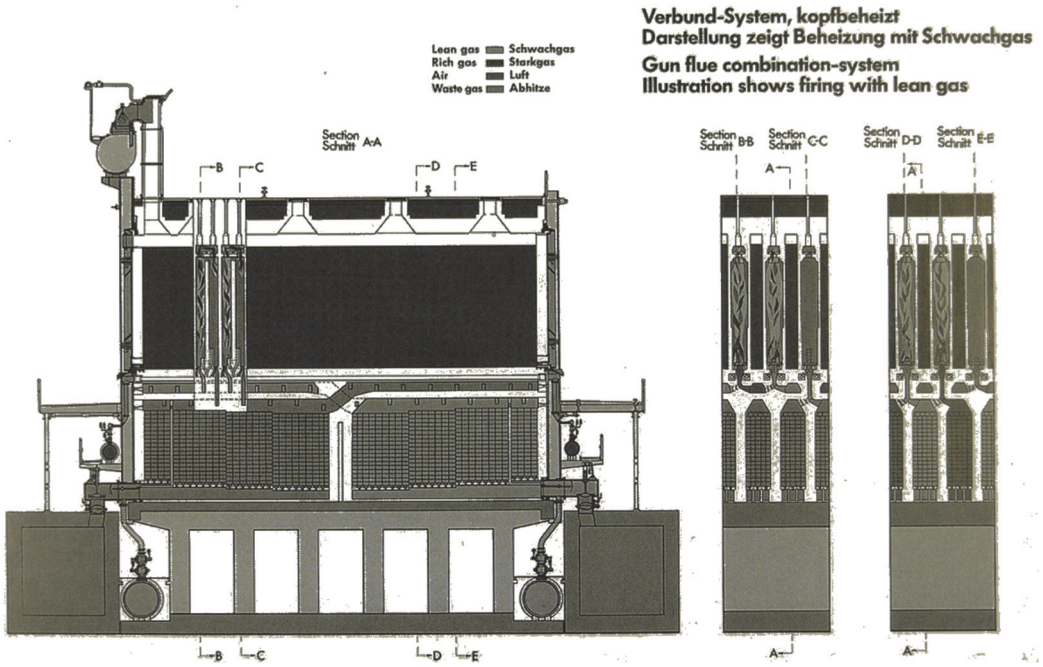

Figure 2-12: Principal set-up of a coke oven chamber [47]

Another utilization of stone coal came up in the last 20 years, where an attempt was made to implement coal powder into iron blast furnaces. The PCI technology leads to an optimized process to obtain pig iron, since the injection into the tuyeres in the lower part of the shaft furnace guarantees an immediate reaction together with the hot blast, resulting in the production of reducing gas. Several advantages are responsible which lead to the conclusion of labelling the process as “state-of-the-art” in modern blast furnace operations. Reduction of the coke consumption, utilization of the hydrogen within the coke as a reducing agent and improvement of the pig iron quality can be named as developments due to the PCI. A drawing of the implementation of a PCI in a modern blast furnace can be observed in Figure 2-13 [48].

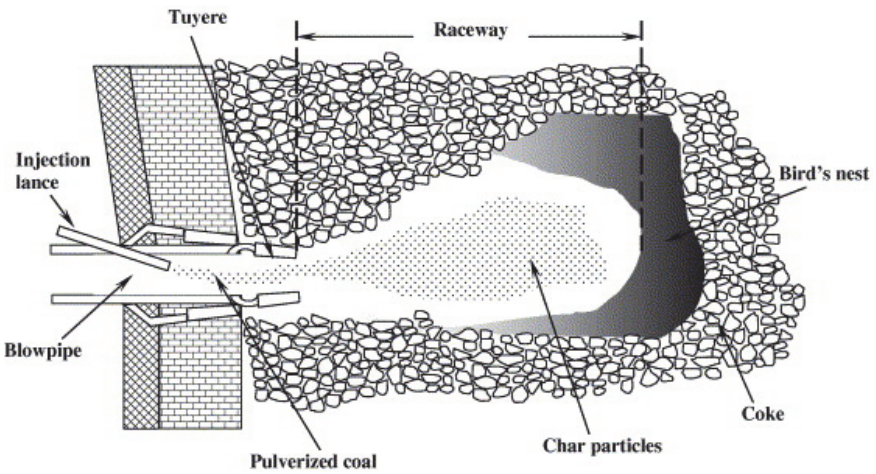

Figure 2-13: Sectional drawing of the bottom part of a blast furnace equipped with a powder coal injection [48]

2.4 Anthracite

Anthracite is the last modification of the coalification of biomasses over millions of years. Since the amount of volatile matter is very low and the carbon content in contrary very high, it is considered as an alternative to the artificial and therefore more expensive coke.

Unfortunately, its thermal resistance is rather low, which causes bursting at increasing temperatures. A possible solution to avoid the destruction of anthracite is to mill it and produce briquettes with several additives to increase the resistance. Literature shows that a mixture of anthracite powder with lignin, collagen and silicon additions increases the thermal resistance and therefore, the compressive strength of a briquette made out of this input materials. An optimization would be the substitution of silicon with silicon carbide nanotubes. The collagen leads to an increased sticking behaviour of the briquette at room temperatures, which is favourable for transportation and storage. However, lignite forces the resistance under pyrolysis conditions in a temperature range between 400 and 1,200 °C. Finally, the silicon carbide nanotubes guarantee the required strength above these temperatures in the melting zone of a metallurgical furnace. However, metallurgical applications are the utilization in EAFs at the charging of scrap and for injection purposes [49–51]. Table 2-6 shows the proximate analysis of three different anthracites.

Table 2-6: Proximate analysis [wt-%] of three different anthracite coals

	from China [52]	from Ukraine [53; 54]	
		No.1	No.2
Moisture	3.40	1.14	3.65
Ash	8.55	11.11	10.7
Volatiles	6.67	7.30	7.03
CFix	81.38	80.45	78.62

2.5 Coke

The first usage of coke was the substitution of charcoal in blast furnaces in the 18th century because of its advantages compared to renewable charcoal. Usually, stone coal is used to serve as a source for the carbonization process. Further applications of coke were the production of salt out of salt brine and the calcination of lime. Today, coke is the most used carbon carrier for metallurgical purposes, mostly because of its purity and strength, since it fulfils the initial requirements for the iron blast furnace [55].

The carbonization process, a type of pyrolysis, is carried out at temperatures higher than 1,000 °C and in the absence of air. Pyrolysis happens after the increase of temperature in a

coal particle and is the first step previous to combustion, gasification, liquefaction and carbonization. The subsequent reaction mentioned before depends on the operating parameters [56]. In case of carbonization, the major product is the obtained coke (or char) that is mainly used for the production of pig iron in blast furnaces. Therefore, the mechanical strength as well as porosity and gas permeability must be rather high, to move the carbon without any massive destruction to the bottom of the furnace. The most common process for the carbonization of coals is externally heated coke batteries, which are operated batch-wise (see Figure 2-12 and Figure 2-14). The indirect heating takes place by the combustion of fuel gas, often by the coke oven gas itself. After several hours, the produced coke is removed from the furnace, quenched and forwarded to further processes [57].

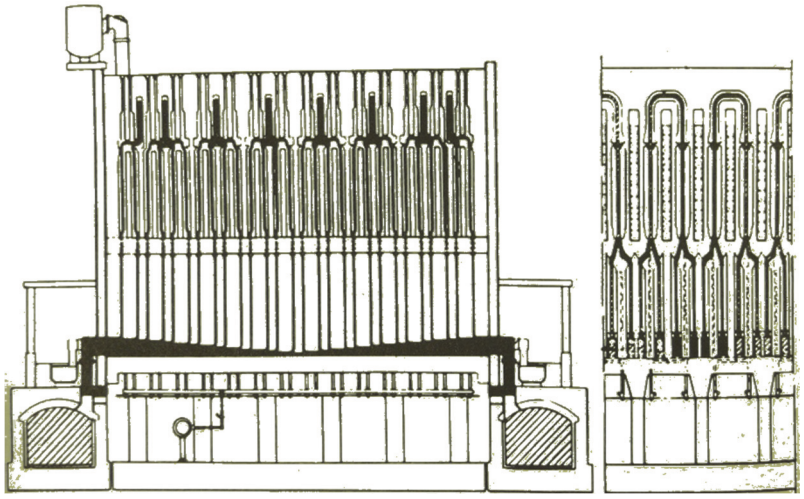

Figure 2-14: Koppers Becker underjet coke oven furnace [57]

Depending on the input material (coal), the parameters in the carbonization process and the designated use, the obtained product can be labelled as [47]:

- “Coke” (obtained from the carburization of stone coal), gas coke, pitch coke, petroleum coke
- Semi coke, high temperature coke
- Industrial coke, furnace (or metallurgical) coke, foundry coke, domestic coke, coke breeze
- Electrode coke, calcined petroleum coke, calcined pitch coke

The big advantage of the charring process is that the amount of fixed carbon increases with the simultaneous decrease of volatiles and ash [58]. Table 2-7 shows the chemical composition of several cokes. Further advantages are that specific values, like sulphur (<1 %), ash (<8.5 %) and volatiles (<1 %) are rather low for the conversion of coal to coke in the absence of air [49].

Table 2-7: Overview of the proximate analysis [wt-%] of eighteen different coke samples [59]

	A	B	C	D	E	F	G	H	I
Moisture	1.9	2.4	2.5	2.4	2.7	1.4	1.1	1.5	1.5
Ash	6.2	5.6	7.7	7.1	9.1	7.0	9.8	9.7	9.6
Volatile matter	34.0	28.9	26.2	22.3	22.8	21.3	20.2	20.2	17.6
Fixed carbon	59.8	65.5	66.1	70.6	68.1	71.7	70.0	70.3	72.8
	J	K	L	M	N	O	P	Q	R
Moisture	0.7	0.7	0.8	0.7	1.1	1.9	0.8	0.8	0.6
Ash	9.1	7.9	10.3	9.3	11.9	9.0	11.8	12.2	11.9
Volatile matter	0.7	0.8	0.3	0.7	0.5	0.6	0.6	0.4	0.6
Fixed carbon	90.2	91.3	89.4	90.0	87.6	90.4	87.6	87.4	87.5

2.6 Petroleum coke

Petroleum coke is a by-product from the production of fuels and organic compounds, respectively, during the refining of crude oil in petrochemistry. The flow sheet in Figure 2-15 shows the production overview of several oil-based compounds, including petroleum coke. The green coke itself is the residue of the coking process, where heavy hydrocarbons are cracked to maximize liquid products. But the major product within this process is petroleum coke, which mainly contains all the undesirable components like sulphur, metals and nitrogen that should not be accumulated in e.g. fuels [60].

The analysis of pet-coke varies, depending on the crude oil and the parameters (temperature, pressure, etc.) of the production unit within the refining plant. Typical ranges of the proximate analysis of crude (green) petroleum cokes are represented in Table 2-8 [61].

Further optimization would be the implementation of a calcining step, as it was mentioned previously. Here, remaining oil or tar components are removed from the pores of the coke typically in a rotary kiln or rotary hearth furnaces. With an incomplete combustion and carbonization, respectively, the carbon content of the pet-coke is increased with a simultaneous reduction of the amount of volatiles and moisture. About 20 % of the world´s produced petroleum coke is sold as calcined pet-coke. In this case, the product is, among others, utilized in metallurgical furnaces as a reducing agent or for other purposes (carbon anodes (primary aluminium production), Söderberg anodes, graphite anodes) [60; 62].

Table 2-8: Typical ranges of the proximate analysis of green petroleum coke (values are on dry base) [61]

	Range [wt-%]
Ash	0.3-0.5
Volatiles	9-21
CFix	83-90

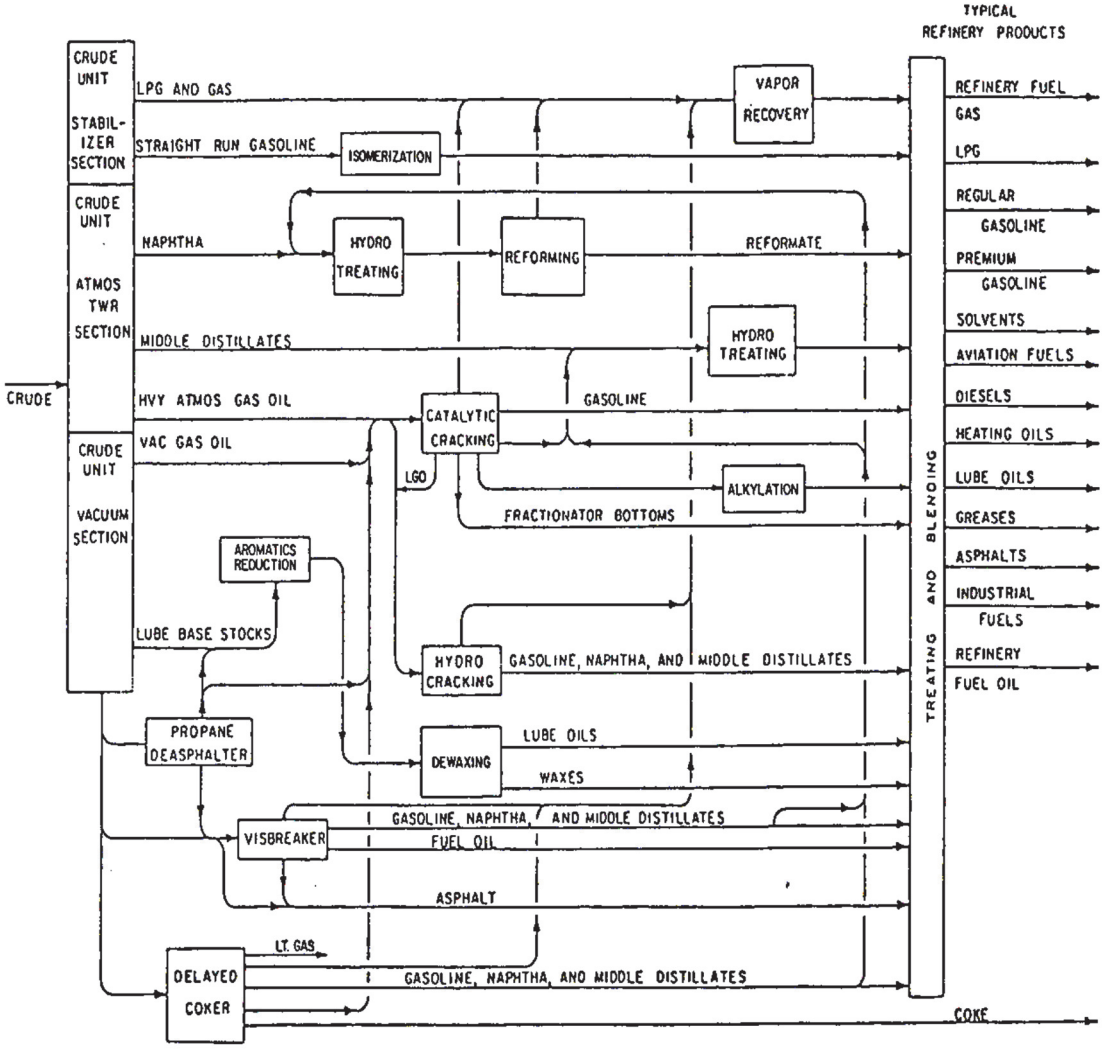

Figure 2-15: Process overview of the origination of crude oil-derived products [63]

2.7 Desulco®

Desulco® (invented word out of *desul*phurized *co*ke) is a product from the company “Superior Graphite Co.” in Chicago, United States of America. The production plant is located in Hopkinsville, USA, whereby a second plant is operated in Sundsvall, Sweden. This type of carbon carrier is often used in the field of re-carburization in the casting industry [64].

The feed material to obtain Desulco® is usually calcined petroleum coke. The purification step is a continuous working electro-thermal furnace at temperatures higher than 2,760 °C. Due to these operating conditions, the matrix gets rid of undesirable substances like moisture, ash and volatiles. Especially the removal of sulphur is an important factor when utilizing a carbonaceous material in metallurgical operations, since this element usually causes a lot of problems. The further graphitization of the carbon leads to a unique morphology of the carbon particles obtained. The typical analysis according to “Superior Graphite Co.” is given in Table 2-9. Obviously, it is not necessary to perform a separate ultimate or proximate analysis because of the applied production process [64].

Table 2-9: Typical chemical analysis of Desulco® coke [64]

Element	Standarized values
C	99.9 %
S	0.014 %
N	42 ppm
H	10 ppm

In Figure 2-16, the production unit of this special type of carbon carrier is illustrated. The conversion takes place in the upper part of a retort where the energy is delivered using three electrodes, increasing the temperature up to at least 1,700 °C, but usually higher (see previous section). The feed material, calcined petroleum coke, is charged at the top of the furnace, moving down during conversion. Here, the carbon is purified by the removal of remaining volatiles and ash. The lower part mainly consists of the cooling system to get rid of the heat prior to the discharge at the bottom of the conversion unit. Further processing after cooling down would be a sieving step with a subsequent packaging [65].

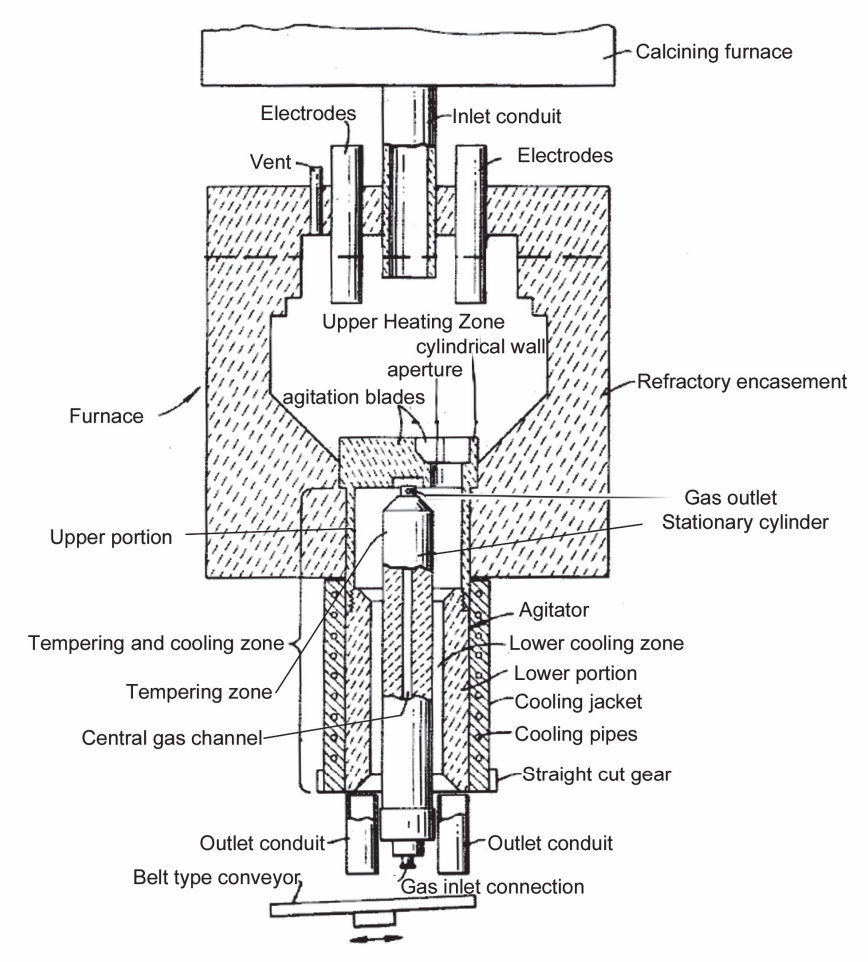

Figure 2-16: Drawing of a production unit for desulphurized coke [65]

3 Alternative reducing agents

The previous chapter describes the state of the art of carbon carriers that are used in metallurgical furnaces and kilns. Because of environmental reasons already mentioned before, new ways have to be found to reduce the emission of greenhouse gases, especially CO_2. One possibility is the utilization of waste biomass which is converted to special charcoal. In this thermochemical conversion process, a by-product is also formed, the so-called pyrolysis gas. Since this gas contains a valuable amount of reducing agents (C_xH_y) as well, it should be considered to think about utilization possibilities; in the case of metallurgical applications, it might serve as an alternative reducing gas or heating gas in various furnaces [66–69].

The main organic components of fresh biomass are cellulose as well as hemicellulose and lignin. The model in Figure 3-1 shows the schematic design of fresh biomass. Of course the amount as well as the ratio of each component varies a lot within the different types of biomass [66–69].

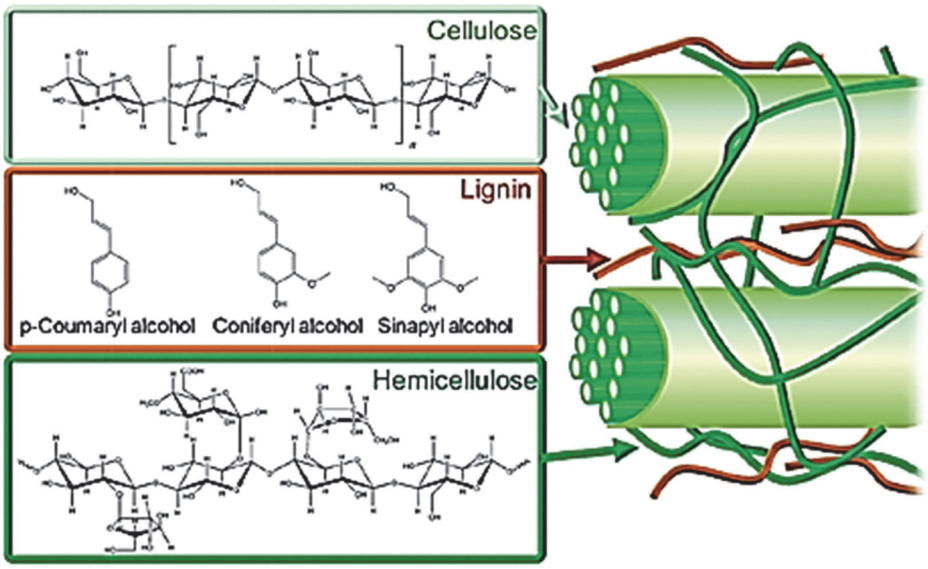

Figure 3-1: Visualization of the organic components in biomass [70]

To upgrade the mentioned biomass, a pyrolysis process is carried out to purify the carbonaceous material. The basic principle as well as the obtained products are described in Figure 3-2.

Historically, the first carbonization reactors were invented to provide charcoal for the medieval iron making process. These very simple earth kilns were of course very inefficient, since the charcoal yield was relatively low; a specific quantity of biomass was combusted to deliver heat energy to run the carbonization process. An optimization of the reactor led to concrete-based walls that guarantee a higher biomass throughput and increasing pyrolysis temperatures.

These types of kilns can still be found in Brazil next to the mini blast furnaces. Finally, the newest commercially used operations are mostly indirectly heated retorts. For this reason, the charcoal yield increases and the pyrolysis gas-based fuel efficiency is very high, leading to an economic process. Unfortunately, all the mentioned methods are not able to produce high quality charcoal, which is why newer technologies have to be found in order to deliver satisfying results. Among others, very popular carbonization reactors are [66; 71]:

- Rotary kilns
- Screw reactors
- Fluidized bed reactors

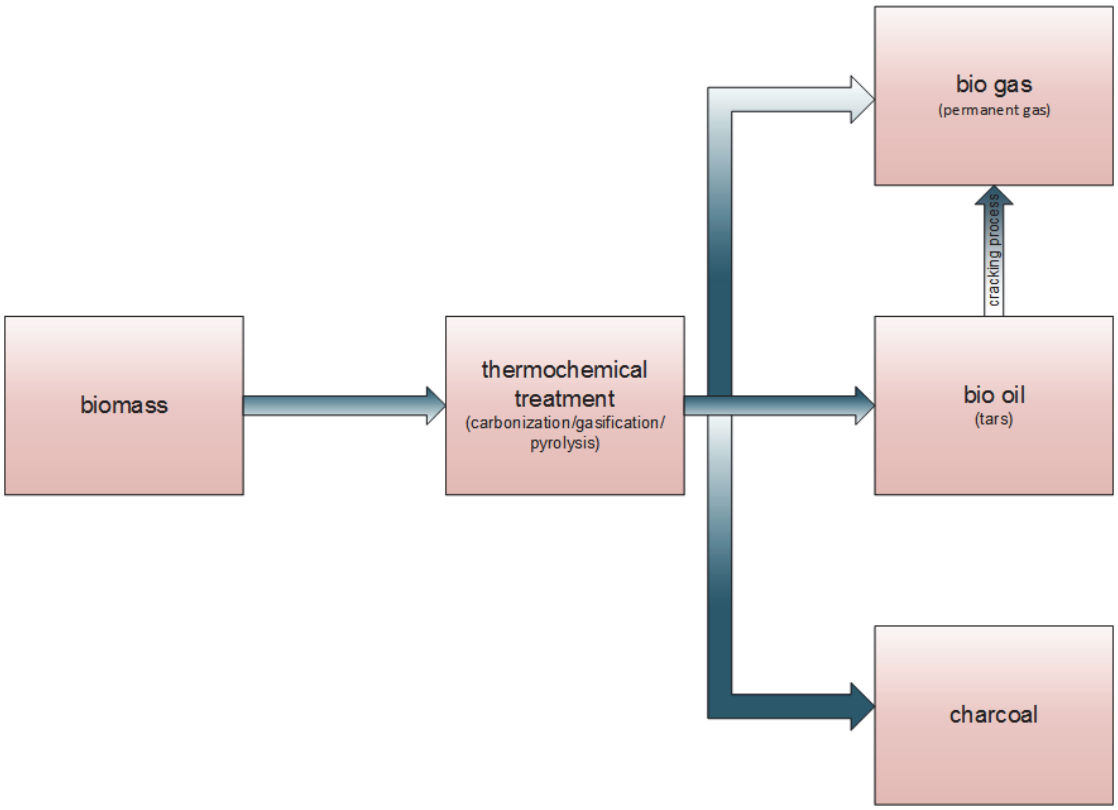

Figure 3-2: Products obtained from the thermochemical treatment of biomass [68]

The thermochemical conversion process was performed in a novel carbonization reactor which is able to treat semi-continuously fresh biomass at untypically high temperatures and varying retention times. Figure 3-3 shows the draft of the reactor that has already been described in previous theses and was utilized in the present work [21; 72].

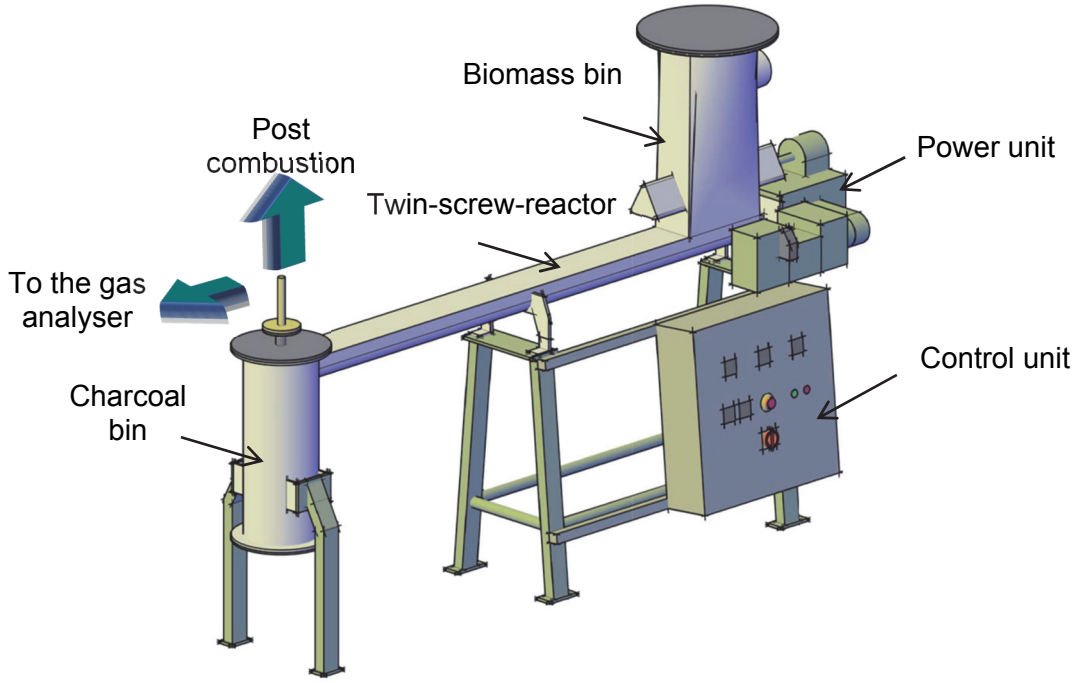

Figure 3-3: Semi-continuous “twin screw reactor” for the production of high quality charcoal

For this conversion in the absence of air, the biomass is stored in a bin until the reactor is at the desired temperatures at the very beginning. Different temperature profiles (equals heating rate of the biomass) can be applied. Afterwards, the biomass is moved by two rotating screws through the heated reactor and because of the absence of air, converted to charcoal. In this process, various hydrocarbons are evolved since they are very volatile, depending on their chemical structure. Since this gas is also combustible, it could be used to heat the furnace wall as well as to operate the carbonization process without any externally provided power. Considerable know-how has been acquired in recent work; therefore, only a short summary is given which describes the carbonization process. Furthermore, it has to be mentioned that all the charcoals used within this thesis were produced with this reactor. This section gives a summary of the recently performed carbonization experiments as well as characterization possibilities and results, along with an interpretation of all these trials. Additionally, the pyrolysis gas is taken under investigation with respect to the condensable as well as non-condensable fraction.

3.1 Charcoal

Charcoal is one of the products in the thermochemical treatment of biomass in the absence of air. Beside this, a volatile fraction occurs during this treatment and can be defined as pyrolysis gas, which is described in Chapter 3.2. Charcoal is known as the first artificial human-made product, since the first cave paintings 40,000 years ago were done using this carbonaceous material. The fields of application in former times were widespread; it is known that further

uses of this renewable resource were cooking and melting of metals. The implementation of charcoal as an energy carrier for the melting or reducing of oxidic ores retained till the production process of coke was applied successfully [69].

The definition of biomass was already given in the introduction of this thesis [13]. In principle, the major components of biomass are hydrogen, oxygen and carbon, as can be seen in Figure 3-4. Beside them, some nitrogen can be found as well as small traces of sulphur. Some inorganic matter is present which consists of Na, K, Mg, Ca in addition to some chlorine. Referring to the proximate analysis of carbonaceous material, these species can be found in the ash fraction. The organic fraction, H, O and C are bond together and can be found as cellulose, hemicellulose and lignin [73; 74]. The exact behaviour of these compounds as well as their behaviour during heating up in the absence of air are described in the following section. Nevertheless, the average chemical composition of various biomasses that were treated in the last couple of years is pictured in Figure 3-4. The analysis methods applied here were already presented in the previous section. Here, a ternary system is shown, similar to ternary slag systems, where each corner represents 100 at-% of H, C and O. Furthermore, the biomass conversion processes are layered to get an idea about the various types of thermochemical treatment. As it is pictured here, due to a carbonization step (labelled as “P” for slow pyrolysis), the amount of hydrogen as well as oxygen is minimized extremely, since biomass is known for its high amount of volatiles, as it can be observed here. By applying the aforementioned technology, it can be stated that the remaining solid gets “purified” with carbon [25; 67].

Taking a closer look at the thermochemical treatments of biomass, the basic principle of each type of biomass treatment can be observed in Figure 3-5. Due to the supply of thermal energy, biomass is heated up and further converted in absence of air. Major steps are the evolution of volatile matter, which can be divided into condensable and non-condensable gases (subsequent chapter). The remaining solid is accumulated by carbon as well as the inorganic matter (ash). Several secondary reactions can occur which are, for instance, polymerization or cracking reactions that lead to a further increase or decrease of each fraction [25; 67].

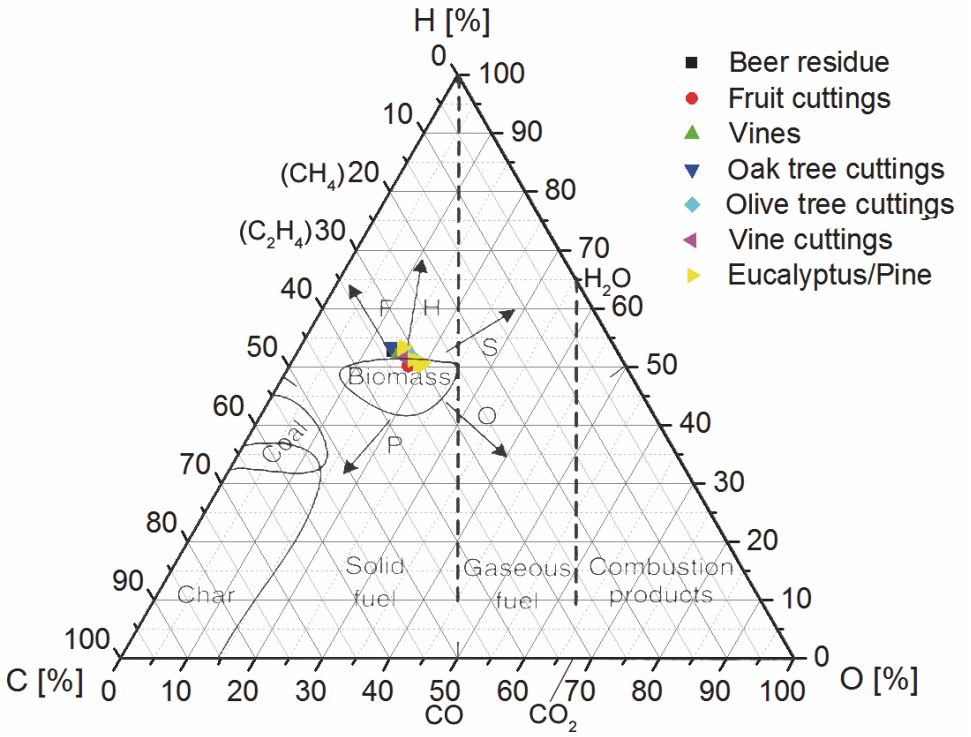

Figure 3-4: Ternary diagram “C-H-O” (in at-%) of several biomasses as well as a second layer representing several biomass conversion processes according to [25]; F = fast pyrolysis; H = hydrogen; S= steam; O = oxygen; P = slow pyrolysis

By varying the initial parameter such as temperature, residence time, heating rate, etc. the quantity and quality of charcoal and pyrolysis gas can be varied. Moreover, it has to be mentioned that the parameter of highest influence for the carbonization of biomass is the raw material itself. Since several theses were written in the past [21; 72], a short summary of their results will be given as well as own results of performed experiments based on the mentioned publications.

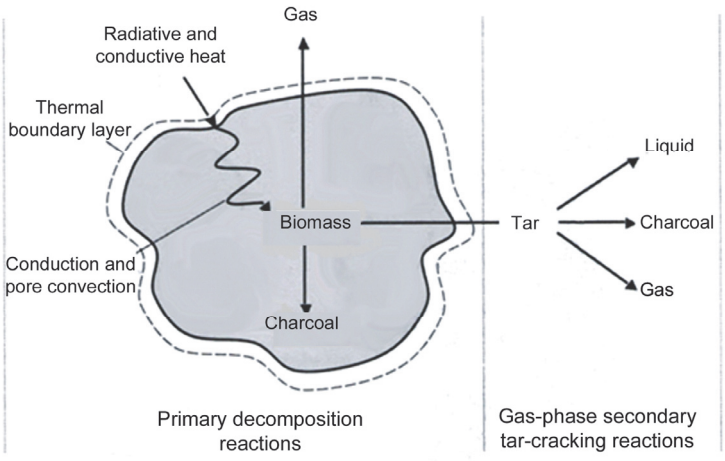

Figure 3-5: Thermal decomposition of a biomass particle under pyrolysis conditions [25]

Beside the fact that the biomass itself influences the result of a pyrolysis, the major impact is the carbonization temperature, as shown in Figure 3-6. Here, all the trials of the recent years are published, beginning with initial trials in the muffle furnace (dotted line). After this batch-

wise process, the semi-continuous production in the “twin screw reactor” was implemented (dashed line). Further optimization was carried out with regards to the ratio of charcoal quality to maximum temperature (solid line). It could be seen that, although the yield decreased significantly at 900 °C, the C_{fix} did not accumulate too much. This was the reason why it was decided that due to this fact and economic reasons, the best range to produce metallurgical charcoal is between 750 and 850 °C.

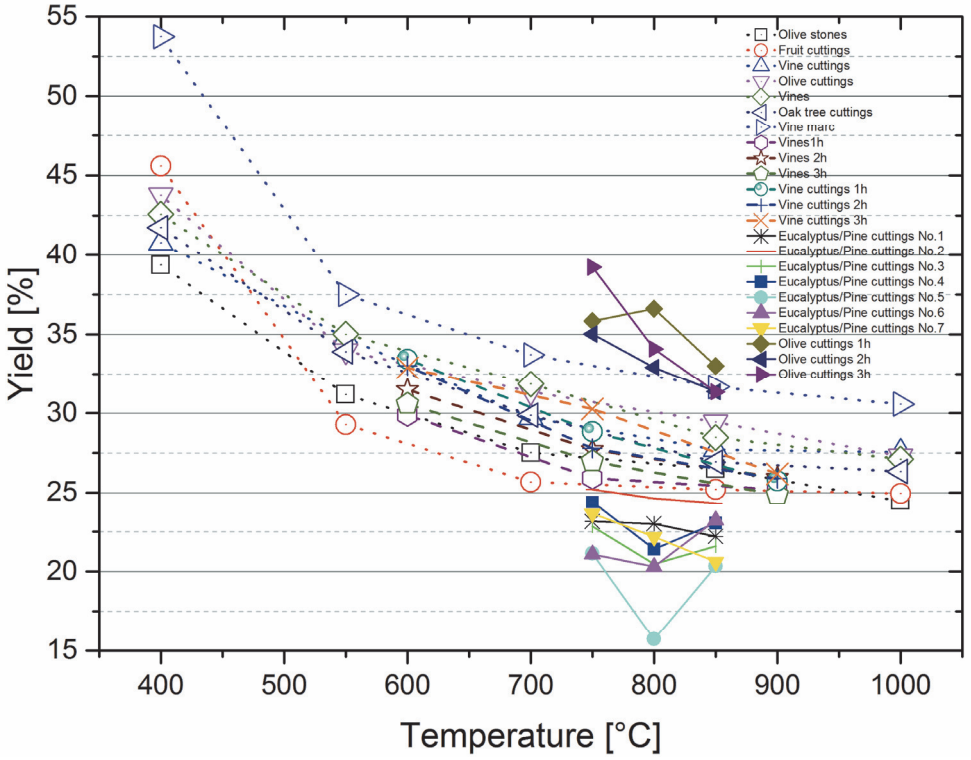

Figure 3-6: Development of the charcoal yield subject to the maximum carbonization temperature; own data and from [21; 72].

In Figure 3-7, the aforementioned progress of the fixed carbon content dependent on the obtained charcoal yield is pictured. Due to the fact that the C_{fix} increases at high temperatures, the charcoal yield is unfortunately rather low. This means that enormous amounts of fresh biomass would be needed to generate a reducing agent that meets the requirements of metallurgical operations. This fact, in combination with the economic reasons, also led to the final decision to lower the maximum carbonization temperature.

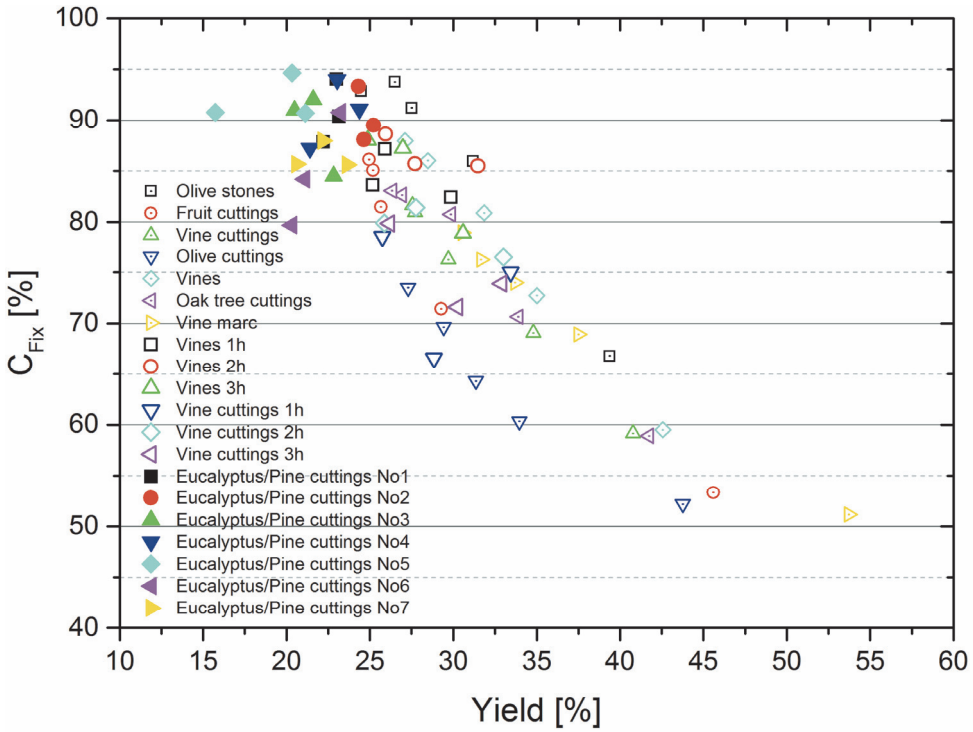

Figure 3-7: Banana-shaped evolution of the fixed carbon content dependent on the obtained charcoal yield; own data and from [21; 72]

Regarding the influencing parameters, various experiments with changing retention times were performed in the “twin screw reactor” to get insight into the behaviour of the yield during the thermochemical treatment. The tests were carried out using biomass from olive cuttings, at a temperature of 850 °C. Unfortunately, the biomass was really inhomogeneous; the woody trunks were mixed with leaves of the trees as well as a high amount of stones. Since it was not possible to remove the small particles, they found their way into the reaction chamber. Therefore, the results concerning the yield have a very high fluctuation rate. Nevertheless, a very slight decrease in the yield at higher residence times can be observed, which means that retention times in-between 0.5 and 2.5 h led to similar yields. With respect to the fixed carbon content, no mentionable impact on the retention time could be observed due to the fact that the input material was very inhomogeneous, as mentioned before. The ash content is accumulated in the charcoal. That means that with an increasing pyrolysis temperature, the relative amount of ash also rises since the inorganic matter is inert to this treatment. In the case of volatiles, the opposite happens. The higher the pyrolysis temperature, the lower the amount of volatile matter; further influences could be observed with varying retention times. With longer retention times, the volatile matter in the charcoal decreases, which is easy to explain since the solid carbon remains in the hot reactor longer. That leads to an extra purification of the carbonaceous material, because the volatile matter has enough time to evaporate at these high temperatures. Moreover, some secondary cracking reactions might occur with the subsequent precipitation of solid carbon, increasing the yield slightly.

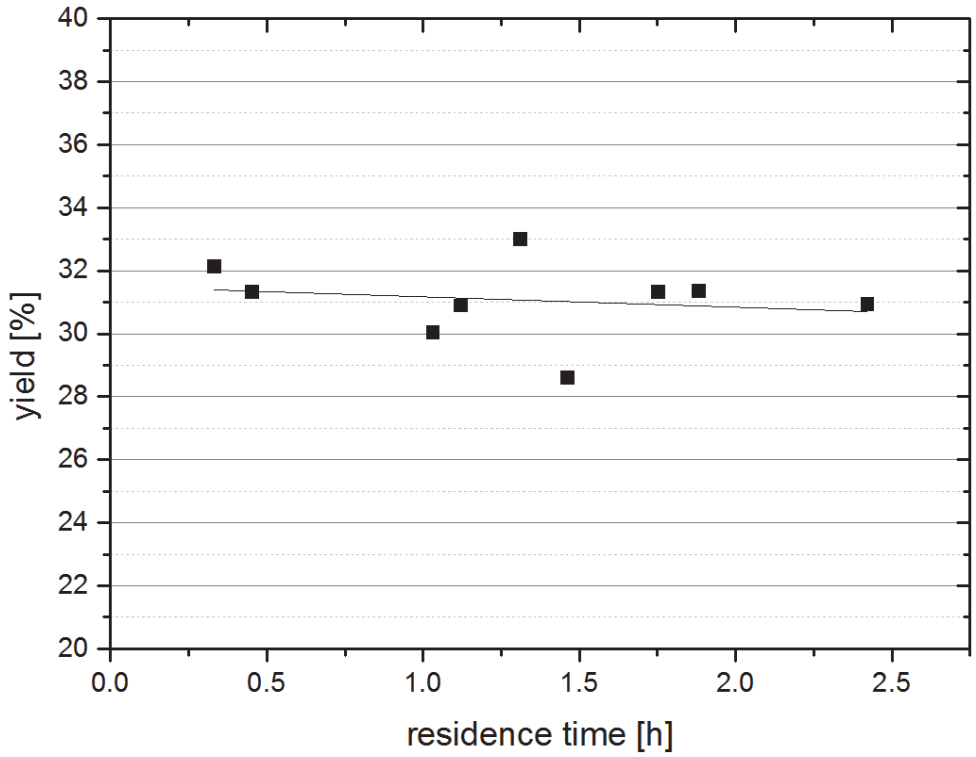

Figure 3-8: Evolution of the charcoal yield at varying retention times in the “twin screw reactor”

Finally, the best parameters to produce charcoal concerning good quality and economics are in-between 700 and 800 °C and retention times of about 1-2.5 h. However, the converted biomass is relieved by hydrogen and oxygen, as it is shown in Figure 3-13 for self- produced charcoals as well as some commercial carbons which may be used in metallurgical operations. What is very interesting is the fact that within this diagram, the evolution of fossil carbons can be observed. Taking the chemical composition and the position in the ternary diagram in Figure 3-13 into account, the biomass is also the origin of fossil fuels, which means high in hydrogen and oxygen. With the subsequent purification which lasts for long periods of time, the chemical composition is shifted to the bottom left corner, increasing the carbon content. This can be easily observed in this figure. The youngest fossil carbon is brown coal, higher in oxygen and hydrogen than stone coal. Further purification to anthracite leads to a decrease in oxygen and hydrogen, as it is shown here and similar to the carbonization of biomass and blast furnace coke for stone coal. Finally, the high quality Desulco® is completely free from oxygen and hydrogen and can be found in Figure 3-13 at the bottom left of the ternary system.

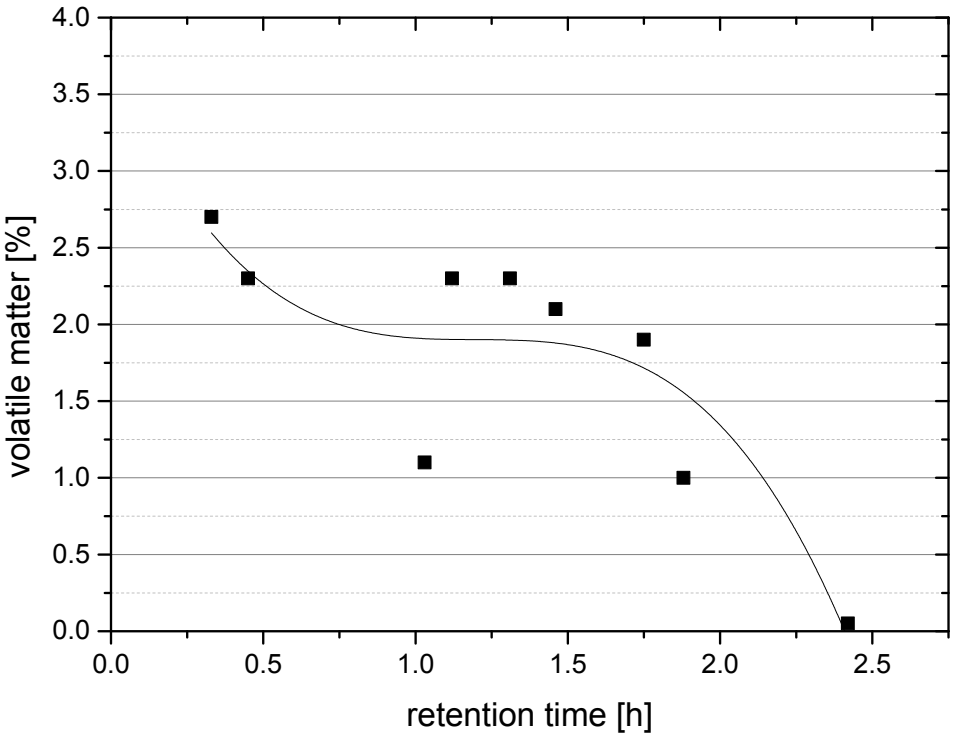

Figure 3-9: Decrease of the analysed volatile matter at increasing retention times

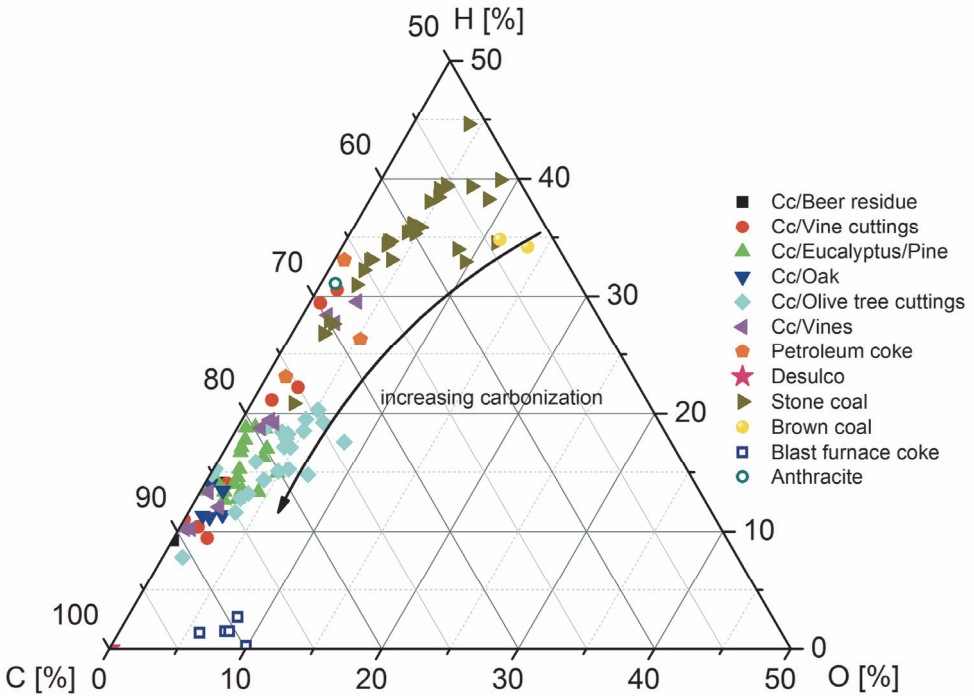

Figure 3-10: Overview of the results obtained in the carburization experiments in the “twin screw reactor” as well as comparable fossil carbons from Chapter 2, according to [25], data from [21; 72] and own experiments

The previously mentioned geological evolution of carbons can be seen in Figure 3-11, where the progress of the ratio of H/C at the ordinate dependent on the ratio O/C at the abscissa of several carbons is pictured. This diagram was first used in “Coal science” and is named after its inventor – van Krevelen [25; 75]. This diagram was originally used to characterize fossil carbons concerning their quality and further utilization. In the subsequent figure, the results

obtained as well as other carbon carriers pointed out in this thesis were plotted according to van Krevelen. It can be seen that the charcoal obtained from the biomass residues is high in quality, as already stated referring to the ternary diagram.

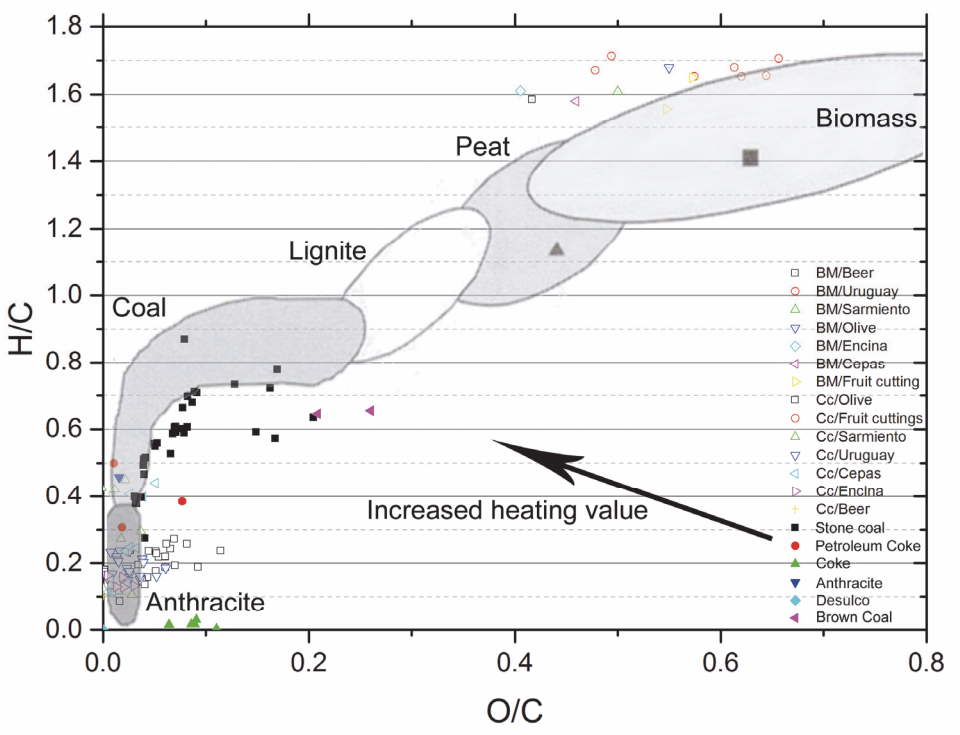

Figure 3-11: van Krevelen diagram with own used biomass/charcoals as well as carbonaceous material from literature provided in Chapter 2, from [21; 72] and own literature, diagram according to [25; 75]

Finally, the influence of the pyrolysis temperature on the specific surface area of the charcoal should be discussed. It can be seen in Figure 3-12 that the surface area increases between 600 and 750 °C. This behaviour can be associated with the decrease in volatile matter within the biomass, leaving a porous structure behind. Surprisingly, after reaching a maximum at 750 °C, the specific surface area decreases. According to [76; 77], it can be stated that due to a further increase in the pyrolysis temperature, the structure of the charcoal is destroyed, resulting in a decrease in the specific surface area.

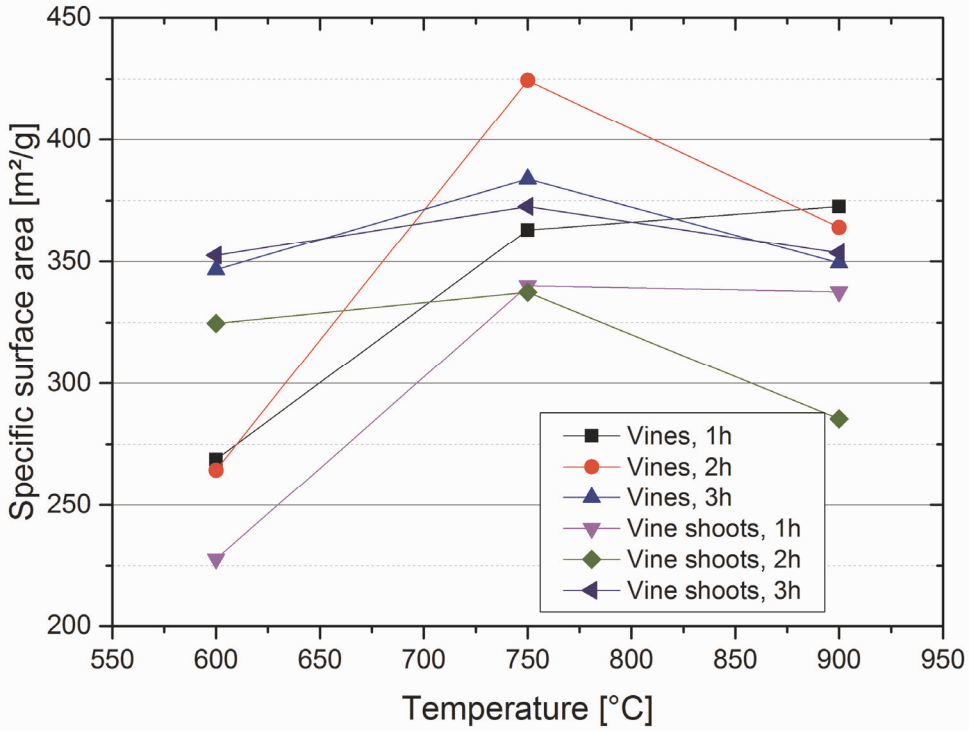

Figure 3-12: Evolution of the specific surface area subject to the pyrolysis temperature as well as the retention time of the biomass/charcoal [72]

3.2 Pyrolysis gas

As already stated, the second product group obtained during pyrolysis is the gas fraction. Biomass releases a huge variety of different gases during its conversion into charcoal, which have to be characterized according to their utilization as a reducing agent or fuel gas. Due to an equivalent value of hydrogen, carbon monoxide as well as hydrocarbons (C_xH_y) within the pyrolysis gas, there is an available reducing potential that should be investigated in order to obtain basic knowledge in this field. The main question, among others, is the chemical composition of the gas fraction that is produced during the carbonization process of the biomass/charcoal. Further thermo-chemical calculations in terms of heat value and volumetric flow should give a rough overview as to whether this type of gas can serve as a reducing agent in metallurgical units.

3.2.1 Characterization of the gas fraction

In principle, the gas fraction obtained during a pyrolysis/carbonization process can be divided into two separate groups; the non-condensable gases (also known as “permanent gas”) and the condensable ones (“tars”). Permanent gas is really easy to determine since it consists of mainly H_2, CO, CO_2 and CH_4. Here, the volumetric composition can be investigated very easily using e.g. infrared, thermal conductivity and paramagnetism, as it is available at the Chair of Nonferrous Metallurgy. Unfortunately, the tar fraction causes problems, especially if a continuous sample taking and subsequent analysis are considered. Moreover, a prediction of

the tar fraction using thermodynamic programs is not successful, as the evolution of non-condensables is a result of kinetic processes [78]. This was the reason why the experiments performed in the following section were executed with the assistance of the “DBFZ – Deutsches Biomasse Forschungszentrum,” which has knowledge and the appropriate equipment in the field of biomass conversion [79].

3.2.1.1 Permanent gas

Permanent gas, which is also known as non-condensable gas fraction, mainly consists of H_2O, H_2, CO, CO_2 and methane. Smaller amounts are light hydrocarbon like C_2H_6 or C_2H_4. When applying the continuous gas measurement unit ABB EL3000 series that is available at the Chair of Nonferrous Metallurgy, attention has to be paid to the estimated gas composition. Especially when measuring a gas fraction which also consists of hydrocarbons, cross influences will occur that lead to a slight increase in the accuracy of the values received by the measurement unit. However, three types of physical principles are available to determine the volumetric composition of a gas at the Chair:

- Infrared spectroscopy (CO, CO_2, CH_4)
- Para magnetism (O_2)
- Heat conductivity (H_2)

Unfortunately, the moisture (H_2O) content cannot be measured online using this device, since the water condenses in the pipes which forward the trapped gas to the gas analyser. Basically, the liquefaction of water could be avoided by the application of a heated pipe, but the maximum temperature in the measurement unit is limited to low temperatures, so a condenser must be applied to remove the H_2O. The only possibility to get information with regard to the water moisture content is to carry out preliminary experiments in a TGA (thermogravimetric analysis) to estimate the summarized content of moisture, or to condense the whole gas fraction in advance and to separate the water from the liquid fraction. Finally, the water amount can be estimated gravimetrically.

However, although there were remarkable problems regarding sampling and its accuracy, comparable results were obtained, which will be explained below. First of all, and very similar to the solid product, the influencing parameters are generally:

- Raw material (biomass)
- Temperature
- Retention time

With regard to the raw material, the highest influence on the average chemical composition of the pyrolysis gas could be evaluated. Since the amounts of cellulose, hemicellulose as well as lignin in the raw material are responsible for gas evolution, the resulting yields of the solid and gas fraction are quite varying. The reason is the interaction of these three hydrocarbons with each other, resulting in various decomposition and polymerization reactions, as it can be observed in Figure 3-13 for four different carbonized biomass residues.

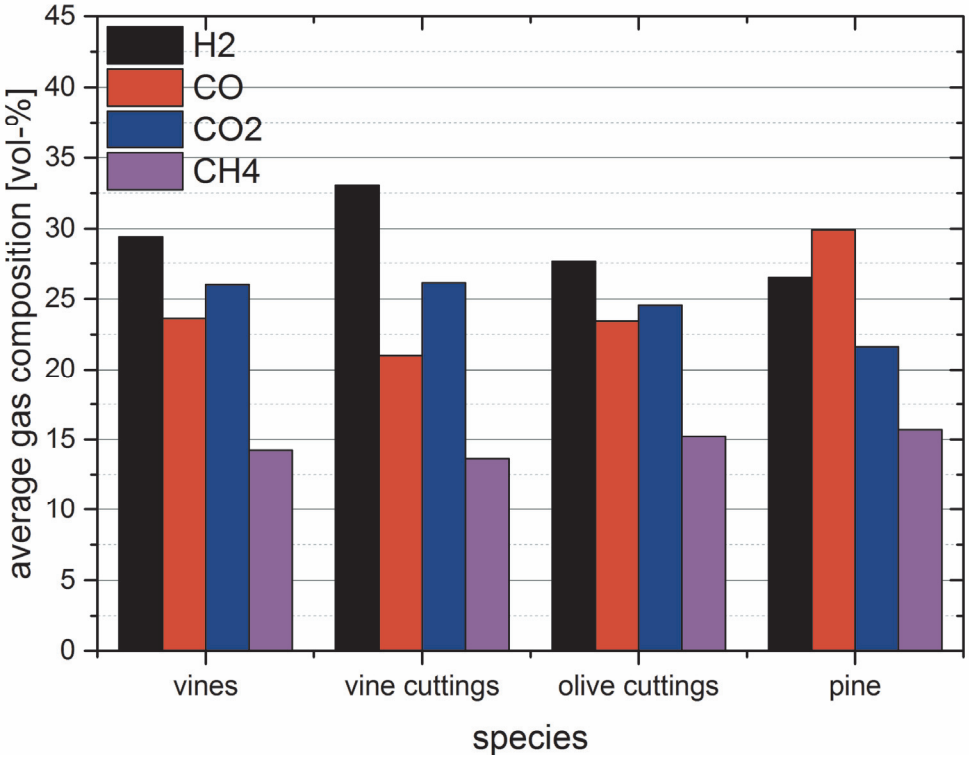

Figure 3-13: Influence of the raw material (biomass) on the average gas composition at a pyrolysis at 850 °C maximum temperature and retention time 2 h

Figure 3-14 shows the influence of the retention time of the biomass/charcoal in the reactor on the average composition of the non-condensable fraction. It can be seen in this diagram that especially “fast” pyrolysis (<0.5 h) leads to a formation of CO_2 and CH_4. It is obvious that this can be related due to the little time for the gas formation, since especially short retention times lead to the production of longer hydrocarbons (bio-oil production), which is expressed in a decrease in the CO_2 and CH_4 amounts. Longer retention times force the heat transfer in-between the reactor (source of heat energy) and the carbonaceous material. This leads to an increase in the CO and H_2 formation because of the fact that the production of tars is just a matter of kinetics. This means the long chained hydrocarbons as well as CO_2 and CH_4 are cracked at longer residence times and reformed, respectively, resulting in a higher yield in syn-gas, as pictured in Figure 3-15.

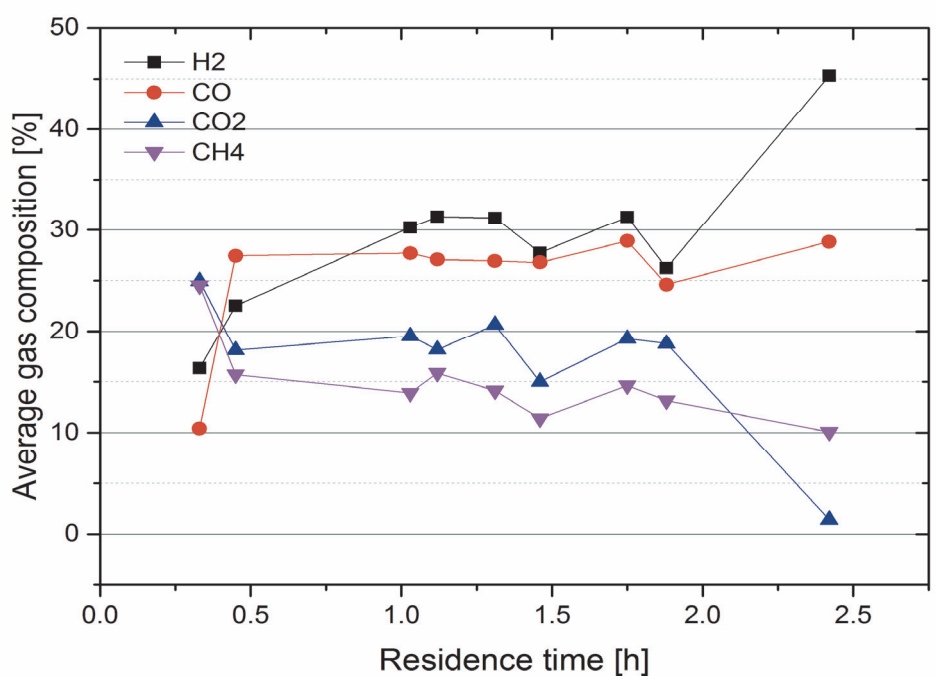

Figure 3-14: Evolution of the gas composition at varying retention times at the pyrolysis of olive tree cuttings, 850° C

Syn-gas (synthesis gas) is usually a mixture of H_2 and CO, but can also contain other reducing agents. This gas could serve as a reforming agent for further gas optimization or for combustion as well as for metallurgical purposes. Especially in the field of the direct reduction of iron ore, synthesis gas is required to reduce the oxidic input material. Technologies like MIDREX, HYL/Energiron, FINMET and Circored can be named as typical representatives in this field of direct reduction. Principally, the metallurgical procedure is based on the utilization of shaft furnaces or fluidized bed reactors to produce direct reduced iron (DRI) or hot briquetted iron (HBI) [80–83].

However, the syn-gas concentration at varying pyrolysis gas temperatures and different biomass is shown in Figure 3-15. As already mentioned, the syn-gas yield increases with higher temperatures, the reason being the cracking of long chained hydrocarbons at such conditions, forming additional H_2 and CO in the pyrolysis gas.

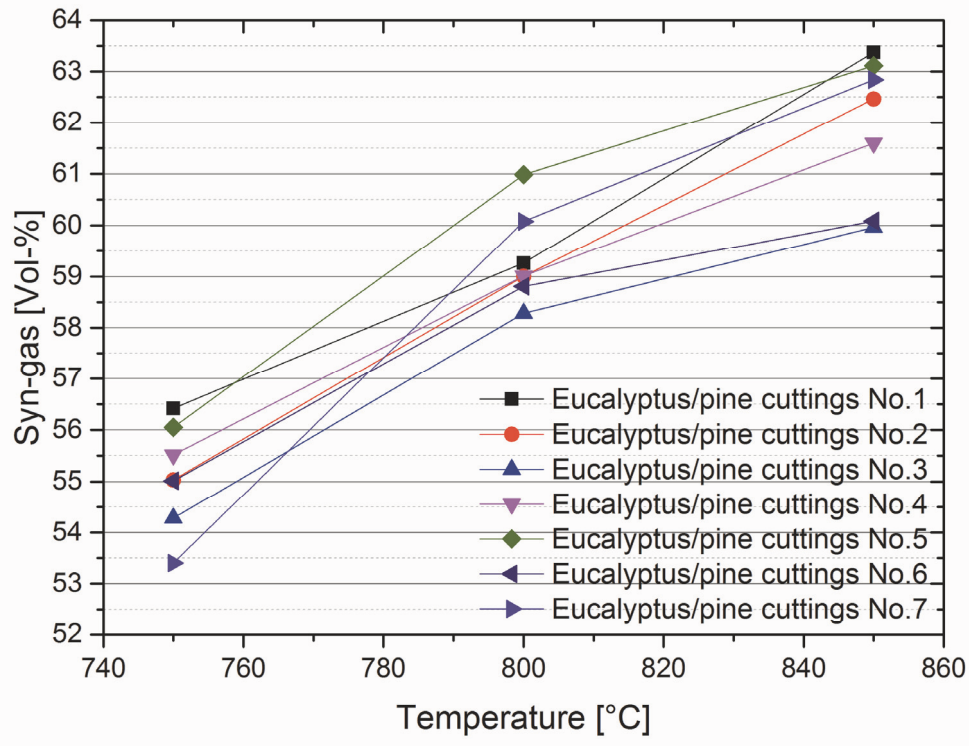

Figure 3-15: Overview of the obtained syn-gas content (H_2 and CO) at varying pyrolysis temperatures

In the next chapter, the origin and chemistry of the tar fraction will be described in detail, since with the know-how obtained here, the utilization possibilities can be evaluated.

3.2.1.2 Tars

During the carbonization of charcoal, a huge amount of gases are produced, which can be divided into non-condensables and condensables. The last fraction is also known as tar. What is typical for this product is its highly viscous behaviour after cooling down to ambient temperature. Various problems can occur if the condensable part of the pyrolysis gas is treated wrong. Consequently, this chapter should serve as a basis for further decisions as to how to utilize this type of product in a smart way.

As it was already mentioned, the utilization as well as the characterization of tars might cause problems because of their strong sticking behaviour at relatively low temperatures. The reason is their relatively low condensation point which is, in dependence of the species respectively, lower than 400 °C. That means that a tar sample has to be kept at elevated temperatures and/or has to be removed from its origin and immediately forwarded to its analysis. This is the major challenge when thinking of a continuous analysis of a non-condensable fraction that is obtained in a continuous carbonization process, as is the case here.

Different methods are available to determine the chemistry of tars. Two well-known and often approved methods (not standards) are the “tar protocol” and the “SPA method.” The SPA method (Solid Phase Adsorption) was the first invention to take tar samples during the pyrolysis

of biomass. Since this method has several disadvantages, a research group was founded by the European Union for evaluating various methods to improve the technique. This resulted in the tar protocol, which allows a semi-continuous sample measurement but continuous gas analysis under carbonization conditions. Therefore, this newer development was chosen to be utilized as the appropriate method during the carbonization of biomass in the twin screw reactor. In Figure 3-16 the experimental set-up of the tar protocol is shown [84].

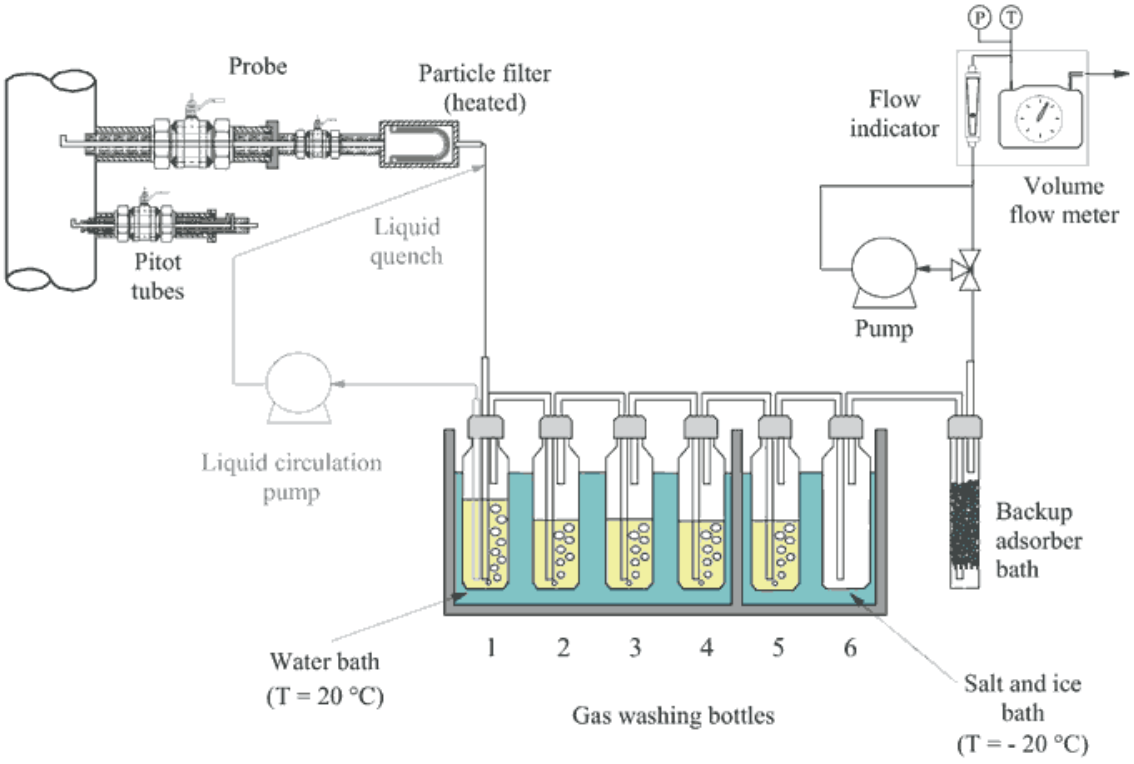

Figure 3-16: Experimental set-up of the tar protocol according to the research group of the European Union [84]

A pump extracts the hot gas by a needle through a diaphragm from the off-gas stream of the pyrolysis reactor. Using a heated plate that keeps the temperature at 500 °C prevents the premature condensation of the condensable fraction. A subsequent decrease in the temperature is done by an iced filter to separate the soot. The following extraction of the tars is carried out with three washing bottles using isopropanol, where the whole condensables are dissolved. Two bottles are used to collect the tar; one is used as the “standby bottle” for unforeseeable events. Finally, the tar-free fraction – basically the non-condensable species from the pyrolysis – leaves the experimental set-up through a dryer, flow meter as well as a gas counting unit. For safety reasons, the exhausted gas is post-combusted and fed to the off-gas system of the building. The samples are sent to the “DBFZ” for sample preparation and characterization regarding the chemical analysis. Because of the uncertainties concerning the species present in the liquid, it was chosen to search for the EPA 16 PAH species since they are well known in any kind of pyrolysis gas [85].

3.2.1.2.1 Literature survey of the chemistry of tar

A short overview of the condensable hydrocarbons obtained during pyrolysis is given in this section. In this part of the report, an analysis of the tar fraction from the pyrolysis of pomegranate seed is cited. The pyrolysis parameters in this scientific publication are almost equal to the ones performed at the Chair of Nonferrous Metallurgy. That means the maximum temperature as well as the retention time of the biomass/charcoal are similar, leading to the assumption that the tar compounds obtained are also nearly equal [86].

In Table 3-1, the different benzene derivates in the tar fraction are given. These species - also known as alkylbenzenes - are basically benzene rings in which one or more hydrogen atoms are replaced by a varying number of alkyl groups (-CH_3) [86; 87].

Table 3-1: Overview of the benzene derivates obtained in the pyrolysis of pomegranate seeds [86]

Benzene Derivates			
Name of compound	Formula	Name of compound	Formula
Methylbenzene	C_7H_8	1,4-Dimethyl-2-(2-methylpropyl)-benzene	$C_{12}H_{18}$
Ethylbenzene	C_8H_{10}	Hexylbenzene	$C_{12}H_{18}$
1,3-Dimethyl-benzene	C_8H_{10}	Heptylbenzene	$C_{13}H_{20}$
Propylbenzene	C_9H_{12}	Octylbenzene	$C_{14}H_{22}$
1-Ethyl-2-methyl-benzene	C_9H_{12}	2,3,5-Trimethoxy-methylbenzene	$C_{14}H_{14}O_3$
Butylbenzene	$C_{10}H_{14}$	Nonylbenzene	$C_{15}H_{24}$
Pentylbenzene	$C_{11}H_{16}$	(1-Methylnonyl)-benzene	$C_{16}H_{26}$
(1-Methylbutyl)-benzene	$C_{11}H_{16}$	Decylbenzene	$C_{16}H_{26}$
		(1-Methyldecyl)-benzene	$C_{17}H_{28}$

In Table 3-2, the analysed phenols in the tar are pictured. Phenols are very similar to the derivates of benzene; instead of an alkyl group, hydroxygroups are attached to a benzene or arene ring [86; 87].

Table 3-2: Phenolic compounds found in the condensable gases during pyrolysis of pomegranate seed [86]

Phenols			
Name of compound	Formula	Name of compound	Formula
Phenol	C_6H_6O	3-Ethylphenol	$C_8H_{10}O$
2-Methylphenol	C_7H_8O	2-Methoxy-4-methylphenol	$C_8H_{10}O_2$
4-Methylphenol	C_7H_8O	2-Hydroxyphenol	$C_6H_6O_2$
2-Methoxy phenol	C_7H_8O2	3-Methoxy-2-hydroxy phenol	$C_7H_8O_3$
4-Ethyl phenol	$C_8H_{10}O$	4-Ethyl-2-methoxy phenol	$C_7C_8O_2$
2-Methoxy-4-propyl phenol	$C_{10}H_{14}O_2$	4-Methyl-2-hydroxy phenol	$C_7H_8O_2$
2-Methoxy-4-(1-propenyl) phenol	$C_{10}H_{12}O_2$	2-Methoxy-4-vinyl phenol	$C_9H_{10}O_2$
2,6-Dimethoxy-4-(2-propenyl)-phenol	$C_{11}H_{14}O_3$	2,6-Dimethoxy phenol (syringol)	$C_8H_{10}O_3$
		2-Methoxy-3-(2-propenyl) phenol	$C_{10}H_{12}O_3$

The acids and esters which are listed in Table 3-3 belong to the fatty acids (or aliphatic monocarboxylic acids) and consist of chains with several carbons [86; 87].

Table 3-3: Results of the GCMS analysis of acids and esters in the tar fraction [86]

Acids and esters			
Name of compound	Formula	Name of compound	Formula
n-Octanoicacid	$C_8H_{16}O_2$	Methyloctanoate	$C_9H_{18}O_2$
n-Hexadecanoic-acid	$C_{16}H_{32}O_2$	Methyl-hexadecanoate	$C_{17}H_{34}O_2$

Table 3-4 gives an overview of the different alkanes which may occur during a pyrolysis process. This chemical compound consists of carbon and hydrogen only, which can be branched or unbranched [86; 87].

Table 3-4: Summary of alkanes of pomegranate seeds obtained at the GCMS [86]

Alkanes			
Name of compound	Formula	Name of compound	Formula
n-Decane	$C_{10}H_{22}$	n-Dodecane	$C_{12}H_{26}$
n-Undecane	$C_{11}H_{24}$	n-Pentadecane	$C_{15}H_{32}$
		n-Hexadecane	$C_{16}H_{34}$

Table 3-5 shows the compounds which contain nitrogen. They can occur in connection with benzene rings as well as in a molecular chain [86; 87].

Table 3-5: List of N-containing compounds detected in the tar in a GCMS [86]

N-containing compounds			
Name of compound	Formula	Name of compound	Formula
3-Methoxypyridine	C_6H_7NO	Hexadecanenitrile	$C_{16}H_{31}N$
1H-Indole	C_8H_7N		

In Table 3-6, the last condensable species which may evolve during a pyrolysis of biomass are shown. Polycyclic aromatic hydrocarbons (PAH) are a molecular system which has more than two benzene rings. They are well known for their carcinogenic behaviour [86; 87].

Table 3-6: Overview of Polycyclic aromatic hydrocarbons in the condensable pyrolysis gas [86]

Polycyclic aromatic hydrocarbons (PAH)			
Name of compound	Formula	Name of compound	Formula
2-Methyl-naphthalene	$C_{11}H_{10}$	1-Methyl-naphthalene	$C_{11}H_{10}$

As seen in the previous tables, the variety of species in the tar is really vast. Therefore, it is important to know how to proceed with the tar after leaving the pyrolysis reactor, if it is not post combusted. This is very important if the environmental legislation and the regulations of the maximum workplace concentration values are taken into account. The evolving chemical compounds are all well known as unhealthy and carcinogenic, respectively.

3.2.1.2.2 Evolution of tar

A high influencing factor is the amount of N, S Cl, K and other trace elements, which are responsible for producing pollutants. As a pyrolysis process is performed during the heating up of the biomass, CO, polycyclic aromatic hydrocarbons (PAH) and soot, together with characteristic smoke markers of pyrolysis such as levoglucosan, guaiacols, phytosterols and substituted syringols are released which are within the tar [88]. As a result, a categorization can be done in four groups depending on the reaction conditions [89]:

- Primary products which are derived from cellulose, hemicellulose and lignin products (like levoglucosan, hydroxylacetaldehydride, furfural)
- Secondary products which are mainly characterized by phenolics and olefins
- Alkyl tertiary products which are mainly methyl derivates of aromatic compounds
- Condensed tertiary products consisting of more or less condensed PAHs

But now the big question is how tar is produced during a pyrolysis/gasification process due to the fact that it is responsible for major issues during the process. The major influencing factor regarding the biomass feed material is the amount of volatiles and the water content in the fresh biomass. The higher the values, the higher the amount of pyrolysis gas and as a result,

the amount of tar in the gas [90]. Typical values occurring during a carbonization procedure in the temperature range of 660 to 800 °C are reported in literature between 1 and 20 g/Nm³ [91; 92].

A good overview of the tar product is given in Figure 3-17, where the primary, secondary and tertiary products depending on the pyrolysis conditions are explained. This means that during a thermo-chemical treatment, the different stages are passed by the biomass, forming the pictured products [93].

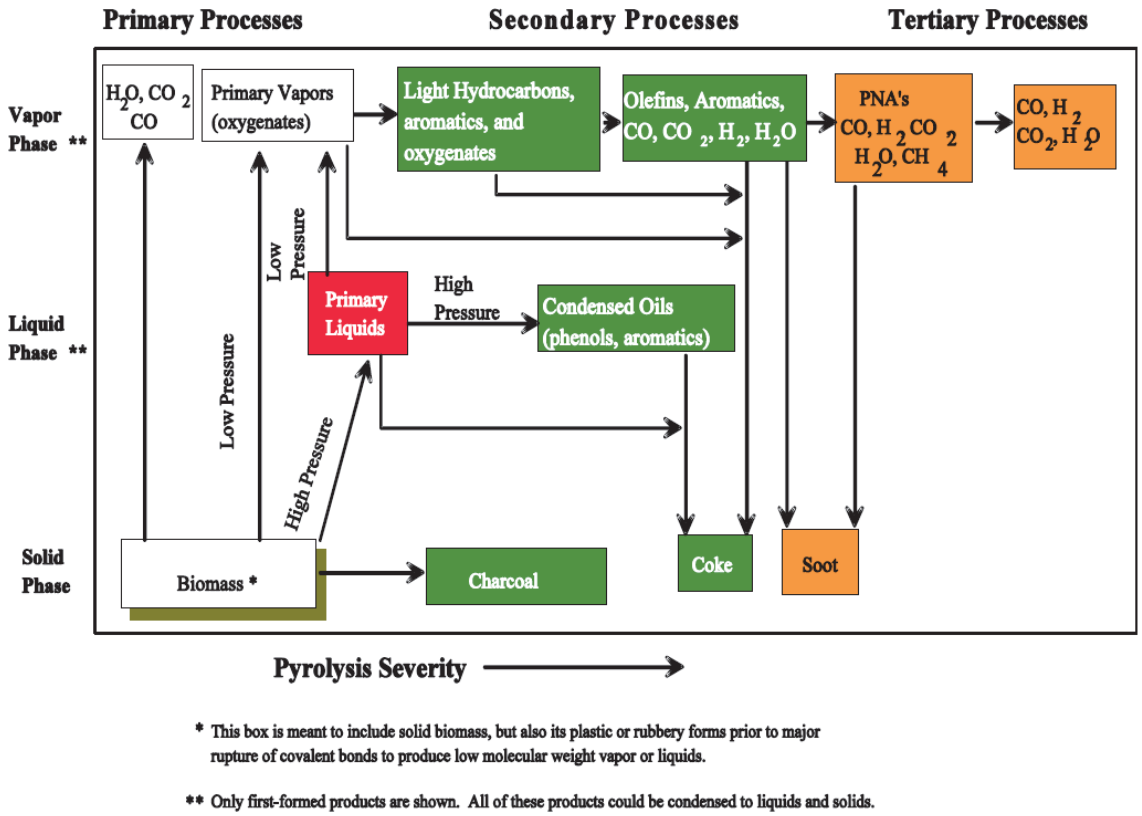

Figure 3-17: Possibilities for gas and tar formation depending on the pyrolysis parameters [93]

A different possibility is given in Figure 3-18, where the maturation of the tar is determined by the pyrolysis temperature [93]. The biomass decomposition at the same time as in this figure can be divided into four stages [90]:

- Evaporation of moisture < 220 °C
- Decomposition of hemicellulose between 220 and 315 °C
- Decomposition of cellulose between 315 and 400 °C
- Lignin decomposition > 400 °C

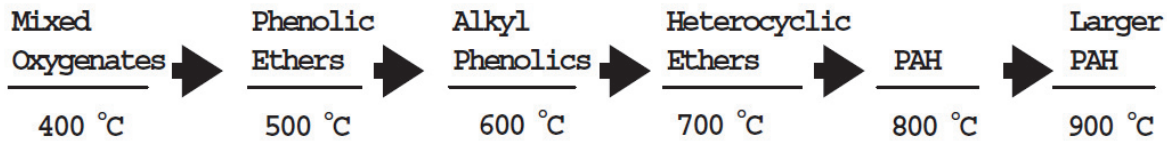

Figure 3-18: Change in the gas evolution during the heating up of biomass with absence of air [93]

Subsequently, the formation of the three different species during the pyrolysis process will be described in more detail.

3.2.1.2.3 Lignin

Usually biomass consists of 20-40 % lignin, depending of course on the biomass type, but it can be said that hardwood contains less lignin than softwood. This fraction consists of different aromatic molecules which lead to the formation of PAHs. The pyrolysis of pure lignin results in (non-condensable) permanent gas, char and condensable tars. The prediction of the distribution of the products is very difficult since the decomposition of this species occurs in a wide temperature range of 100 - 900 °C. The main products in the gas phase are [90]:

- H_2O, methanol
- Phenolics (at least one OH group bond to an aromatic hydrocarbon)
- Gases (methane, ethane, ethylen, propane and carbon oxides)

3.2.1.2.4 Cellulose

The pyrolysis of cellulose takes place in the temperature range of 327-407 °C, where the main product is tar compounds. As the empirical formula of cellulose is $H(C_6H_{10}O_5)_nOH$ (n is variable between 200 and ~10,000), the products are a wide variety of carbohydrates (mostly furans and aldehydes) which are responsible for the formation of tar [90].

3.2.1.2.5 Hemicellulose

This part of the biomass is the least stable polymer. This is the reason why the decomposition during pyrolysis is the fastest (220-315 °C), whereby the remaining char of the hemicellulose is approximately 20 % of the original polymer. The structure is very complex, which is responsible for the bonding of the lignin and the cellulose. The main compounds from the pyrolysis of hemicellulose are methanol, acetic acid, furfural, acetone and C_2, C_3 gases [90].

Taking into account that there is also ash participating the conversion process, the chemical reactions would change, since some of them (especially sodium and potassium) may act as a catalyst. As an example, the products would change in their amount, creating new chemical compounds, as it can be seen in Figure 3-19 [88]:

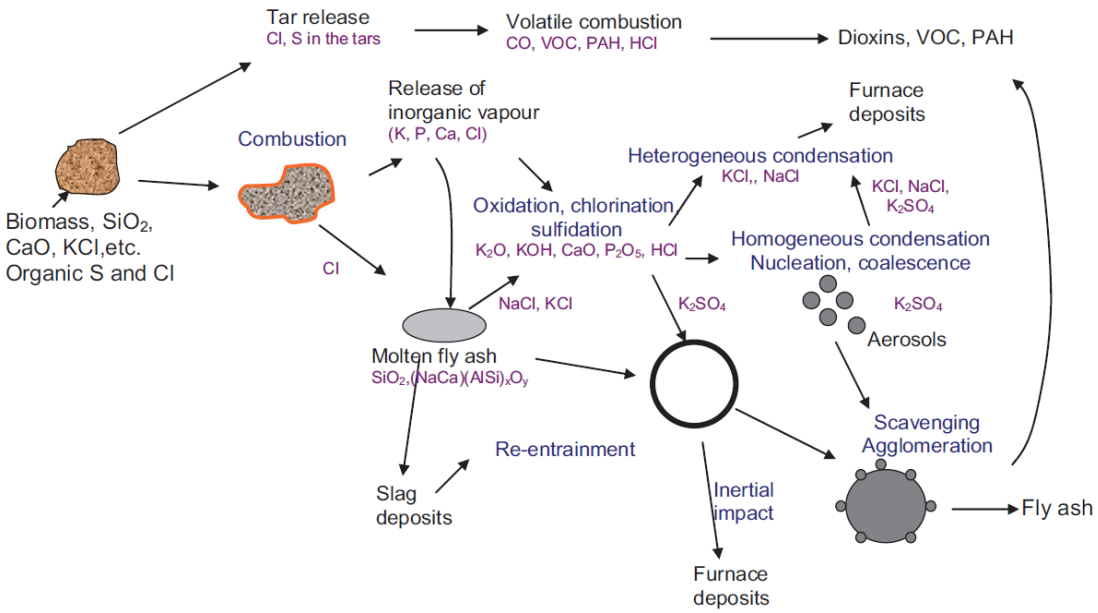

Figure 3-19: Tar, gas and fly ash evolution in incomplete combustion, which can be compared with a pyrolysis process [88]

3.2.1.2.6 Tar removal

There are also different methods available to reduce and control the tar concentration in the pyrolysis gas, which should be mentioned here. The first method – the primary one - is to remove the tars inside the reactor, whereby this technique is only possible with proper adjustment and design of the reactor, which is very difficult to realize. Possibilities are the secondary methods for the controlling of condensable hydrocarbons [90; 94]:

- Mechanism methods
  scrubber, filter, cyclone and ESP
- Self-modification
  similar to primary methods
- Thermal cracking
  drastic increase in pyrolysis gas temperature to 1250 °C and higher
- Catalyst cracking
  tar removal by catalytic reactions using Ni-based, alkali metal, dolomite or novel metal catalysts
- Plasma methods
  destruction of organic compounds with corona discharges

3.2.2 Results

The first step of the measurement of the pyrolysis gas is the removal of the solid particles like soot and other dusts. The amount of these particles was performed during the tar measurement in all trials, between 2.4 and 4.8 g/m³$_N$, which means that the deviation of the

results was in a close range. Furthermore, the overall tar content was measured, where results of tar are obtained from 17.9 to 53.2 g/m³$_N$ [79].

As already explained, the gas was analyzed regarding the 16 polycyclic aromatic hydrocarbons, as they are within the pyrolysis gas and the methods for analysis are standardized and can be performed very easily.

A big disadvantage of this test series was the incomplete analysis of all the hydrocarbons, seeing as 20-30 % of the overall tar fraction was higher hydrocarbons which are not part of the 16 EPA PAH. According to the DBFZ, it was not possible to get more information about these components because it was not part of the contract between the DBFZ and the University of Leoben. Another handicap was that with the described tar separation unit, no water/steam could be obtained, which would also be very interesting, as it would conclude the mass balance.

In order to complete the mass balance, the permanent (non-condensable) gas was measured, whereby very similar results as in previous reports were obtained, as can be seen in Table 3-7. It must be said that the amounts of C_2H_6 (ethane) as well as C_2H_4 (ethylene) were measured [79].

Table 3-7: Average values from the permanent gas measurement [79]

Permanent gas	H_2	CO	CH_4	CO_2	C_2H_6	C_2H_4
Vol-%	36.5	33.3	13.8	18.0	3.2	~ 0

Nevertheless, the results show a very constant tar production during the steady-state gas section of the carbonization process, as it can be observed in Table 3-8 for 1m³ of tar. The values in this table are investigated by the DBFZ and summarized and converted by the author of the related reference, respectively [79].

At last, calculations were performed concerning the heat value of the gas with the program HSC Chemistry 6.1. It was shown that the condensable tar fraction influences the overall heat value in a minor way. The summarized heating value of the gas is 12 MJ/m³ pyrolysis gas at 1000 °C using the data obtained in Table 3-7 and Table 3-8. The released energy amount of the non-condensable gas is about 98.7 % of the total energy output in this case. By comparing the value with e.g. methane (35.7 MJ/m³), the energy available from pyrolysis gas is unfortunately really low.

Table 3-8: Results of the tar measurement with the maximum and minimum values obtained during the experiments [79]

Species		Value [dm³/m³ tar]	
Name	Formula	Minimum	Maximum
Naphthalene	$C_{10}H_8$	165.8	126.8
Acenaphthene	$C_{12}H_{10}$	5.9	5.7
Acenaphthylene	$C_{12}H_8$	216.9	196.2
Fluorene	$C_{13}H_{10}$	84.7	82.0
Phenanthrene	$C_{14}H_{10}$	203.4	188.7
Anthracene	$C_{14}H_{10}$	69.8	60.6
Fluoranthene	$C_{16}H_{10}$	81.2	77.0
Pyrene	$C_{16}H_{10}$	79.1	76.2
Benz(a)anthracene	$C_{18}H_{12}$	28.9	23.3
Chrysene	$C_{18}H_{12}$	28.0	24.8
Benzo(b)fluoranthene	$C_{20}H_{12}$	11.0	9.1
Benzo(k)fluoranthene	$C_{20}H_{12}$	21.1	18.2
Benzo(a)pyrene	$C_{20}H_{12}$	30.4	28.1
Dibenz(ah)anthracene	$C_{22}H_{14}$	2.3	2.2
Benzo(ghi)perylene	$C_{22}H_{12}$	11.1	10.1
Indeno(1,2,3-cd)pyrene	$C_{22}H_{12}$	18.6	14.7

Table 3-9 gives insight into a part of the calculation of the heat value of permanent gas. Assuming that 100 % of this gas is combusted in an oxygen containing atmosphere, an energy of 11.74 MJ/m³ is released at an agreed temperature of 1,000 °C, if the products of the combustion are CO_2 and H_2O (except in the combustion of H_2, CO as well as CO_2; here the products are H_2O and CO_2, respectively). Furthermore, the heat energy of methane is marked for comparison purposes, since this species is the major component in natural gas.

Table 3-10 shows the calculation of the heat energy in the combustion of the condensable fraction as well as the final heat value obtained with the addition of the two sums (condensable and non-condensable species).

Table 3-9: Part of the combustion calculation of the permanent gas fraction

Species	Vol-%	m³/m³	MJ/m³ (Species)	MJ/m³
H_2(g)	36.5000	0.35	-1.4808	-0.5126
CO(g)	33.3000	0.32	-1.2321	-0.3891
CO_2(g)	18.0000	0.17	-31.4469	-5.3679
CH_4(g)	13.8000	0.13	-35.6957	-4.6714
C_2H_6(g)	3.2000	0.03	-21.5239	-0.6532
C_2H_4(g)	0.0000	0.00	-28.8705	0.0000
C_8H_{10}(g)	0.0157	0.0001	-14.1342	-0.0021
C_7H_8(g)	0.0649	0.0006	-18.7172	-0.0115
C_6H_6(g)	0.5690	0.0054	-24.3836	-0.1316
	105.4496	1		
Sum				**-11.7393615**

Table 3-10: Calculation of the heat energy of the tar fraction obtained during the pyrolysis of biomass in the “twin screw reactor”

	mg/dm³(Tar(liq))	MJ/m³	MJ/m³ (Species)
$C_{10}H_8$(NPHg)	2671.01	9.34×10^{-04}	-0.0193
$C_{12}H_{10}$(BPHg)	133.55	3.88×10^{-05}	-0.0008
$C_{12}H_8$(ANPHg)	4560.26	1.34×10^{-03}	-0.0346
$C_{13}H_{10}$(Fg)	2149.84	5.62×10^{-04}	-0.0111
$C_{14}H_{10}$(PAg)	5537.46	1.31×10^{-03}	-0.0216
$C_{14}H_{10}$(Ag)	1824.10	4.42×10^{-04}	-0.0079
$C_{16}H_{10}$(FLUg)	2508.14	5.34×10^{-04}	-0.0112
$C_{16}H_{10}$(PYRg)	2442.99	5.19×10^{-04}	-0.0097
$C_{18}H_{12}$(BAg)	977.19	1.79×10^{-04}	-0.0047
$C_{18}H_{12}$(Cg)	977.19	1.79×10^{-04}	-0.0023
$C_{20}H_{12}$(BaPg)	423.45	6.94×10^{-05}	-0.0008
$C_{20}H_{12}$(BkFg)	814.33	1.39×10^{-04}	-0.0026
$C_{20}H_{12}$(BaPg)	1172.64	2.03×10^{-04}	-0.0023
$C_{22}H_{14}$(DBahAg)	97.72	1.47×10^{-05}	-0.0002
$C_{22}H_{12}$(BghiPg)	456.03	7.39×10^{-05}	-0.0010
$C_{22}H_{12}$(I123cdFg)	618.89	1.22×10^{-04}	-0.0024
Sum (Tars)	27364.82	6.66×10^{-03}	**-0.1325**
Sum (Permanent gas + tars)			**-11.8718**

3.2.3 Interpretation of the results

This chapter dealt with the analysis of the gaseous fraction, and particularly the problems occurring with tars. Moreover, the applied techniques how to take samples were mentioned, since especially the condensable fraction is very often the problem due to its sticking behaviour when cooling down.

It can be stated that the main components of the gas phase are H_2, CO and CO_2. Unfortunately, the H_2O content is also very high, but exact values cannot be measured using the applied technology at the Chair of Nonferrous Metallurgy. Similar problems occur if the volumetric flow of the gas should be investigated. Of course, quite a few possibilities using physical methods are feasible (such as the Venturi effect), but were not possible in this case for several reasons. The major problems could be identified, such as the resistance of the measurement units (the pressure gauges) to heat as well as the fact that the “twin screw reactor” cannot be operated at higher pressures, which means if the diameter of the off-gas pipes is reduced (in case of the Venturi-based measurement), the increased pressure inside the reactor is released by “leakage” (e.g. the gap between the biomass chamber and the charging door).

However, the question of the best utilization possibility will be discussed in the following chapter. The main problem of the pyrolysis gas itself is the condensation problem of the tars when reaching temperatures below 400 °C, and in this connection, the sticking problems and further clogging effects by blocked pipes are the major challenge.

3.3 Utilization possibilities

The next pages within this chapter deal with possible utilization and optimization methods of the two fractions obtained after the carbonization process in the twin screw reactor (charcoal and pyrolysis gas). Furthermore, current metallurgical application fields for these two products are described and future utilization possibilities are mentioned.

3.3.1 Charcoal

Previously investigated utilization possibilities for charcoal in metallurgical furnaces could be found in huge quantity in the field of producing pig iron in blast furnaces. Here, in principle, two options are available to use charcoal as an alternative reducing agent. The first one is the utilization of charcoal as the only reducing agent in the furnace. This method was state-of-the-art in the medieval operated ancient furnaces and is still very common, especially in Brazil, in so-called mini blast furnaces, where huge quantities of biomass are still available very cheap. The big disadvantage is the fact that due to the low compressive strength of the charcoal, the heights of these furnaces are limited to relatively low values. The small hearth diameters of

~4 m in this connection lead to a very low metal production in comparison to coke-operated blast furnaces. However, as the iron producing process is very high in the evolution of CO_2, some alternative ways have been developed [95–98].

For instance, blending the fossil coke with charcoal leads to a significant decrease in the effective CO_2 production in steady hot metal production. Quantities up to 20 % charcoal do not influence the sinter or the process performance. Up to the given amount, the maximum sintering temperatures are reduced and the sintering times increase [99–102].

Similar research was carried out in the field of powder coal injection to blast furnaces [44; 99; 103–105]. Since the CSR and coke stability according to ASTM would result in stability too low for coke blends with charcoal addition, the main focus of research in this field should lie on the substitution of fossil fuels in the injection by the tuyeres. In this case, the coal-charcoal blends can reach up to 15 % charcoal, as well. If a total substitution is considered, CO_2 taxes can be reduced by 19-28 %, depending on the blast furnace size and the country of its operation. Unfortunately, the charcoal prices vary tremendously, from very low to very high values, which leads to the conclusion that according to [44], charcoal injection would only be possible in Brazil, and maybe in China, India and the USA, from the economic point of view. For instance, in Western Europe, CO_2 taxes higher than ~100 €/t CO_2 would lead to a reasonable economic process.

Finally, it should be mentioned that the previously performed experiments were carried out using various types of biomass. Furthermore, the pyrolysis conditions (temperature, pressure, retention time and the reactor) varied greatly. The following considerations can be referred to the production of charcoal using the “twin screw reactor.”

The charcoal obtained from trials using the “twin screw reactor” showed promising results regarding its utilization in metallurgical furnaces. The conversion of special types of biomass to charcoal achieved good C_{Fix} values, which is the main goal of those trials. The charcoal produced is definitely suitable for the recycling of EAFDs in the Waelz kiln process, as this was already described in a doctoral thesis [21]. Due to the low strength, the alternative reducing agent will definitely not be used in shaft furnaces, because the reducing agent should have a high compressive strength, which is not the case with charcoals. This means the produced alternative reducing agent will only find its way into metallurgical furnaces when grainy carbon particles are recommended, or it is blended with fossil coke, as mentioned before.

The products obtained in the Waelz kiln are crude Waelz oxide and Waelz slag. Since the slag still contains some valuable metals, a post-treatment of the gained slag should be considered to save resources as well as avoid landfilling. A detailed explanation of these concerns is provided in Chapter 6.2. However, charcoal would be a very good option for a utilization of the

Waelz slag in a submerged arc furnace, as in this type of furnace, an agglomeration step is often recommended anyway. Due to this, a crushing of charcoal with a subsequent mixture with the residue is easily possible, resulting in an e. g. agglomerated self-reducing briquette. A total recovery of the remaining heavy metals is possible with the production of an iron alloy as well as a saleable slag which can be used as the base material for construction purposes.

A second very good option for the utilization of the charcoal in the field of recycling is the so-called iron bath process “2sDR” (cf. Chapter 5), which is part of a modern recycling technique to recover heavy metals from metallurgical residues like dusts and slags. The process itself will be described in detail in the subsequent chapters. Initial trials to generate information about the dissolution behaviour of various carbons in an iron bath were performed in advance in a small-scale heat resistance furnace, since the knowledge achieved here is one of the keys to the success of the process. Results obtained here were used to scale up these trials to approximately 30 kg input material in an induction furnace. Finally, the whole recycling process was designed with regards to the preliminary results. In this last case, a TBRC (top blown rotary converter) served as the furnace to recycle steel mill dusts that have already been heat treated with the utilization of a carbon-containing iron bath.

3.3.2 Pyrolysis gas

For the second (by)-product – the gas fraction – several options are available concerning the further procedure. Of course, the simplest way to get rid of it would be a post-combustion immediately after leaving the reaction chamber. But it is obvious to say that this type of treatment is the most inefficient one. It has to be mentioned that it is very important to keep the obtained pyrolysis gas at temperatures higher than 500 °C. Since the long chain hydrocarbons would condense and cause sticking and blocking in tubes, it is very important to forward the produced gases as fast as possible to the place of their transformation to heat/energy. An optimization would be the energetic use of the pyrolysis gas for heating the carbonization reactor and/or to produce process water. If an alternative utilization of the pyrolysis gas is considered, a huge variety of utilization possibilities are available, which is described within this chapter. However, for metallurgical purposes, the gas might be forwarded directly or upgraded using the methods described below. Since the pyrolysis gas trials gave a good overview regarding the chemical composition of the gas and tar fraction, the pyrolysis gas was used as the burner gas in the TBRC at the Chair of Nonferrous Metallurgy for clinkering crude Waelz oxide (WOX). Therefore, the twin screw reactor is operated simultaneously with the TBRC supplying heat energy in terms of combusting the pyrolysis gas with oxygen using an optimized burner. The detailed experimental procedure as well as the obtained results are described in Chapter 6.1.

Previous studies using this technology can be found at [21]. In this case, a heavy metal-containing residue – Waelz slag – was treated in an externally heated retort to recover the remaining Zn (as ZnO) and to produce metallic iron. The reducing agent was an artificial mixture of H_2 and CO in initial studies; after evaluating the results, the pyrolysis gas generated during the carbonization process was utilized to recycle this residue.

As previously mentioned, the optimization methods for pyrolysis gas are manifold. Among others, the most important ones are described in the following subchapters. All of them have the goal of maximizing the amounts of CO and H_2 to produce synthetic gas that might find its way into metallurgy for reduction purposes.

3.3.2.1 Steam reforming

To destroy the long chain hydrocarbons, water is evaporated and intensively mixed with the hot pyrolysis gas. If the humidity in the biomass is high enough, it might be possible that no water must be added, since the water content in the biomass is sufficient. However, the result would be an increase in the CO and H_2 content in the final gas stream by a cracking process. In general, the theoretical chemical reaction for this process would look like equ. 3-1; if the maximization of hydrogen is the target of the process, a supplementary water gas shift reaction could be added according to equ. 3-2 [106]:

$$C_xH_y + x\,H_2O \rightarrow \left(x + {}^{y}/_{2}\right) H_2 + y\,CO \qquad \text{equ. 3-1}$$

$$CO + H_2O \rightarrow CO_2 + H_2 \qquad \text{equ. 3-2}$$

Although these two chemical reactions run at high temperatures spontaneously, recent research activities are focused on the utilization of several types of catalysts to shift the reaction at lower temperatures to make the process more feasible. Figure 3-20 shows the basic principle of the reactions in equ. 3-1 and equ. 3-2 with the application of a catalytic support [106].

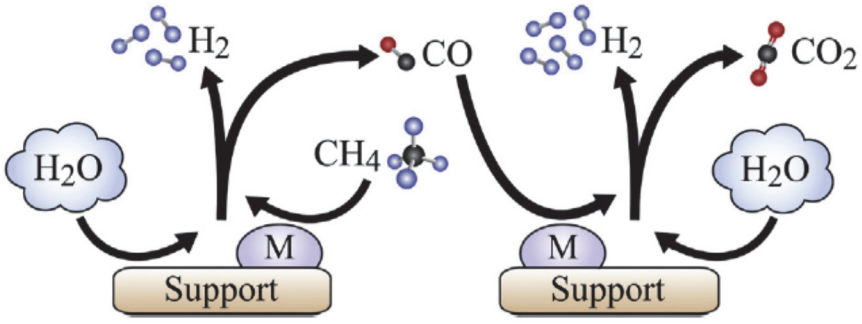

Figure 3-20: Schematic drawing of a steam reforming process of CH_4 with a subsequent water gas shift reaction for increasing the H_2 amount, using a metal catalyst (M) [106]

Several types of catalysts are available, which will be mentioned in the following paragraph since the technology is quite similar.

3.3.2.2 Catalytic upgrade

Catalysts are well known in the field of cracking processes in the petroleum industry, to reduce the amount of long chain hydrocarbons and improve the output of more valuable products. Since the basic principle of pyrolysis gas optimization is comparable, the available types of catalysts were used also in several studies in this field of gas upgrading and tar minimization. Different shapes and modifications of so-called zeolite catalysts are applied that are identified for their cracking ability and to decrease the yield of the liquid fraction. Other already known catalysts are (calcinated) dolomite, alumina, silica and alumosilicates, but the obtained yields are smaller than those received with zeolites. Zeolites are artificial alumosilicates and are formed out of SiO_4 and AlO_4 tetrahedra and are used as catalysts in the petroleum industry. They are considered to be a potential candidate for hydrogen storage in the near future, as well. In this connection, the structure can be improved by cations which may lead to an increased behaviour for the cracking of long chain hydrocarbons and the storage capacity of hydrogen, respectively. It should also be mentioned that especially for the utilization in the field of biomass conversion, nickel was found to be a good option for decreasing the condensable gas fraction. It is mostly plated on several supporters like alumina, zirconia, dolomite, etc., which are also used in the steam reforming of pyrolysis gas [107].

3.3.2.3 Thermal cracking

Thermal cracking is the decomposition of long chain hydrocarbons only by temperature. With increasing temperatures, usually starting at approximately 500 °C, the condensable gases are destroyed by the high energy supply. Among the major influencing parameters – temperature – smaller impacts positively influence the evolution of additional non-condensable gases by secondary pyrolysis reactions. Higher residence times, for instance, lead to a better heat exchange and therefore better cracking. With this, the already explained water gas shift reaction and the methanation reaction lead to a subsequent increase in the gas yield [108–111]. This theory has also been proven by [108] and own studies mentioned earlier.

3.4 Overview of utilization possibilities

Figure 3-21 will give an overview of the applications in the field of EAFD recycling, where alternative reducing agents can be utilized.

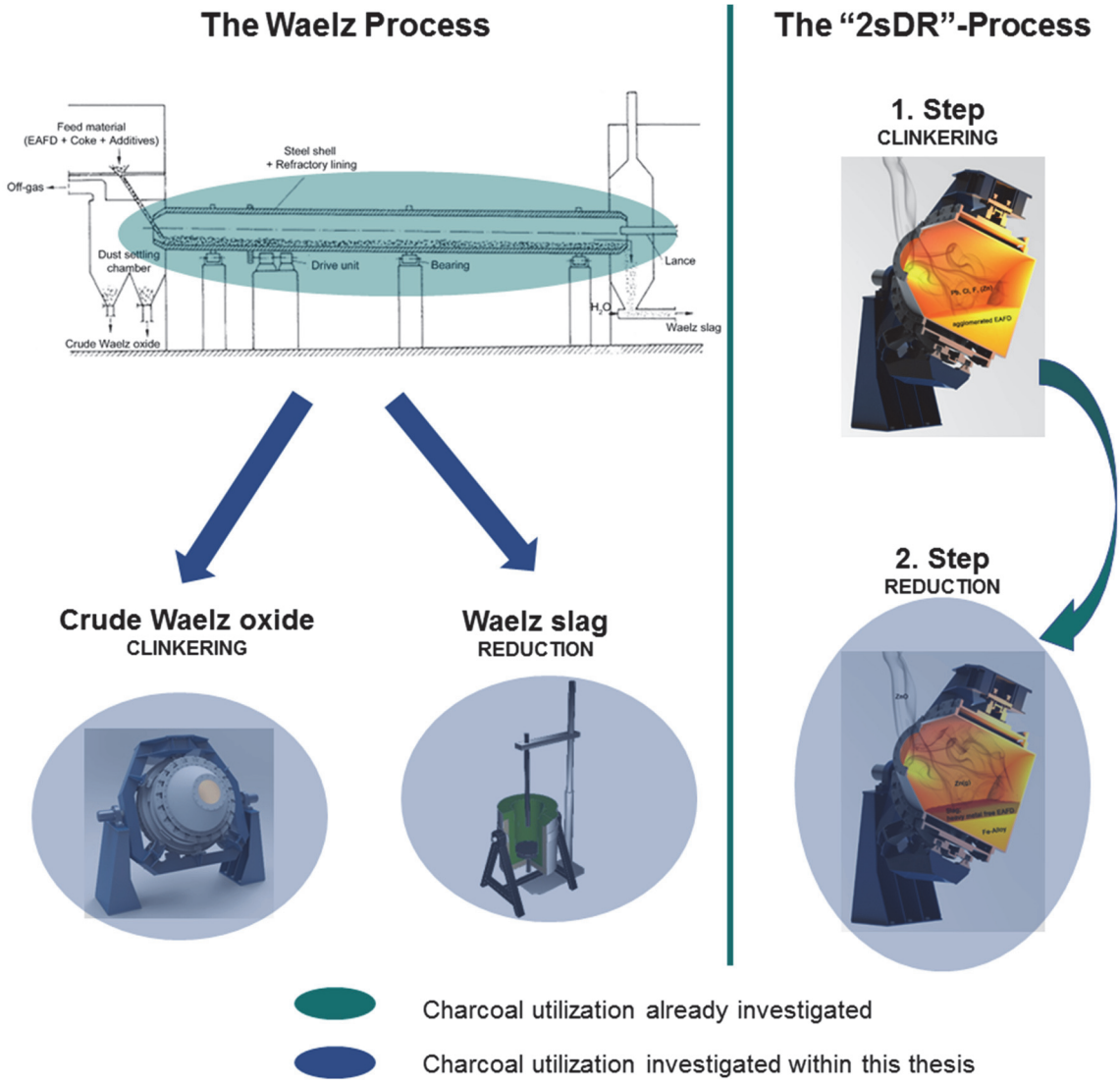

Figure 3-21: Overview on the utilization possibilities of charcoal at the recycling of EAFDs

4 Carburization of iron

The possible utilization of charcoal is the main goal within this thesis. Several experiments in the field of biomass optimization have been performed recently to find some suitable options for metallurgical purposes. The goal of this research is the implementation of charcoal in an iron bath to increase the carbon content, which is called carburization. The high carbon-containing iron produced could be used as a master alloy in the casting industry as well as a reducing agent for zinc and collector of metals like chromium and nickel in the so-called “two step dust recycling” process (2sDR) for the recovery of heavy metal-containing residues, especially steel mill dusts. The first step of the research focuses on the dissolution behaviour of different carbons, especially charcoals with different properties and petroleum coke as well as Desulco®, as a representative of fossil carbons, which is generally used in the casting industry for adjusting the carbon content.

These experiments were conducted at the very beginning using a hot stage microscope, where the carbon served as the subsurface and a small pure iron cylinder was set on its surface. These initial experiments were performed in advance to get information on the general feasibility of the concept. After these successful trials, further tests were carried out in a heat resistance furnace on a small scale, using pig iron granules as the base, with the subsequent addition of carbonaceous material.

Further up-scaling led to the application of an induction furnace, where experiments were carried out at bigger size, using approximately 25 kg of low alloyed steel. The reason for utilizing an induction furnace was the fact that the carbonaceous material would be dissolved easily because of the moving iron bath, which is caused by the induction effect. Furthermore, this type of furnace is able to reach temperatures up to 1,750 °C by applying the appropriate refractory material.

Finally, the results obtained here served as a basis concerning dissolving and burn-off behaviour at the last increase in the experimental set-up. A TBRC (top blown rotary converter) served as a metallurgical aggregate to recover heavy metals like Zn, Fe, and Cr, Ni from dust produced during the melt-down of steel scrap inside the EAF (Electric Arc Furnace).

This chapter will summarize the experiments which were performed in the aforementioned furnaces in the laboratories of the Chair of Nonferrous Metallurgy and at the Christian Doppler Laboratory for Optimization and Biomass Utilization in Heavy Metal Recycling, respectively.

4.1 Theoretical background – carbonization

The experiments shown in this chapter deal with the carburization of an iron bath for a subsequent utilization in a new recycling process to recover heavy metals from metallurgical residues, which will be explained in detail later. The aim of the initial pre-study is to increase the carbon content in an iron melt up to the eutectic point – or in other words – to regions in the iron carbon binary diagram with low melting temperatures, as it can be seen in Figure 4-1.

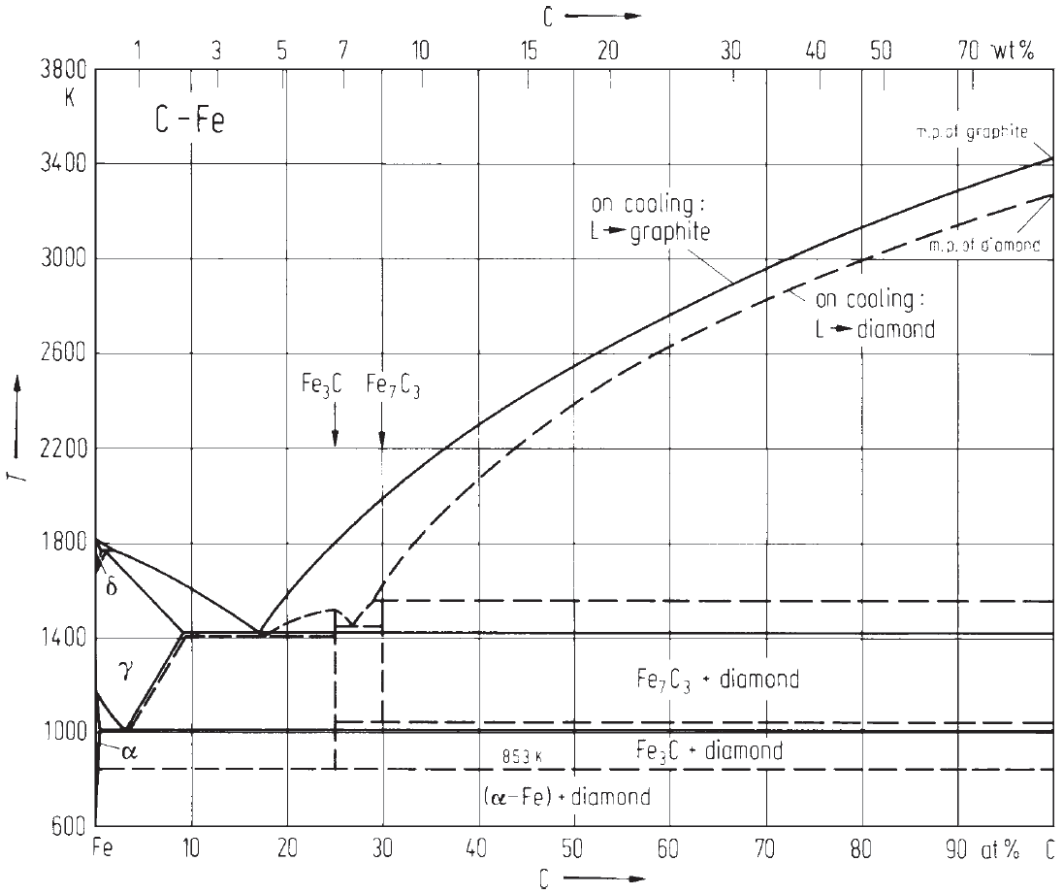

Figure 4-1: “Iron –Carbon” binary diagram [112]

For this, two options are available in this diagram. The first desired carbon content that is more the well-known one, is at 4.302 wt-% carbon in a liquid iron melt, according to the iron-carbon binary phase diagram in Figure 4-2. The second one can be found at higher carbon contents in between the Fe_3C and the Fe_7C_3 phase at around 7-8 wt-% carbon in the metastable system. This increase in the carbon converts the charged pure iron into cast iron related to the requirements of the iron and steel industry. The further increase to higher carbon contents would transform the liquid metal into an unusable material if the liquid iron carbon mixture were solidified. However, since this is not considered in this research, the reduction potential would increase immensely for the subsequent reduction step. An important specification for the reduction of the heavy metal residues is the fact that the lowest carbon content after the consumption of it should not be less than 2.14 wt-%. The melting point of the alloy would

exceed too much and this would lead to avoidable financial expenses due to the high energy demand for smelting. Nevertheless, although the high carbon-containing iron produced would be a possible master alloy in the casting industry, the product will not be utilized in this industry, because of the fact that the applied carburization agent, the charcoal, would not be carbon-neutral anymore. Only if some CO_2 is produced by the reduction of oxidic residues, this neutrality can be guaranteed and therefore, the overall emissions of a metallurgical process can be decreased [112].

In Figure 4-3 the schematic experimental procedure can be seen, using the iron-carbon binary diagram already used in Figure 4-2. In this case, the target was to reach 4.0 % carbon in the induction furnace, charging three times the similar amount of carbonaceous material on the molten surface, resulting in the final carbon content. The loss of material due to combustion by the atmospheric air is excluded, since it would be the result of this investigation. Finally, the material was tapped and forwarded to its analysis by a spark spectrometer.

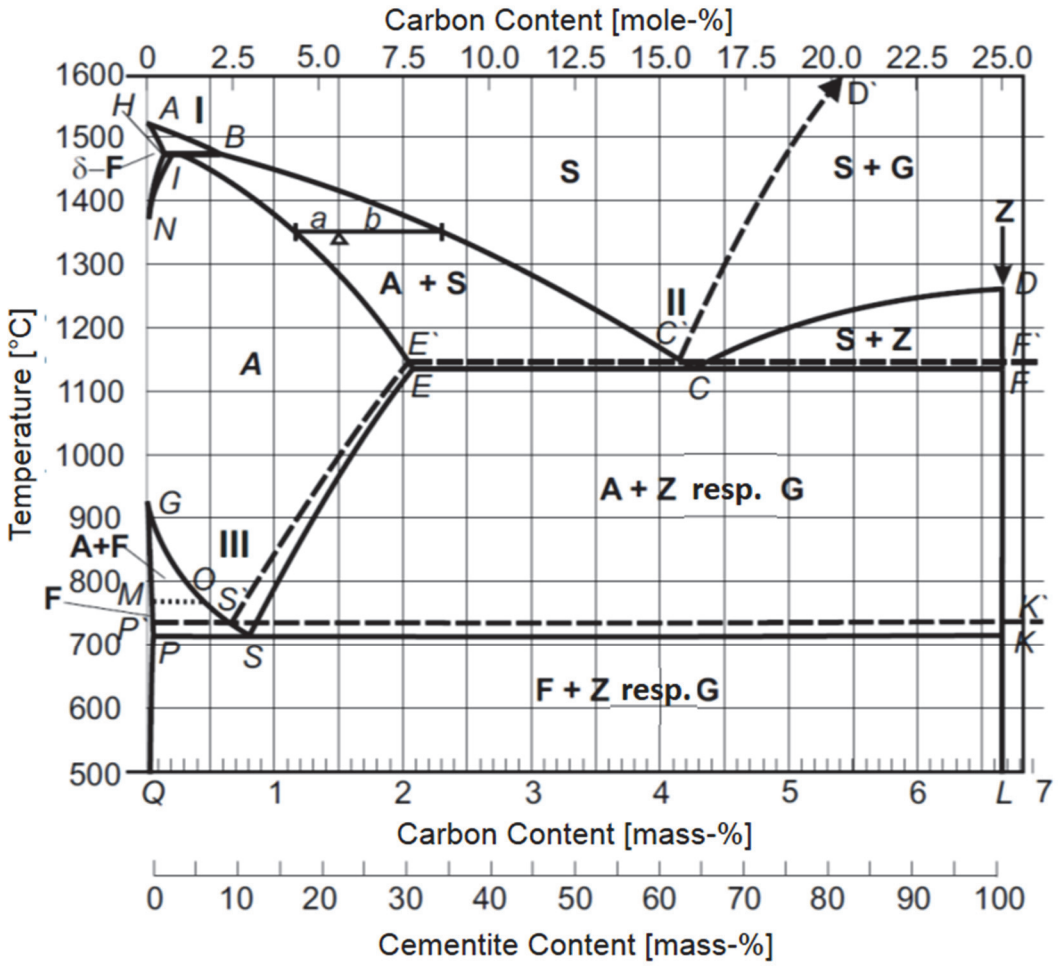

Figure 4-2: More detailed and technical binary diagram “Iron-Carbon” under standard conditions. — Metastable Fe-C diagram; - - - Stable Fe-C diagram; ····Magnetic change; I Peritectic system; II Eutectic system; III Eutectoid transition; *a,b* “law of the lever” for 1.5 % C at 1,350 °C (example) Phases: Melt (S); δ-Ferrite (δ-F); Austenite (A); Ferrite (F), Cementite (Z); Graphite (G); [113]

In the subsequent table, additional information regarding the binary diagram “Iron-Carbon” in Figure 4-2 is given.

Table 4-1: Additional description of the binary diagram “Fe-C” in Figure 4-2 [113]

Labelling in Figure 4-2	Temperature [°C]	Carbon [wt-%]
A	1 536	0.0
B	1 493	0.533
C, C’	1 147, 1 153	4.302, 4.256
D, D’	1 252, 4 000	6.689, 100
E, E’	1 147, 1 153	2.140, 2.098
F, F’	1 147, 1 153	6.689, 100
G	911	0.0
H	1 493	0.086
I	1 493	0.160
K, K’	727, 736	6.689 ,100
M, O	769, 769	-
N	1 392	0.0
P, P’	727, 736	0.034, 0.032
Q	≤ 20	≈ 0.0
S, S’	727, 736	0.758, 0.688

Of course, special focus has to be placed on the properties of the renewable carbons produced for the carburization of iron. According to the requirements of the casting industry, carburization agents should have the following specifications for their utilization in an iron bath [114; 115]:

Carbon content

The value of the carbon in the carbonaceous material should be as high as possible. Commercially used petroleum coke fulfils this requirement, but low-grade charcoal does not. During the last years, a specially developed continuous carbonization process was introduced at the Chair of Nonferrous Metallurgy, which enables the possibility to produce high-quality charcoal with carbon contents up to 95 % to compete with the fossil carbon industry.

Ash content

It is obvious that the ash content within the carbon should be as low as possible since high amounts would have an impact on the dissolution behaviour and there would be something like an undesirable slag formation.

Sulphur

Like the ash content, the amount of sulphur in the carbons has to be very low. In this case, there is a big advantage of renewable carbons over the fossil ones given that there is almost no sulphur within the biomass.

Moisture content

Finally, regarding the moister content, there should be a special focus on this parameter. The reason for this is an energy loss due to the additional energy for evaporation and there might be the fission of water into hydrogen by carbon according to the water-gas shift reaction. This led to a hydrogen-containing and explosive atmosphere.

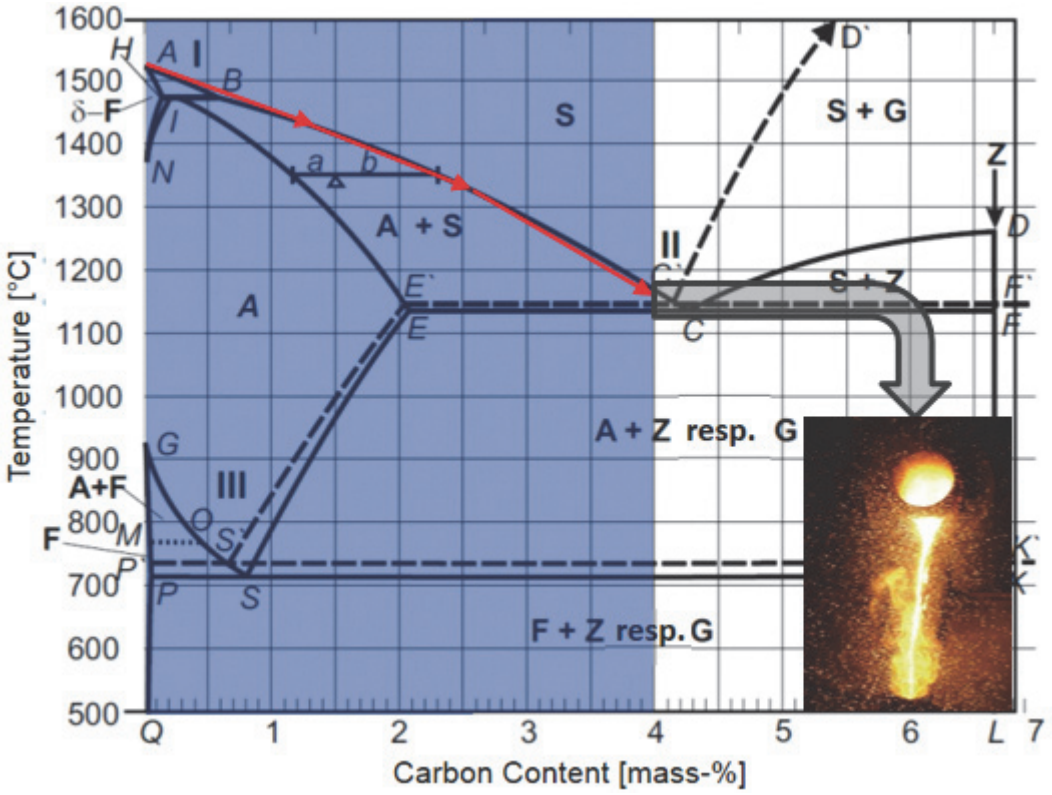

Figure 4-3: Schematic overview of the experimental procedure of the carburization experiments; in this case, the carbon content was increased to 4.0 % using an induction furnace; diagram from [113]

With regard to the experimental procedure itself, some literature was found which dealt with the carburization of various carbonaceous materials. Usually petroleum coke or Desulco® is applied in commercially used cast iron smelters like the induction furnace. This furnace, for example, is a well-known technique to smelt relatively clean iron and steel scraps for the production of high quality cast iron. A carbonization of the molten iron is often mandatory to adjust the correct carbon content, since the input material is low in carbon. Normally, a lot of different solid carbon carriers like petroleum coke, high carbon coke, anthracite and other fossil ones are used commercially. Since the basic idea is to use the dissolved carbon as a reducing

agent in a new innovative recycling process and not for the production of cast iron, attention has to be paid to the possible CO_2 emission occurring in the reduction step of oxidic residues. Due to the fact that fossil carbons are not sustainable concerning the emission of CO_2, the carbonization of iron by the use of charcoal from residues from the agricultural and forestry industry is considered, as already mentioned. The results obtained in the final scale (~25 kg) will be compared with other carbonaceous material where the dissolving behaviour is already known, as shown in Figure 4-4. With this, the subsequent recycling process can be adjusted to the results obtained in these preliminary examinations.

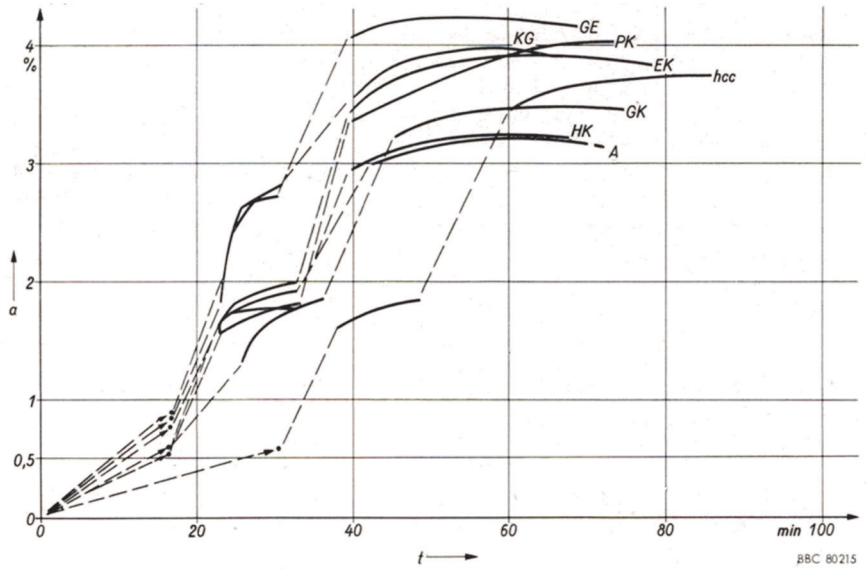

Figure 4-4: Carbonization of steel melts at 1,550 °C with different carbon carriers, a…carbon content of the melt; PK...petroleum coke; GK...gas-coal; hcc...high carbon coke; EK....electrode coal; HK… char carbonized at low temperatures; A...anthracite; GE...graphite electrodes; KG...coal granules [114]

4.2 Experimental procedure

Since the experiments were performed in several furnaces located in the laboratories at the Chair of Nonferrous Metallurgy, a short overview of these facilities should be given as well as some essential parameters.

4.2.1 Hot stage microscope

The hot stage microscope serves as basis for many investigations in the field of metallurgy as well as process optimization. Basically, the microscope consists of three main parts: a light source, the high-temperature heat resistance furnace (T_{max} = 1,700 °C) and a camera, as it is pictured in Figure 4-5. A sample is placed on its sample holder and charged into the furnace. Inside, the material is heated up according to the requirements (heat rate, final temperature). Furthermore, during the heat treatment the sample is flushed by a gas, which could be used to provide an oxidizing, neutral or reducing atmosphere. Due to the increasing temperature,

the cylindrical-shaped sample changes its figure from the cylinder to a sphere, then a hemisphere, until it is totally molten.

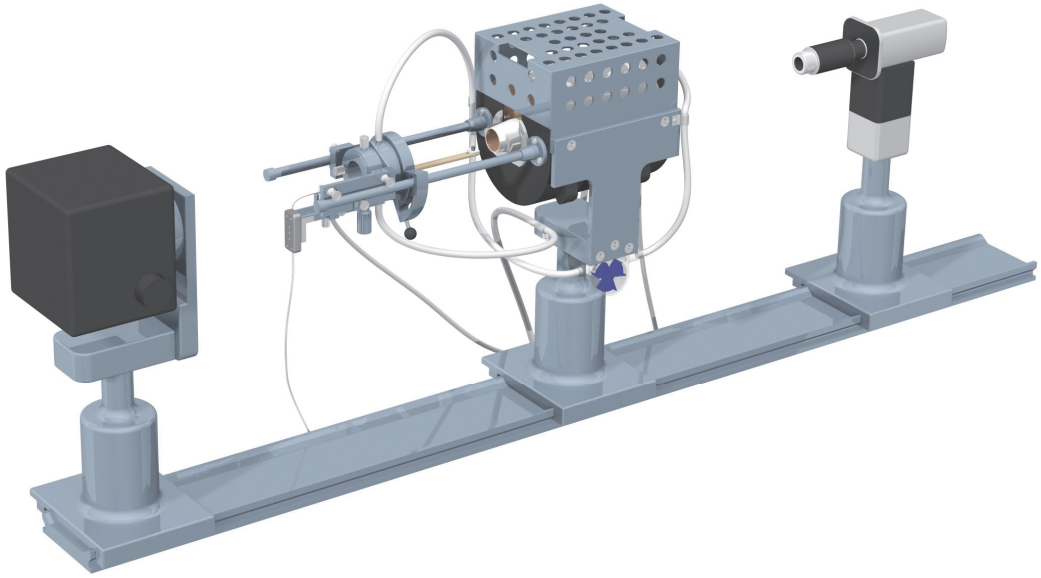

Figure 4-5: Drawing of the hot stage microscope available at the Chair of Nonferrous Metallurgy; the main parts are the light source (left), the furnace (middle) and the camera (right)

The investigated characteristic temperatures of a material are usually:

- Sintering point
- Softening temperature
- Hemisphere temperature
- Melting temperature

The experimental set-up in the case of determination of the dissolution behaviour resulted in the comparison of the estimated softening temperatures. The sample holder was filled with carbonaceous material, as shown in Figure 4-6. The pure iron (chemical analysis, see Table 4-2) was shaped into a cylinder (2 × 2 mm) and set on the carbon surface. The increase in the temperature led to the above-mentioned formation of a sphere as well as a hemisphere, which was later dissolved in the carbon. The softening temperature of the tested carbons should serve as tentative test that should provide information as to whether the charcoal produced is able to substitute the fossil carbons at all.

Table 4-2: Chemical composition of the applied iron

ARMCO © pure iron	C [wt-%]	Mn [wt-%]	P [wt-%]	S [wt-%]	N [wt-%]
Grade 4	0.01	0.06	0.005	0.003	0.005

However, the results obtained showed a definite utilization possibility in comparison to the fossil petroleum coke.

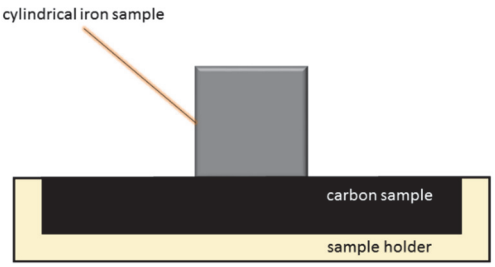

Figure 4-6: Cross-sectional view of the experimental set-up of the sample and the sample holder inside the hot stage microscope

Table 4-3 shows the results of the trials carried out using the experimental set-up as well as the main ash constituents and the theoretical melting point, according to FactSage™.

Table 4-3: Results of the hot stage microscope measurement as well as the major ash components as well as the theoretical melting point according to FactSage™

Name of the Charcoal	Softening temp. [°C]	Al_2O_3 [%]	CaO [%]	MgO [%]	SiO_2 [%]	Fe_2O_3 [%]	Na_2O [%]	K_2O [%]	T_m Fact Sage [°C]
Eucalyptus/ Pine No.2	1,510	0.540	77.510	6.060	2.710	1.840	4.250	1.670	2,400
Eucalyptus/ Pine No.6	1,539	3.230	52.850	11.400	12.420	5.760	3.470	2.900	2,300
Olive tree cuttings	1,491	4.030	23.520	3.130	55.770	4.090	1.340	7.060	1,300
Vines	1,528	3.174	44.074	8.872	17.457	6.830	0.720	3.790	1,850
Pet-coke	1,325	16.920	8.900	1.900	50.180	11.020	1.090	1.400	1,420

As it is shown in Table 4-3, it can be recognized that the lowest softening temperature could be observed applying the fossil petroleum coke. As regards the ash composition, some conclusions can be made in advance. It can be seen that high MgO contents lead to higher softening temperatures. Moreover, high alumina and quartz amounts decrease the softening point. These considerations are based on their specific melting temperature, which is very high in the case of MgO (2,800 °C) and slightly lower, respectively (SiO_2 1,713 °C; Al_2O_3 2,050 °C). If more than three components are investigated simultaneously, a thermochemical software like FactSage™ has to be applied.

The achieved results can be observed in Figure 4-7. In general, the softening temperatures obtained in the hot stage microscope trials correlate with the calculated melting temperatures using FactSage™.

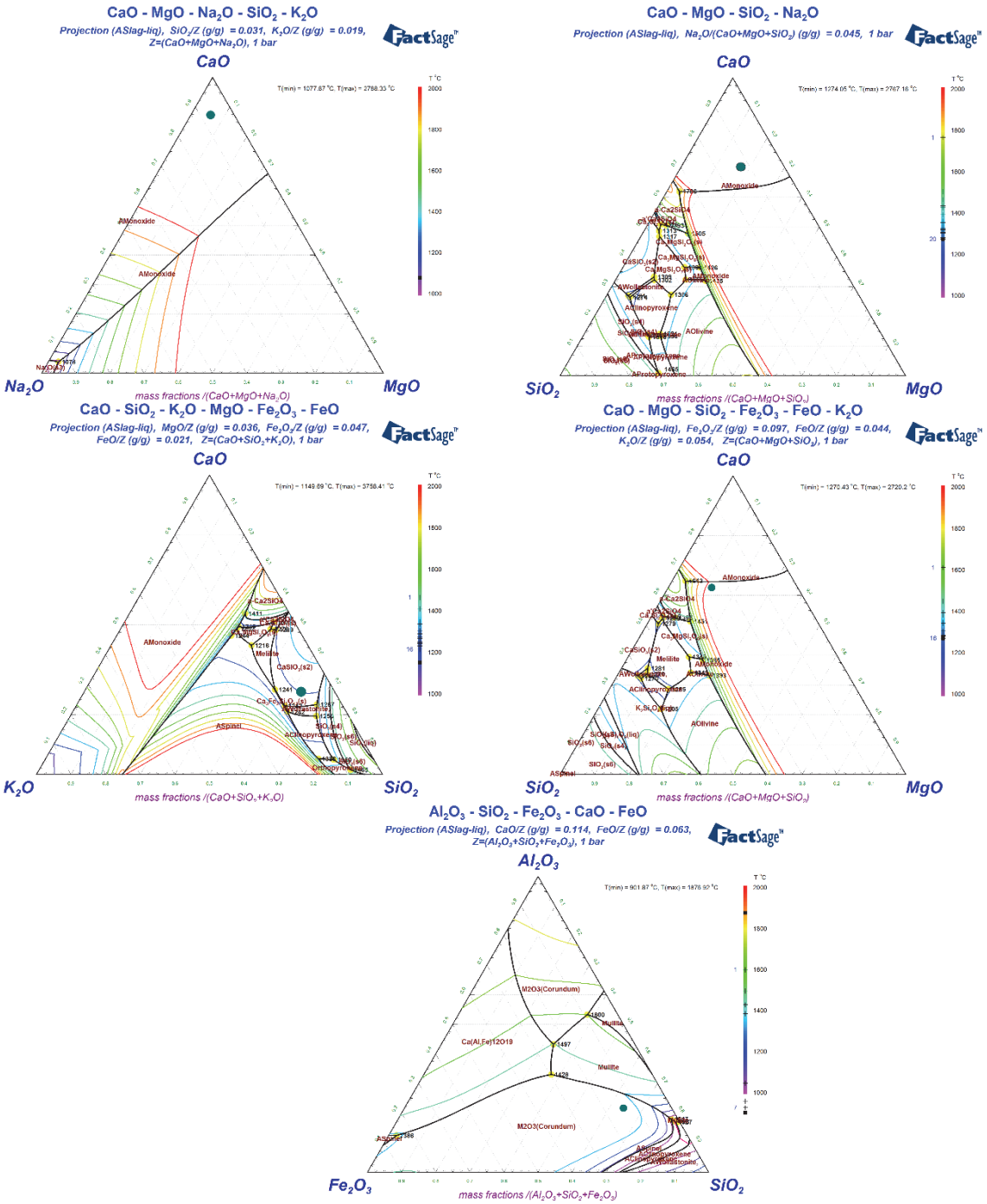

Figure 4-7: Calculated ternary systems using FactSage™. The green dot represents the ash analysis of the carbonaceous material:
top left: charcoal “Eucalyptus/Pine No.2”; top right: charcoal “Eucalyptus/Pine No.6”;
middle left: charcoal “Olive tree cuttings”; middle right: charcoal “Vines”; bottom: “Petroleum coke”

4.2.2 High temperature chamber furnace

Since the previously performed experiments in the hot stage microscope mainly showed the influence of the mineral matter, the trials in the heat resistance furnace should serve as a basis to gain knowledge about the burn-off behaviour of carbonaceous substances in an already carbon-containing iron bath. The furnace type applied is a heat resistance furnace with a maximum temperature of 1,750 °C. Furthermore, the heating rate as well as several holding

temperatures can be adjusted. Figure 4-8 and Figure 4-9 show a photo of the metallurgical furnace utilized, which is also located at the Chair of Nonferrous Metallurgy.

Figure 4-8: High-temperature heat resistance furnace “Heraeus K 1750”

For these trials, pig iron granules served as the raw material, whereby the carbonaceous material was added in advance, due to the experimental set-up. An Alsint crucible was used which was filled with a small amount of granules. Afterwards, a specific amount of carbon was added with regard to the carbon content already available within the pig iron and the fixed carbon content in the carbonaceous material. The crucible was closed with an Alsint cup and the finished mixture was forwarded into the furnace. Afterwards, the furnace was heated to 1500 °C within 3 h and the final temperature was kept for 30 minutes. Finally, the heating elements were switched off and the high carbon-containing iron regulus produced solidified and cooled down until ambient temperature was reached.

The samples were weighted to analyse the increase in the mass and forwarded to their analysis. Here a combustion infrared detection technique from “LECO Corporation” was applied to get information about the carbon content. Unfortunately, a simple spark analysis couldn´t be performed since the carbon content was too high.

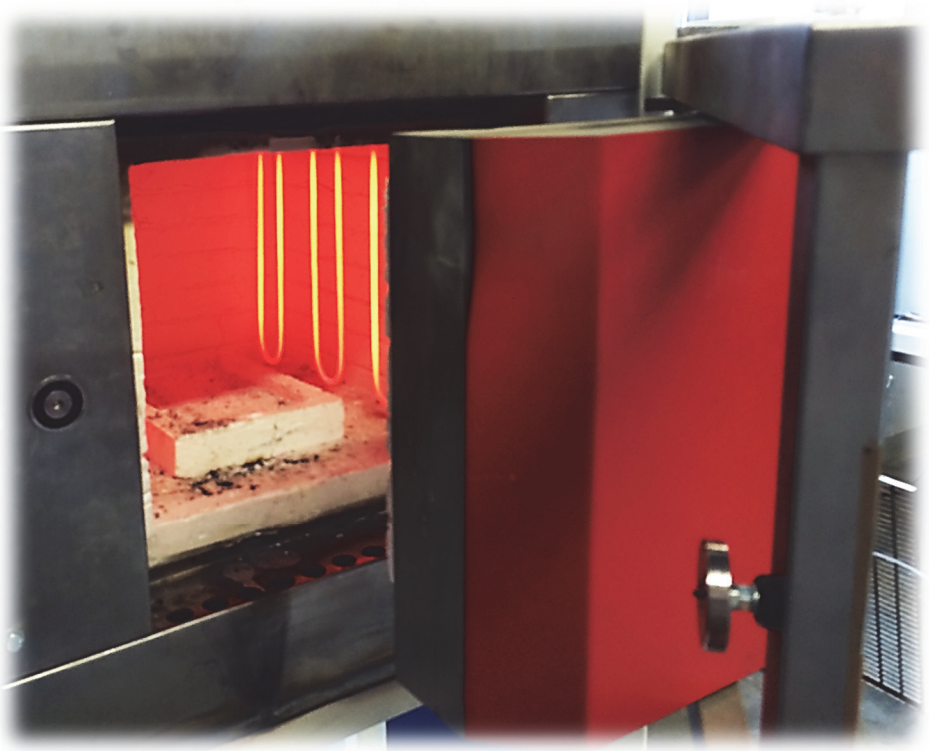

Figure 4-9: Photo of the inside of the applied furnace

Table 4-4 shows the proximate chemical analysis of the applied carbonaceous material. The chemical analysis of Desulco® can be found in Table 2-9. Roughly 150 g of pig iron granules were used and based on this, the necessary carbon amount was calculated to reach the target value.

Table 4-4: Proximate analysis [wt-%] of the used carbons

Carbon	Volatile matter	Ash	C_{Fix}	Moisture
Pine/Eucalytus blend No1	1.75	1.90	93.35	3.00
Pine/Eucalytus blend No2	0.90	6.65	90.80	1.65
Olive tree cuttings	2.19	32.56	60.45	4.80
Pet-coke No1	1.87	1.70	90.65	5.78
Pet-coke No2	10.40	0.34	83.71	5.55

In Figure 4-10, the results of the first trials are shown. The increase of the carbon content in the iron should result in the eutectic composition of 4.3 %. As it illustrated here, the best carbonization result could be obtained with Desulco®, but this is obvious, since this carbonaceous material is especially designed for this purpose. Surprisingly, the Pine/Eucalyptus No. 1-charcoal achieved a very good value, similar to the 2nd subspecies of the biomass. As assumed, the charcoal made from olive tree cuttings delivered a very poor result. Although the crucibles were covered with an Alsint hood, the char was totally exhausted. Concerning the remaining fossil carbons, it could be observed that there was a definite carburization, but the results were not the best. Concluding, it could be seen that a

carburization up to 4.3 % C in an iron alloy using alternative carbons is definitely possible and very promising; of course, the artificial Desulco® especially developed for carburizing purposes delivered the best results.

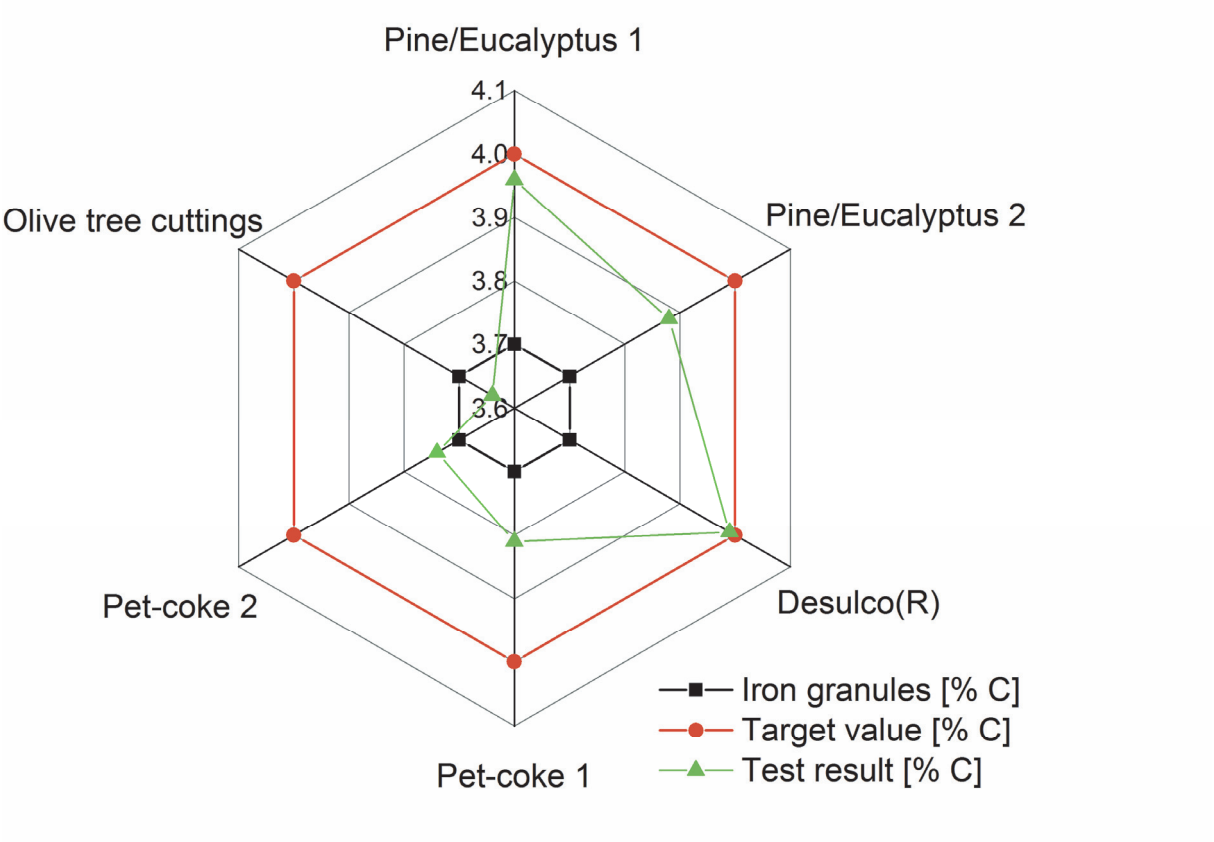

Figure 4-10: Net diagram showing the results of the increase in the carbon content to max. 4.3 % C

Figure 4-11 shows the obtained results of pig iron granules, if a target value of 4.0 % C in an iron alloy is desired. The big difference is that according to the Fe-C diagram in Figure 4-1, the alloy is over eutectic, which means when cooling down, primary cementite is precipitated instead of ferrite. Again, the target temperature was 1,500 °C in the chamber furnace, which should be sufficient to melt the pig iron and dissolve the charcoal supplied.

The results showed quite surprising values, seeing as the achieved carbon yields were in general very low in comparison to those of the first trials. Even the best carburization, Desulco®, was not able to increase the amount of dissolved carbon higher than 4.11 %. Nevertheless, Pine/Eucalyptus No. 1 and 2 again showed competitive results similar to the first trial. An unexpectedly good value was achieved using petroleum coke No. 1, since the carburization yield was much higher than before. Again, petroleum coke No. 2 and charcoal originated from olive tree cuttings could be named as inappropriate for the carburization of iron.

In conclusion, it should be mentioned that the experiments revealed that these tentative tests showed that the maximum carbon content should not exceed 4.3 % C in the iron, according to

the Fe-C diagram the eutectic point. Furthermore, the analysis of the iron alloy was not very easy, since common spark analysing software is usually standardized to maximum contents of 4.3 % C. A “LECO” unit was the only possibility to gain knowledge about the dissolved carbon.

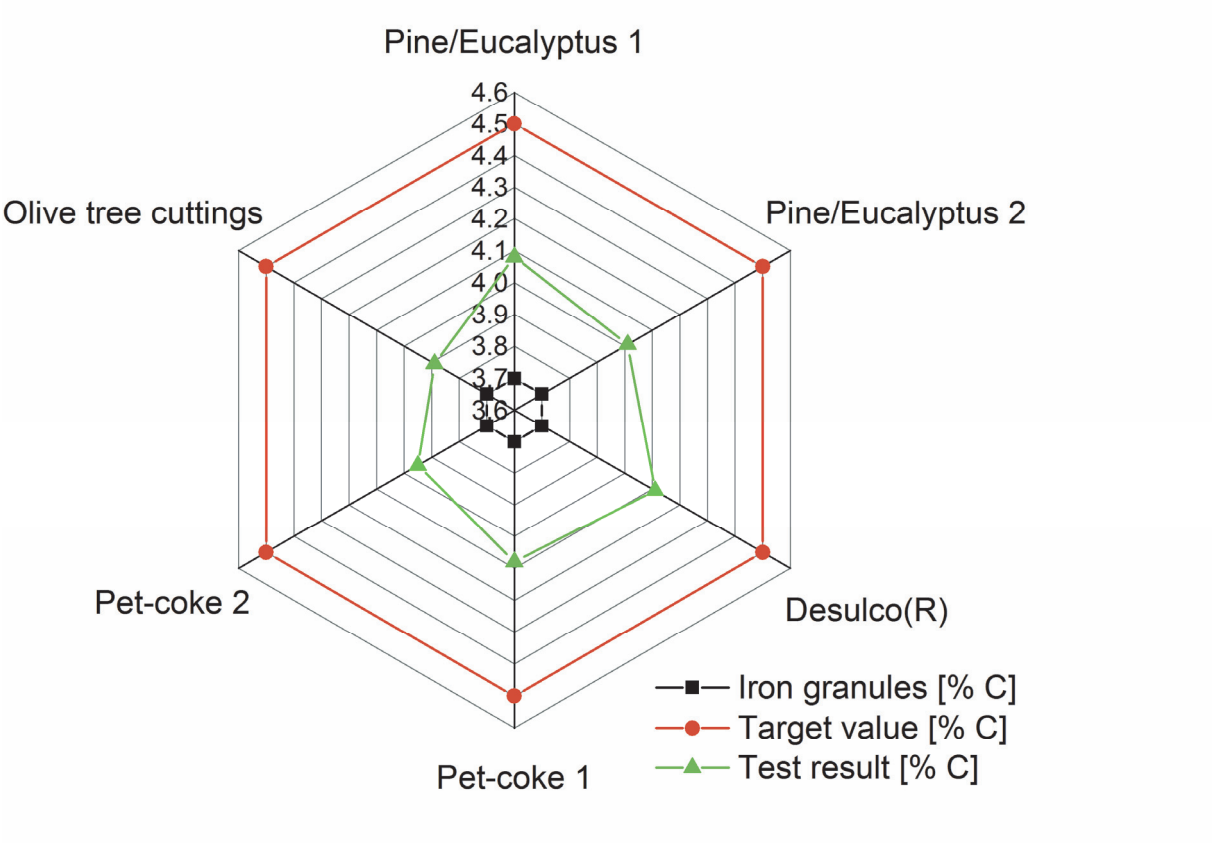

Figure 4-11: Obtained results of the carburization diagrams up to 4.5 % C represented in a net diagram

4.2.3 Induction furnace

The final carburization tests prior to the recycling experiments were carried out in the induction furnace at the Chair of Nonferrous Metallurgy, which is able to melt 100 kg of iron.

The melting unit itself was produced by “ITG-Induktionsanlagen GmbH” for melting down iron in the casting industry. The key data of the furnace are:

- Voltage: 600 V
- Frequency: 3.9 kHz
- Max. power: 80 kW
- Refractory material: Ankerindux from RHI AG

A picture of the tilted furnace can be seen in Figure 4-12. In this figure, the control unit as well as the cooling system are missing.

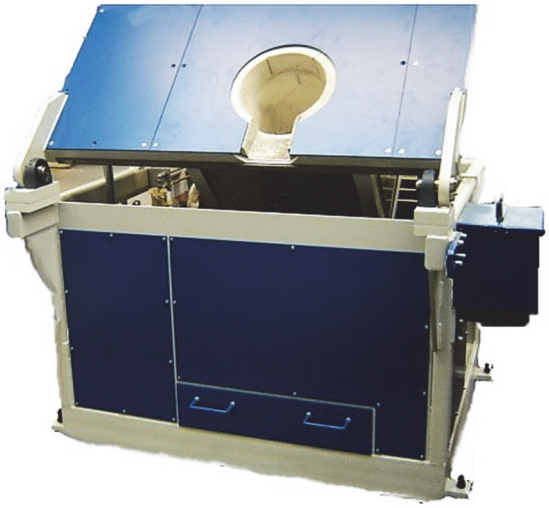

Figure 4-12: Picture of the tilted induction furnace produced by “ITG-Induktionsanlagen”

In Figure 4-13 a draft of the experimental set-up is pictured. The furnace was lined with “Ankerindux” delivered by RHI AG, which was an appropriate refractory ramming material. The life time of this material was 10 trials with temperatures up to 1,750 °C for a couple of hours in each experiment. To protect the molten iron surface against the oxygen from the air, a refractory cover, “Ankermix,” also from RHI AG, was used to have long-lasting protection. Furthermore, a nitrogen purging was installed to support the removal of the oxygen, as can be seen in Figure 4-13. Finally, a recess was drilled into the cover to charge the carbon carrier onto the iron bath and have a good view of the iron melt during the experiments. This hole also allowed a semi-continuous temperature measurement as well as the possibility to take samples. Since the temperature was measured almost every 10 minutes, a constant temperature could be provided.

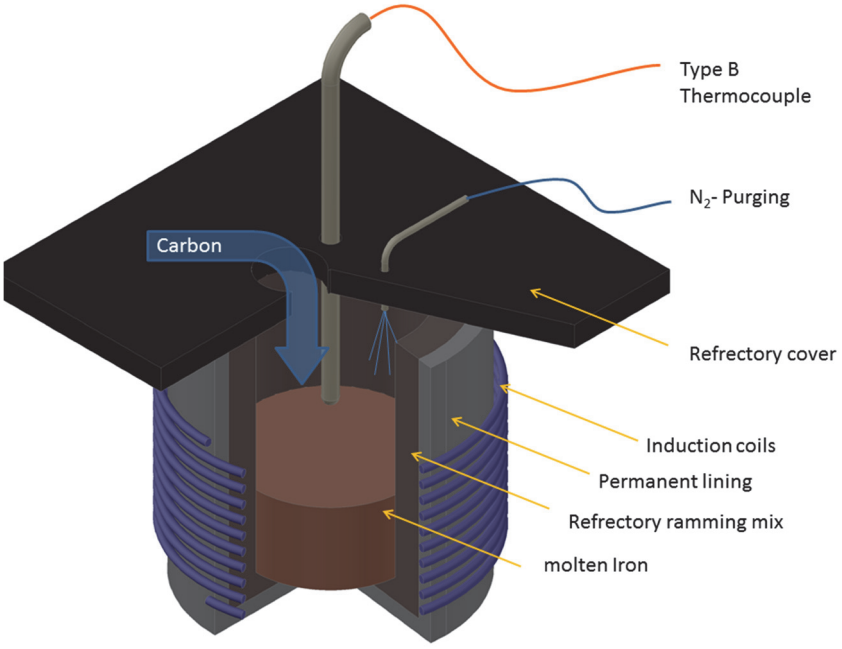

Figure 4-13: Simplified draft of the experimental set-up

For validating the change in the chemical composition, basically the evolution of the carbon content, samples were taken by applying a vacuum inside a cavity to produce a cylindrical shape which looks like a “lollypop”. This kind of specimen is optimized for analysis in a spark spectrometer by optical emission spectroscopy. Both measurement devices can be seen in Figure 4-14.

Figure 4-14: Vacuum sample taker (top) and temperature measurement lance (bottom), both with single use attachment for sampling and temperature measurement, respectively

The target in this test series was to compare different carbons regarding their usability as a carburization agent in an iron bath. Initial trials in the heat resistance furnace and the hot stage microscope demonstrated that it is definitely possible to use an alternative carbon carrier like charcoal in this field, although they have higher ash melting points. These carbonaceous materials serve later as a reducing agent for the oxidic residues from metallurgical processes which are charged on the iron bath.

During this test series, pure iron bars were cut into 10-20 cm pieces which were placed into the furnace. Approximately 25 kg of the pure iron were charged in each trial into the cold furnace at the beginning to have reproducible conditions for the carburization tests. In Table 4-5 the chemical analysis of the standardized iron is given.

Table 4-5: Chemical analysis of the pure iron used in the trials

ARMCO © pure iron	C [wt-%]	Mn [wt-%]	P [wt-%]	S [wt-%]	N [wt-%]
Grade 4	0.01	0.06	0.005	0.003	0.005

The second raw material for these tests was the different carbon carriers which should be tested with regard to the carburization behaviour in the liquid metal. A particular focus was placed on the solubility time as well as the burn-off behaviour of the carbons when charging them onto molten iron in larger scale and by the application of stirring using the inductance effect. In Table 4-6 the chemical analysis (proximate analysis) is listed.

Table 4-6: Proximate analysis [wt-%] and the sulphur content in different carbonaceous material used in the trials

	C_{Fix}	Ash	Volatiles	Moisture	Sulphur
Eucalyptus No.4	91.86	2.11	2.20	3.83	0.01
Eucalyptus No.6	90.80	6.65	0.90	1.65	0.03
Olive tree cuttings	57.36	37.70	2.42	2.52	0.06
Petroleum coke	90.65	1.70	1.87	5.78	3.89

Melting 25 kg of iron lasts approximately 60-90 minutes in the induction furnace, where from the beginning of the experiment, nitrogen was purged into the crucible to remove the ambient oxygen, as mentioned above. The amount of carbon (charcoal or coke) was around 1 kg of carbon carrier in each trial, depending on the exact iron input. It is assumed that under ideal conditions (100 % of carbon in the coke/charcoal, no burning off), 1 kg of carbon in 25 kg iron would result in 4 % of carbon in the melt. This value should not be exceeded, as more dissolved carbon leads to a precipitation of primary cementite if the temperature decreases during the experiment. After melting the iron, a sample was taken to analyse the initial chemical composition prior to the carburization step.

The overall carbon sample was divided into three charges, each 333 g, if the amount of iron in the melt was exactly 25 kg. In doing so, the solubility time as well as the burn-up behaviour depending on the carbon content in the melt could be investigated. The three charges were poured into the melt approximately every 15 minutes, so that the carbonaceous material had enough time to dissolve. In between the charges, samples were taken to show the change in the chemical composition of the melt. Finally, the high carbon-containing melt produced was tapped and granulated for a better handling for future experiments. Therefore, a water basin was adapted by applying a water jet splashing in the poured iron for an optimized heat removal. By mounting a compressed air supply in a closed circular pipeline inside the water bath, a turbulent flow inside the basin could be provided. The set-up of the water basin can be seen in Figure 4-15.

Figure 4-15: Water basin optimized for the granulation of liquid iron

In order to compare the different trials, so-called “carburization diagrams” were drawn, where the carbon content is plotted against the experimental time. The burn-off from each charge and the theoretical carbon content are shown.

The following subchapter focuses on the results of each carburization trial as well as particular features which occurred by adding charcoal or petroleum coke to the iron bath.

4.2.3.1 Charcoal “Eucalyptus No.4”

At the beginning, the “best” alternative carbon carrier should be described. In Figure 4-16 the carburization diagram is pictured. As can be seen in this figure, the burn-off behaviour decreases with higher carbon in the melt. A possible reason for this behaviour seems to be the remaining oxygen above the surface of the molten iron. Due to the charging of the charcoal, the carbon reacts with the oxygen and produces CO, which is released through the top cover. This theory is supported by the fact that in every trial, a combustion flame could be observed at the top due to the combustion to CO_2. Figure 4-16 shows the nominal as well as the actual value of the carbon content in the molten iron. The result shows that the estimated value is 3.99 % C and the achieved one is 3.21 % C. Thus, the overall burn-off of the charcoal in the iron melt results in 19.5 % C.

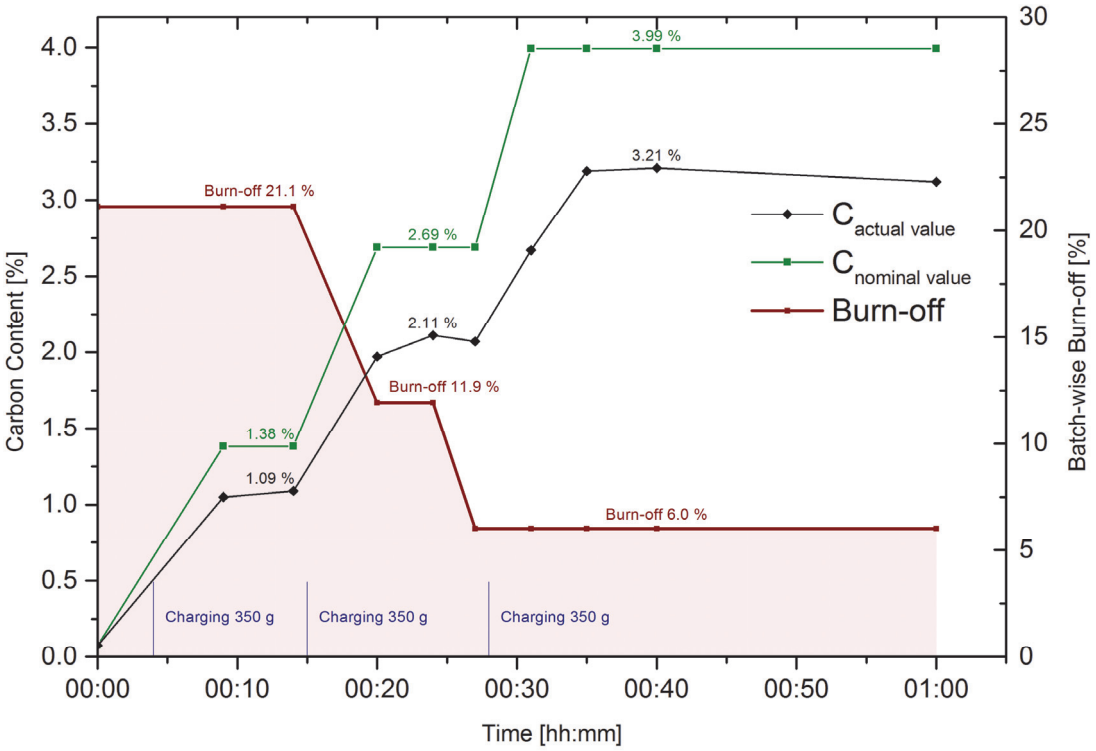

Figure 4-16: Carburization and burn-off behaviour of charcoal “Eucalyptus No.4”

4.2.3.2 Charcoal “Eucalyptus No.6”

The basic idea of these trials was to get information about differences in the composition of the input material. Although the previous and current charcoals are both originated from eucalyptus, they are from different subspecies. In comparison to the previously investigated charcoal, the current one contains more ash (No.4: 2.11 %; No.6: 6.65 %, compared to Table 4-6). The aim now is to see if there are differences due to the higher ash content.

Figure 4-17 shows that there is a significant difference between the Eucalyptus No.4 and No.6-charcoal. So the conclusion is that the higher ash content influences the dissolution of the charcoal in a bad way, since the final carbon content is 2.75 % and the overall burn-off was 30.4 %. Even though there are some alkalis like sodium and potassium within the charcoal which may influence the solubility in a positive way, the ash melts and captures the carbon inside the resulting molten slag. Nevertheless, the carbon content reached 2.75 %, the 2nd best result during this investigation. Perhaps the carbon in the iron would increase with longer experimental time, but this would not be very economical since a fast dissolution rate is recommended in this case.

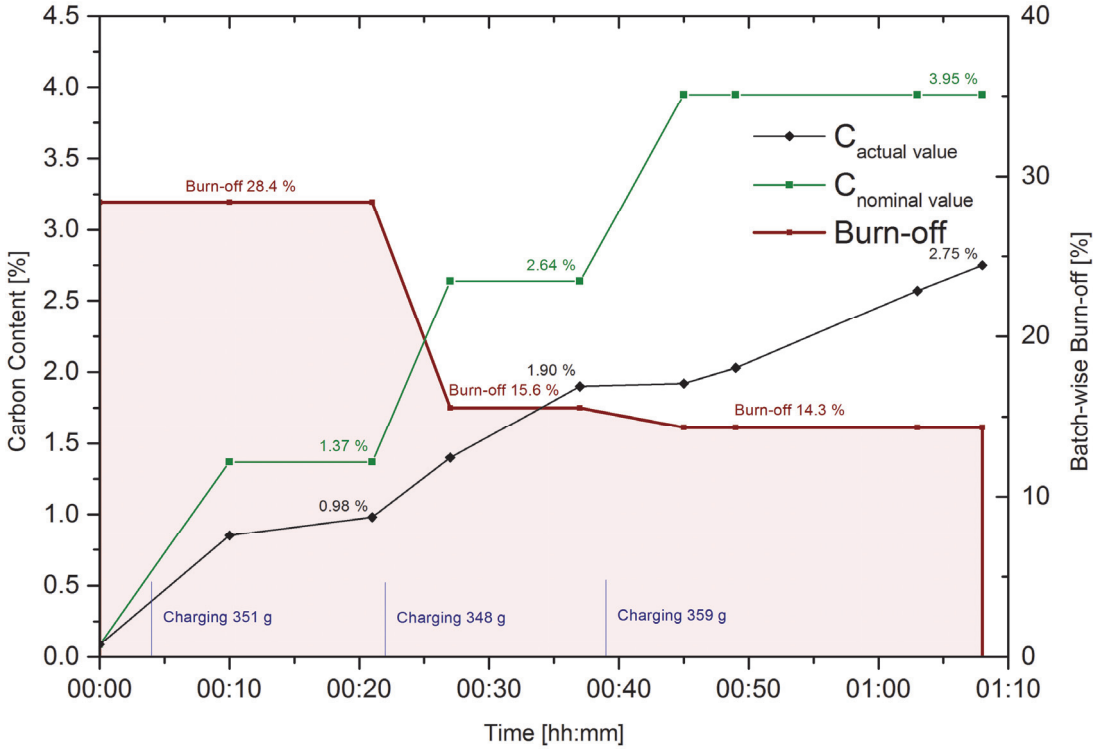

Figure 4-17: Dissolution as well as burn-off behaviour of charcoal made from eucalyptus trees (species No.6)

4.2.3.3 Charcoal “olive tree cuttings”

This trial was carried out with the “worst” charcoal available from the previous pyrolysis experiments. The carbon content was the lowest and the ash content was the highest (cf. Table 4-6). Due to the high ash content, the melting behaviour of the components within the slag becomes important. After a chemical analysis of the ash it was found that a major difference between the “eucalyptus” and the “olive trees” was the SiO_2 content, which is very high for “olive tree cuttings.” Taking into account that CaO and MgO are also within the ash, SiO_2 influences the melting and softening point of the resulting slag to lower temperatures according to Table 4-3. This slag totally covers the iron bath and prevents the dissolution of charged charcoal into the melt later. That’s the reason why the maximum carbon content in the melt reached only 0.71 % C, with theoretically 2.15 % C available from the charcoal. The overall burn-off in this case was 45.90 %, which is a very unusually high burn-off rate in comparison to the previously performed carburization experiments. In Figure 4-18 the carburization diagram recorded during this experiment is shown.

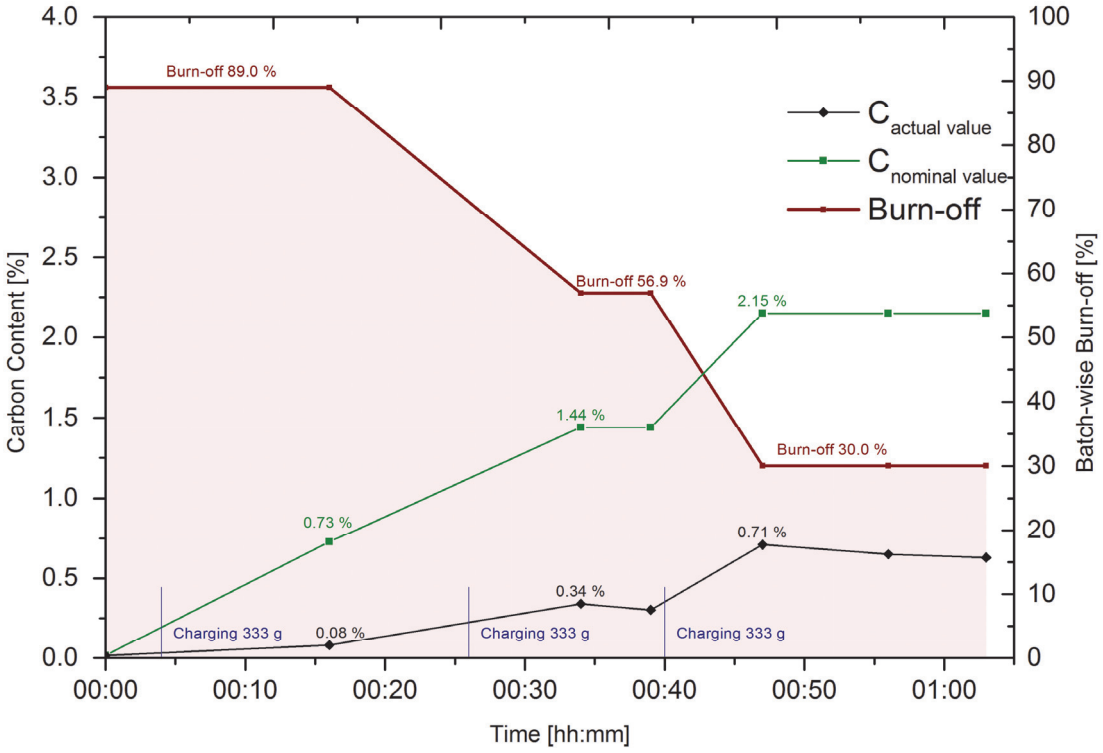

Figure 4-18: Carburization diagram of charcoal made from olive tree cuttings

4.2.3.4 Reference fossil coke “petroleum coke”

The last trial was performed with the utilization of petroleum coke (Figure 4-19) to get an idea about the dissolution behaviour of fossil carbons in the iron bath. A big difference regarding the chemical composition is the higher sulphur content, which is undesired because of the possibility of evolving SO_2 into the off-gas stream. Although the overall burn-off was slightly higher (45.9 %) than with charcoal from eucalyptus, the dissolution rate was the highest. This results in a 2.06 % C in the melt before tapping. The theoretical carbon content without burn-off would be 3.79 % C. Due to the slightly increased sulphur within the coke, a typical sulphur smell could be recognized. An anomaly in this experiment was the high flame which evolved from the high reactivity and the very small particle size in comparison to the charcoal.

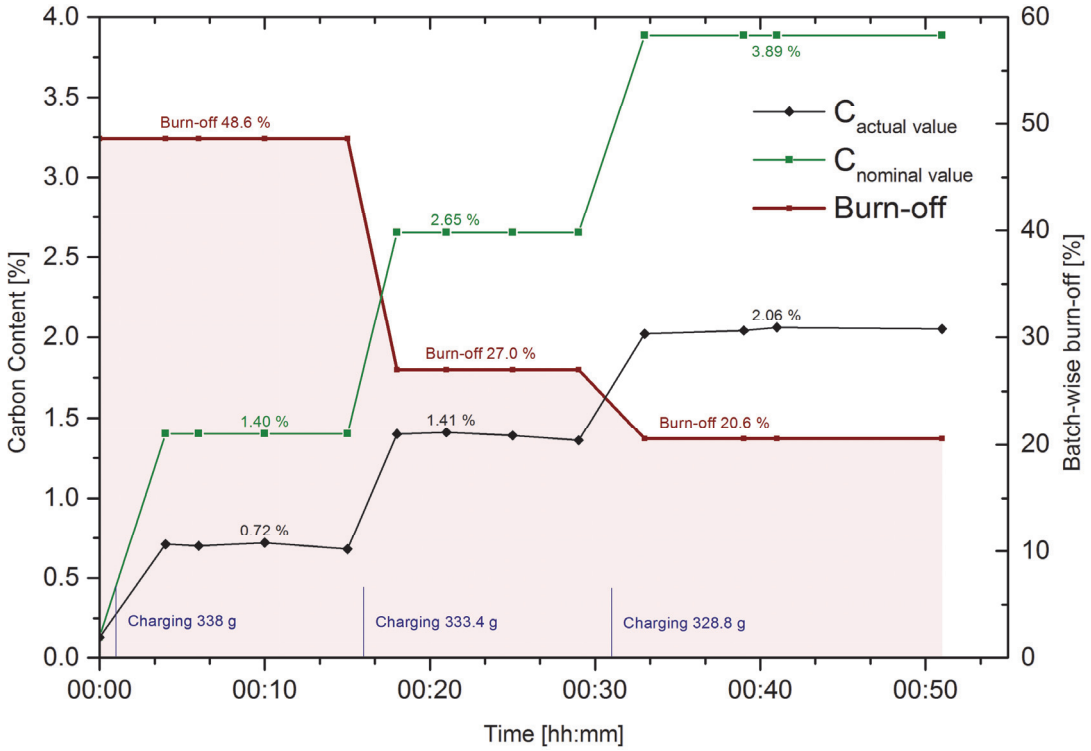

Figure 4-19: Results of the carburization behaviour of the fossil reference “petroleum coke”

4.3 Conclusion and further processing

With regard to the initial trials in the hot stage microscope, some important conclusions could be arrived at. The major interest was the question as to which final temperature for smelting the iron would be sufficient, to dissolve the carbon in the liquid.

Hot stage microscope investigations as well as simultaneously performed calculations with FactSage™ mainly showed the influence of the mineral matter within the carbonaceous material on the dissolution behaviour in iron. The ash from the charcoal made from olive tree cuttings had the lowest melting point, and the ash from charcoal “Eucalytus/Pine No.2 and No.6” the highest. “Vines” and the pet-coke achieved intermediate results. The softening temperatures from the hot stage microscope correlate with those calculated using the thermodynamic software. Due to the low melting temperature of the ash from charcoal “Olive”, the dissolution behaviour will be worse, since the ash is melting previous to the iron, collecting the carbon and preventing it to dissolve into the iron. Contrary, high ash melting temperature, like those of “Eucalyptus/Pine No.2 and No.6” will promote the carburization, since they will not be liquid when the iron melts. These conclusions will be confirmed by the further performed carburization trials in the chamber furnace as well as in the induction furnace.

The small-scale carburization experiments in the chamber furnace showed a good basis for further decisions for trials in larger scale. The bad dissolving behaviour of the charcoals from olive tree cuttings labels this type of carbon as completely inappropriate for these purposes.

Additionally, the excellent carbon yield in the melt of Desulco® could be proved, as already expected since this type of carbonaceous material was designed exactly for this purpose. Surprisingly good yields could be produced with the two remaining renewable species, various subspecies of pine and eucalyptus tree cuttings. These two as well as the olive charcoal were also further investigated in the larger-scale trials, similar to the pet-coke. The results achieved by the two petroleum cokes could be retrieved in the middle field of the ranking. Based on their relatively high specific weight in comparison to charcoals, they sank into the liquid iron by gravitation.

However, one very important piece of information was the fact that carburization cannot be performed very easily if carbon contents higher than 4.3 % are required in the iron. Of course, from the materials technology point of view, iron-containing alloys more than 4.3 % C are very rare (e. g. powder metallurgy), which is why almost no information is available in this field. But in the present research field, higher quantities of dissolved carbon are necessary, which was stated at the beginning of this chapter. This led to the conclusion that higher temperatures and stronger reducing conditions or an oxygen-free atmosphere might be possible; therefore, further investigations have to be carried out after this thesis in the future to solve this problem. Finally, the results obtained in the small-scale trials led to the experiments in a range of 25 kg iron.

The aim here was to test the utilization of charcoal as an alternative carburization agent in an iron bath using an induction furnace. Due to the different structure of the renewable carbons in comparison to the fossil ones, there might be some differences in the solubility behaviour. Based on the previous research using smaller amounts of material, these trials in the induction furnace were adopted to this scale. The aim was, as before, that the experiments should be compared regarding their final carbon content as well as the dissolution rate, which is important for further economic considerations. It could be found that the best performance concerning the solubility was demonstrated by petroleum coke. The fossil carbon was slightly faster than the charcoal from pine and eucalyptus tree cuttings, blend No.4, but the burn-off behaviour is better when using the renewable input material. From this point of view, it seems that charcoal should be preferred since the solubility rate is higher, causing lower amounts of carbon carrier.

The results obtained using pine / eucalyptus blend No.6-charcoal were not so bad, but due to the higher ash content in comparison to the best charcoal, the dissolution rate was lower. This results in a lower increase in the carbon content in the molten iron. Perhaps the final carbon content would increase to higher values but the solubility rate is too low, so this would be too uneconomical by comparing the speed with petroleum coke. The last alternative carburization agent originated from olive tree cuttings. Although the small-scale experiments labelled this type of charcoal as an unsuitable option, it should serve as a bad example in this test series.

The results obtained here were, not surprisingly, a very low carbon content in the melt. Furthermore, the huge amount of ash within the charcoal melted, forming a slag which covered the melt. Due to this fact, further charging of charcoal or other additives will not be possible anymore without removing the slag.

Finally, it can be stated that it is definitely possible to use renewable carbons instead of fossil ones for the carburization of molten iron. As suggested in the previous paragraph, it is very important to focus on the ash content of the carburization agent. Moreover, the most important influencing factor seems to be the fixed carbon content within the charcoal. Results have shown that this value should be higher than 85 % C.

The experiments were performed as a pilot test to get an idea about the solubility behaviour of carbons in an iron bath. Further experiments will be carried out in larger scale with the application of a TBRC (Top Blown Rotary Converter), where the produced high carbon-containing iron will be part of the “two-step dust recycling” process for the recycling of steel mill dusts. The detailed description of the process set-up as well as the theoretical background will be explained in Chapter 5.

5 The “2sDR” process

The “2sDR” (two step dust recycling) process is a new method to recover heavy metals from steel mill dusts without producing any new wastes. The process consists of two separately performed steps, beginning with clinkering and a subsequent reducing step. The next subchapters will serve as a background for the applied process, where in the following section, charcoal was also utilized to lower the CO_2 emissions in the subsequent reducing step. Based on the results obtained in the previous carburization process, the second step in this process was adopted.

5.1 Overview of the recycling of EAFDs

Melting down steel scrap in an electric arc furnace (EAF) leads to the formation of high amounts of so-called electric arc furnace dusts (EAFDs). Usually, these generated dusts contain a huge variety of species, but the majority is zinc and iron. Depending on the input material, the values of the components can vary considerably, which means that high amounts of halides as well as lead, chromium and nickel might also be found. The origin of the main components, zinc and iron, can be found exemplarily in the zinc-coated iron blankets, generally obtained from the shredding of scraps from the automotive industry. By charging the feed material into the EAF, it is heated up immediately by electrical energy (up to 1,700 °C) and melted down to form liquid metal. Due to the low vaporization temperature of zinc (907 °C), fumes arise from the metal/slag bath and are drawn into the off-gas stream. Reoxidation takes place here, forming ZnO. The necessary oxygen is delivered by the ambient oxygen, which of course is also carried away into the off-gas system [116–120].

The high amount of iron in the dust is caused by the formation of small iron droplets during charging, tapping, etc.. These are partly oxidized and also forwarded to the off-gas system and can be found in the bag house filter. Although the origin of zinc and iron is relatively different, a huge amount can be found chemically bonded to zinc ferrite. What is more, a significant amount is bonded to halogens, such as chlorine and fluorine. In the case of chlorine, this element can be associated with organic coatings in combination with other hydrocarbons such as organochlorides. One very popular example is the underbody protection of cars. Fluorine might be found in the bag filters due to the utilization of CaF_2 in casting powders to protect the liquid steel surface against the atmosphere’s oxygen during the refining of steel. Since the off-gas systems are linked, fluorine can be also found in the filter dust. Further sources can also be flame retardants, similar to bromine, originated also from the feed material of the EAF. Finally, slag particles as well as some sodium and potassium, are usually found in the EAFD [116–120].

In respect of the amounts of dust generated each year, several estimations have to be applied to get an approximate value. First of all, the steel production via the EAF route has to be taken into account, which was 452 m. tonnes in 2013. Assuming that between 15 and 25 kg/t of EAFD is produced per tonne of steel, an average amount of 6.8 -11.3 m. tonnes of dust was generated in 2013. Unfortunately, less than 44 % of the residue produced is recycled, whereof ~80 % of the amount recycled is treated with the Waelz process. According to the European Union and the US EPA, the Waelz kiln process is known as the “best available technique” and the “best demonstrated available technology,” respectively, for the recovery of zinc from residues. As with every process, the Waelz process also has some initial requirements for its feed material. In general, nowadays, a zinc content above 20 % Zn in the feed material (currently, typically EAFD) is usually seen as an appropriate amount to run the process economically [116; 121–124]. The following table shows a typical chemical analysis of EAFD as well as the products obtained from the Waelz kiln process.

Table 5-1: Typical values [wt-%] of the feed material of the Waelz kiln as well as its products [125; 126]

	Zn	Pb	FeO	CaO	MgO	SiO_2	Cl	F	S
EAFD	17-32	0.1-3	23-45	3.5-15	1.7-9	1-8	0.1-4	0.1-1.5	0.2-1
Unwashed WOX	55-65	2.3-5.5	2.1-5.4	1.2-4.0	0.2-0.5	0.2-1.5	0.1-6.4	0.1-0.5	0.2-1.0
Waelz slag	0.2-2.0	0.5-2	30-50	< 26.0	< 6.0	< 10.0	< 0.1	0.1-0.3	~1.5

It can be stated that two fractions are produced in the Waelz process. The main one is Waelz oxide (WOX), which contains the majority of zinc (ZnO) and Waelz slag. Several impurities are found within the WOX; the aforementioned chlorine and fluorine are undesirable since the product is usually processed in primary zinc metallurgy. In this case, the zinc oxide and halides are leached using sulphuric acid. The leach is purified and forwarded to the zinc winning electrolysis where zinc is obtained again as metal on the cathodes. The dissolved halides within the liquid will influence the process in a bad way. Chlorine, for instance, corrodes the lead (alloyed with silver) made anodes and forms poisonous chlorine gas. Fluorine corrodes the oxidic passive layer on the aluminium cathodes, by the formation of HF and ZnF^+, which leads to sticking problems of zinc on the cathodes. Usually, the WOX is washed in a Na_2CO_3-containing solution, where these halides are dissolved within the liquid and the zinc stays in the solid part but relatively purified. [118; 120; 127].

Nevertheless, a further problem of the Waelz kiln process can be found when taking a closer look at the by-product, the so-called Waelz slag. Here, the total iron within the charged EAFD is lost, which is the majority of the slag. Furthermore, several heavy metals like Cr, Ni, Mo, Cu or even remaining Zn and Pb can be found, forming partly soluble chemical bondings. At the

moment, the produced slag can be found in some countries in road construction. In the near future, this utilization possibility will be forbidden, especially in the European Union, because of the substances contained in the Waelz slag. With these new legislative regulations, which have already been introduced in some countries, the residue must be labelled as hazardous waste, which will definitely lead to considerable financial efforts to get rid of the slag and dump it in special landfills. Taking a look at the slag components again, it can be seen that a total recovery of these heavy metals is definitely feasible since a huge quantity is lost from the disposal of the slag [128].

Therefore, various options that deal with this topic have been invented in the past, offering alternatives to the “old-fashioned” Waelz kiln. These concepts included pyrometallurgical as well as hydrometallurgical processes. Unfortunately, none of these processes were successful, owing to several reasons.

Some of the alternative routes generated new wastes or were not able to treat a certain variety of steel mill dusts occurring in metallurgical facilities. Furthermore, proposals for new concepts did not take into account the fact that a huge quantity of zinc is bonded to iron, forming zinc ferrite, which is definitely a factor that has to be kept in mind when processing EAFDs [129–133]. As an example, the first drafts of the hydrometallurgical Ezinex and Zincex process did not consider this problem properly. Especially the Zincex process is said to produce no wastes, although according to [131] roughly 820-990 kg/t residues are produced per ton of Zn (including leaching residue, gypsum and iron residue). Further optimization of the processes developments included an additional facility to deal with the ferritic bonding.

It can be stated that hydrometallurgical methods for processing steel mill dusts vary between the type of acid as well as important parameters such as pH, temperature and pressure applied where the dust is leached. Among others, some of the important methods are the leaching of EAFD in [134]:

- Sulphuric acid: good leaching behaviour; unfortunately, the leach has to be purified since Cl and F are totally dissolved. The removal of zinc ferrite is possible but regrettably only at higher temperatures and increasing acid concentrations. However, as well known from the zinc primary industry, a subsequent iron precipitation has to be performed, causing a huge amount of residues [132; 135].
- Soda leaching: usually this type of leaching is used to get rid of chlorine and fluorine within the Waelz oxide. But it can be also used to precipitate zinc bicarbonate [136–138].

- Solvent extraction: one popular example is the Ezinex process mentioned above. Especially the high investment costs are responsible for this process almost not being in use [129].
- Sodium hydroxide: basically a good option to leach the residue with NaOH with a subsequent precipitation using CO_2. However, a huge number of process steps and high temperatures are necessary; therefore, this process set-up seems incomplete, since zinc ferrite cannot be leached, which leads to significant losses.

The main conclusion regarding all of the methods is that until now, no industrial facility has been built using such technologies. Some of them didn´t take into account how to get rid of the problematic halides, while others did not show in detail how to proceed with them within the process [132; 135; 137; 139–142]. Meanwhile, newer publications in this field of hydrometallurgy are aware of the fluorine and chlorine problems occurring in the leaching of zinc from EAFDs. However, most of these publications take into account the chlorine removal [143; 144]; only some of them try to separate the fluorine from the leach [145; 146].

Taking a closer look at pyrometallurgical processes, it can be seen that often, rotary hearth furnaces have been utilized to serve as an aggregate to reduce the zinc oxide in advance with a subsequent production of direct reduced iron (DRI). The Fastmet/Fastmelt technology as well as Inmetco process can be named as representative developments. The big problem for this type of furnace is that instead of iron, the remaining residue is often reduced to wustite and this leads to an agglomeration build-up with the slag and further blockings at the DRI discharge. Similar problems occur in the Primus process, where a multiple-hearth furnace serves as the main aggregate for alternative steel mill dust processing routes [147–149].

Especially the scale-up to pilot scale has often led to unsolvable problems. Some of these inventions can be associated with the utilization of a submerged arc furnace (SAF). Several projects have experienced problems with the implemented refractory material and have therefore been stopped [147; 148; 150].

However, since most of these tests were performed several years ago, there is definitely a possibility of new invented refractories so that the furnaces would run economically now.

Nevertheless, even though the disadvantages listed regarding the products obtained in the Waelz kiln have been known for a long time, it is still the preferred route to process steel mill dusts.

5.2 Set-up of the “2sDR” process

The intensive research activities within the last years finally resulted in the “2sDR” process, which will be described in the succeeding chapters. Moreover, to increase the sustainability as regards the evolving CO_2 emissions, this process also took place using charcoal as a reducing agent, lowering the greenhouse gas emissions and creating a “greener” recycling process.

Basically, this process consists of two separately performed steps, where the main focus lies on the total utilization of all products obtained and without the generation of any wastes. In terms of the process itself, the EAFD needs to be agglomerated in advance to form pellets. There might be the option to add slag-forming additives such as silicon oxide, to improve the melting performance in the reduction step. The first part of the thermal treatment consists of oxidic clinkering to remove the halide as well as the majority of the lead. The clinkered material is forwarded (under hot conditions on an industrial scale) to the second part, the reduction in a carbon-containing iron bath. Here, the reduction of the oxidic components takes place where all materials charged onto the iron bath are converted to products; an iron alloy, a heavy metal free slag and a clean ZnO. The following subchapters describe the applied process steps in detail.

5.2.1 Clinkering

The first treatment of the pelletized residues is performed in an oxidizing atmosphere. Applied metallurgical reactors could be, for instance, a rotary kiln as well as a top-blown rotary converter (TBRC). Since this type of aggregate is available at the Chair of Nonferrous Metallurgy, further examinations are referred to as TBRC.

Concerning the clinkering of materials, in principle, the process has been known for a long time. Clinkering was first used to obtain relatively pure ZnO from smelting intermediates obtained in nonferrous metallurgy and low quality ores. In that case, the process was run subsequent to a Waelz kiln process, similar to today´s process for the recycling of EAFDs. During the clinkering, the highly volatile PbO was evaporated. In comparison to the steel mill dusts, these intermediates did not contain any halides, which is why the process set-up was very easy. However, the chemical analysis as well as the phase distribution of an EAFD is very complex; especially the interactions between these compounds while heating up in an oxidizing atmosphere are a challenge and actually not well understood. Only one doctoral thesis is available which deals with this topic; so, a short summary will be given to explain the essential facts to run the clinkering step in order to obtain a halide and lead-free feed material for the reduction step [134]:

- A good removal efficiency of chlorine compounds could be observed, according to thermodynamic calculations.
- Troubles might occur with $CaCl_2$ at high vaporization times.
- Since CaF_2 is a very stable fluorine compound, other species associated with fluorine can be removed more easily.
- A fast heat-up of the EAFD is recommended to obtain a good removal efficiency of halides to avoid the building of undesirable and hard to remove compounds.

Based on this research, the maximum temperature of 1,150 °C should not be exceeded, since this would lead to an increasing energy demand. Treatment times around 3 h guarantee an efficiency in the chlorine and fluorine removal of more than 90 % and 85 %, respectively. Two products can be obtained from the first step of the process; the clinker, which is low in Cl, F, and Pb and the dust where the undesirable fraction can be found as well as some amounts of Zn lost due to the chemical bonding to halides. Since the losses are lower than 8 % of the overall zinc input, it is acceptable because of the pure clinker achieved. Figure 5-1 shows the experimental set-up of the clinkering process with the utilization of the TBRC.

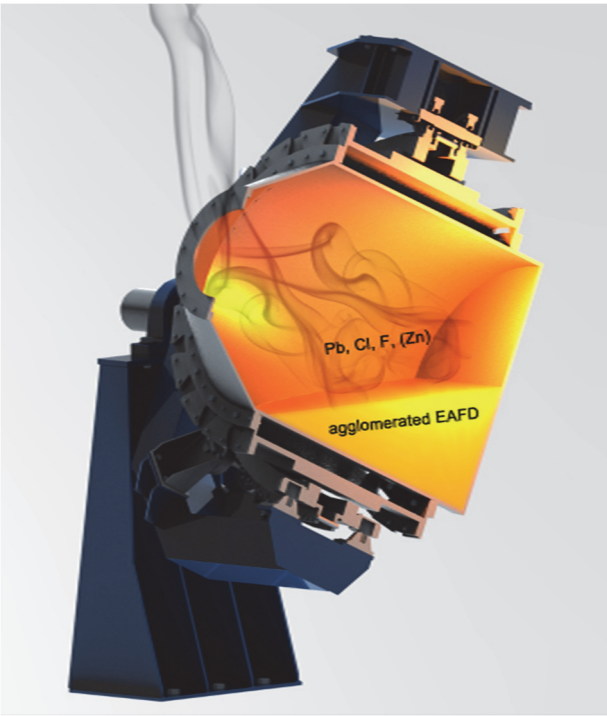

Figure 5-1: Scheme of the clinkering step using a TBRC

The presented vapour pressure curves in Figure 5-2 and Figure 5-3 explain the theoretical basics of the clinkering process with the variation of temperature and pressure of selected chlorines and fluorides. In general, it can be stated that F-compounds need higher temperatures than those linked to Cl. Indeed, as indicated beforehand, the efficiency of chlorine is slightly higher than the flour removal performance.

Figure 5-2 shows selected chloride compounds which are present in the steel mill dust. It can be seen clearly that especially $CaCl_2$, NaCl and KCl are very hard to remove according to thermodynamic calculation. The average working range can be observed as the turquoise temperature range meets the atmospheric pressure line at 10^5 Pa. It has to be mentioned that this figure only represents theoretical considerations. The doctoral thesis [151] concludes that there are definitely several chemical reactions proceeded in parallel (e.g. with PbO), which results in higher yields in the Cl removal. This theory could also be proven in the clinkering experiments carried out during the research of the “2sDR” process.

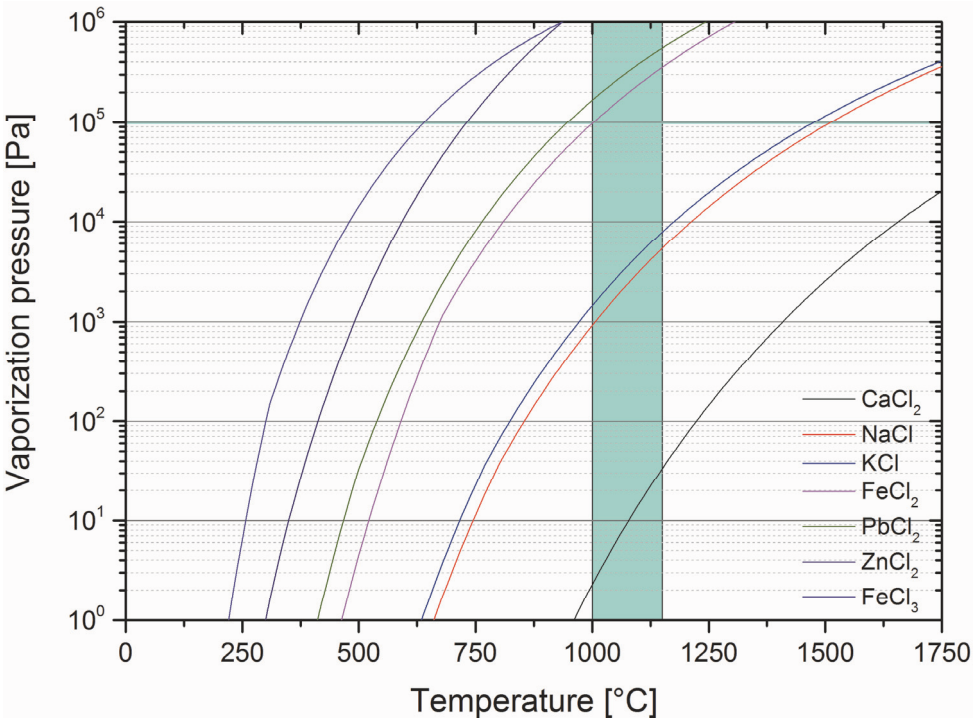

Figure 5-2: Vaporization pressure of selected chlorides at changing temperatures. The interception of the turquoise lines represents the working conditions for the clinkering step

Figure 5-3 shows the dependence of the vaporization of selected halides at various temperatures. It can be stated that in general, fluorides are more stable than chlorides, which means that the vaporization temperature is slightly higher under oxidizing conditions. This leads to the fact that on the whole, the fluorine content would unfortunately stay at higher concentrations than the chlorine content after the clinkering process.

Results obtained for the clinkering trials which will be presented later will confirm the thermodynamic considerations. However, since the overall input of fluorine is relatively low (usually in between 0.1 and 0.5), most of the F is bonded to CaF_2 and can be found in these configurations in the EAFD.

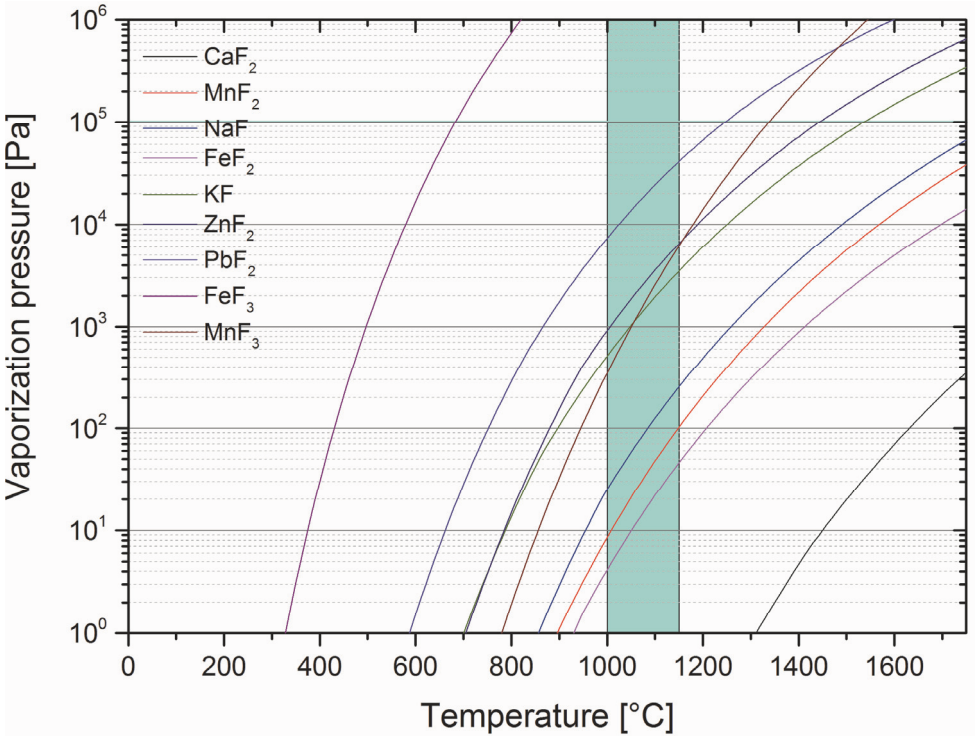

Figure 5-3: Thermodynamic calculation of several fluorides to determine their vaporization temperature depending on the pressure

Finally, the clinkered material, more or less free from halides, can be fed into the second step. Saving energy should be aspired in every process, particularly in the metallurgical industry, so it is considered to charge the hot material into the second step.

5.2.2 Reducing step

The clinkered EAFD is charged onto the molten carbon-containing iron bath in the second part of the process. The main objective is the removal of the zinc to obtain high-quality ZnO since the halides are almost completely removed. The material is collected in the bag house filter of the furnace, and is ready for the production of metallic zinc by leaching in sulphuric acid with subsequent winning electrolysis.

With respect to the iron bath process, it has to be mentioned that the idea to recover metallurgical wastes using this set-up is actually not new. In several studies, an attempt was made to introduce, generally said, a metal bath, for this purpose. References [152–155] could be mentioned as examples for an iron bath process, for utilizing copper reference no. [156] can be cited. Since this new technology is based on a mini mill solution, no pilot plants have been available until now. Furthermore, this technology is not a centralized facility; like the Waelz process, it will be fitted to the demands of the steel mill next to the recycling plant. In the near future, pilot scale experiments will be performed which lead to the further scale-up to industrial scale.

Nevertheless, the major tasks of this process are to reduce the oxidic substances in the clinkered residue (ZnO, Fe_3O_4) to metals with the addition of carbon. Carbon is actually dissolved in the iron bath and added by charging carbonaceous material onto the iron bath together with the residue. The theoretical background of the carbon-containing iron bath was already discussed earlier in this thesis, so a short summary of the topic will be provided. A typical experimental set-up of the process can be found in Figure 5-4.

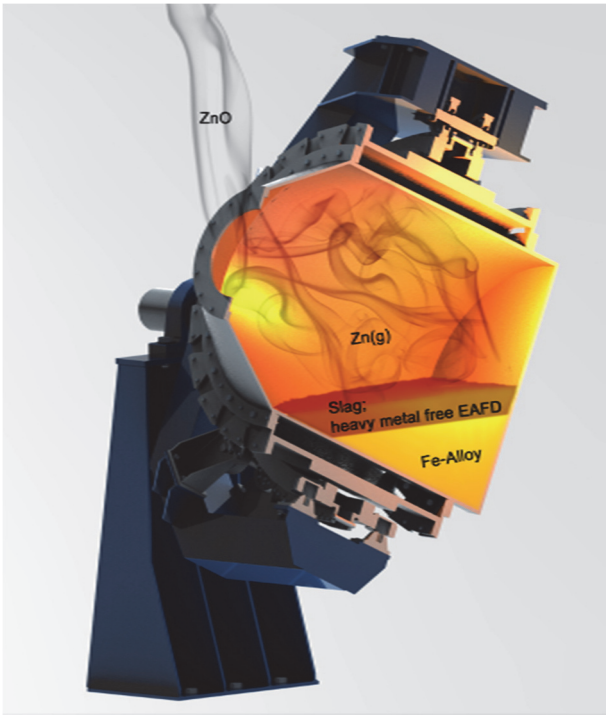

Figure 5-4: Experimental set-up of the second step of the 2sDR process in the TBRC

Due to the difficulties with higher carbon contents (> 4.3 % C), the decision was made to limit the maximum amount to 4.3 % C. Furthermore, the minimum should not be lower than 2.06 % C, as the melting point of the iron alloy according to the Fe-C binary diagram would increase, which leads to an inefficient mode of operating. This means the applicable carbon amount is equal to 2.24 %, meaning 52 % of the overall carbon content in the melt. Since the kinetic of dissolved carbon is very high, it is mandatory that there is always a specific amount of carbon in the melt. However, to increase the batch size, carbon can be added together with the residue, supporting the reduction, not influencing the carbon dissolved in the iron. But this effect is limited due to a high burn-off rate of the charged carbon within the charcoal/EAFD mixture, since homogenization is not easy because of the hot clinker.

Basically, the batch starts with charging clinkered EAFD onto the carbon-containing iron bath. During this procedure, further carbon is added as well as slag-forming additives, depending on the chemical composition and the final melting temperature of the formed slag, respectively. The end of the process is defined as the point where the zinc is completely fumed and the iron is totally removed from the slag.

The products obtained are:

- Relatively pure ZnO; only traces of Cl and F can be found
- Heavy metal-free slag
- Iron alloy enriched with Fe, Cr, Ni, etc. from the EAFD

Regarding the thermochemical background, several publications can be found dealing with the fuming of zinc out of the lead shaft furnace (Figure 5-5). Actually, this process is more than 100 years old, but the principles are generally still applicable for the 2sDR process.

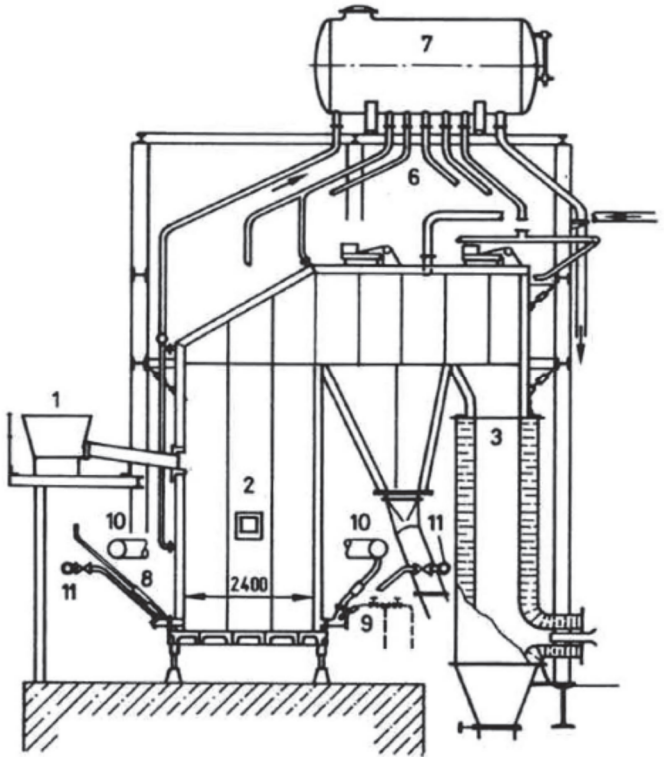

Figure 5-5: Slag fuming furnace for the producing of zinc out of the slag obtained in the lead shaft furnace 1: slag feed; 2: fuming furnace; 3: post combustion chamber; 6: cooling water discharge; 7: cooling water collector; 8: pyrite injection unit; 9: oil injection unit; 10: hot blast bustle pipe; 11: cold blast bustle pipe [157]

The process started with the tapping of the slag out of the lead shaft furnace. The applied carbon carriers for such a slag fuming were, among others, powdered coal and fuel oil, whereby the last example was favoured due to the increase in turbulence with the high amount of volatile matter. In doing so, CO is produced due to temperatures higher than 1,000 °C (usually 1,150-1,373 °C), which acts as a reducing agent. Beside other problems, a theoretical furnace temperature lower than 1,000 °C would not be very reasonable, since the wetting angle between ZnO and the carbonaceous material would be too small. Figure 5-5 shows an old type of slag fuming furnace with an attached post combustion chamber for the complete re-oxidation of Zn (and SnO) [157; 158].

However, the carbonaceous material forms a bubble in the molten slag, consisting of CO and surrounded by the slag and the liquid oxidic residue. In the case of the slag fuming process, zinc oxide is reduced, further volatized and re-oxidized in the upper part of the furnace. Furthermore, the iron oxide Fe_3O_4, which is the most stable form in liquid slags under these conditions [159], is reduced to FeO (wustite). There is a remarkable zinc content in the remaining slag, due to the operating conditions as well as the target of the fuming furnace. Basically, prior to the evaporation of the Zn, it is accumulated in the bubble, consisting of CO. According to thermodynamic calculations using HSC Chemistry software, Fe_3O_4 should be reduced first under these conditions (Figure 5-6). Nevertheless, ZnO is smaller and therefore transported faster to the boundary layer CO-bubble/slag. This leads to the fact that the Zn already produced reduces the iron oxide, producing ZnO again and FeO at temperatures higher than 1,300 °C. In this conjunction, the remaining Zn content in the fuming process is relatively high (~2 % in the slag) and the carbon demand increases if higher Zn yields are required [158; 160].

In comparison, the metal bath process operates at a higher temperature for the recovery of Zn and even Fe out of metallurgical residues. At higher temperatures, the iron oxide is converted to iron and with this, the Zn amount decreases to very low quantities in the remaining slag. Due to its higher density, the liquid iron (as well as other heavy metals like Cr, Ni, etc.) moves down, leaving a clean slag behind which can be further treated to be suitable for construction purposes [161].

$$ZnO + CO \rightleftarrows Zn + CO_2 \qquad \text{equ. 5-1}$$

$$Fe_3O_4 + CO \rightleftarrows 3FeO + CO_2 \qquad \text{equ. 5-2}$$

$$C + CO_2 = 2CO \qquad \text{equ. 5-3}$$

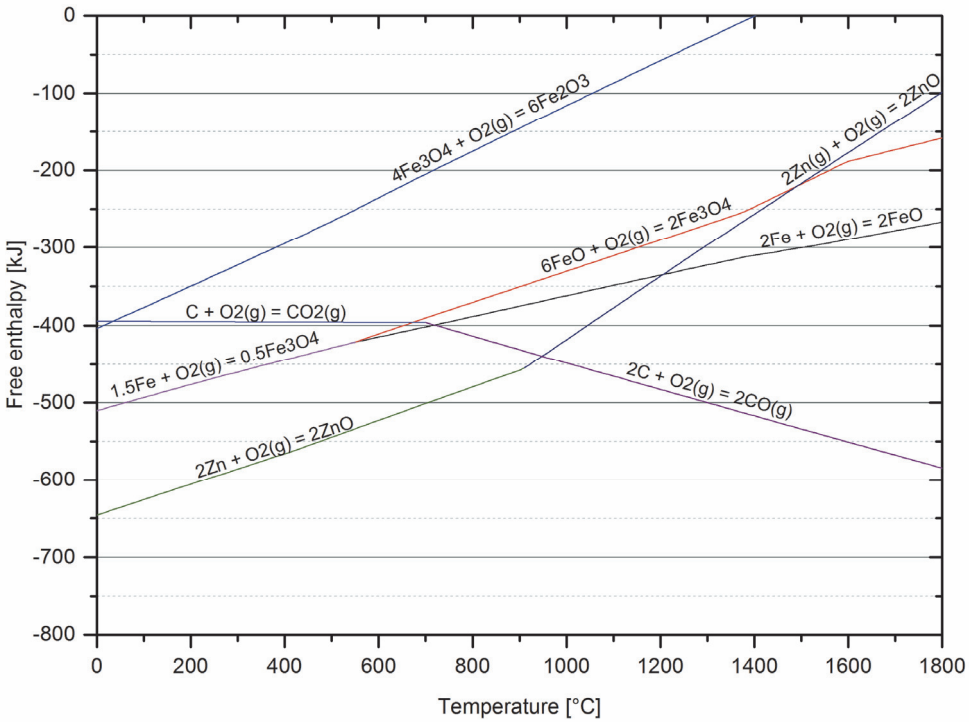

Figure 5-6: Gibbs energy of selcted components depending on temperature

The aforementioned reaction system is pictured in Figure 5-7, where a char particle is set in the middle of a CO bubble, surrounded by liquid slag. The char is converted to CO, which is consumed by Fe_3O_4 and ZnO, producing CO_2. Since the temperature is above 1,000 °C, the CO_2 is immediately reduced to CO. The reaction speed depends mainly on the kinetics of the slag, or in other words, the transportation of the educts to the boundary layer, the reaction at the boundary layer, and finally the movement of the products into the slag. Concluding, the reaction behaves as follows [158–160]:

- High Zn contents in the residue lead to a shorter residence time of the reducing agent
- Increasing Fe^{3+} contents leads to a low fuming efficiency of the Zn and the demand of carbon increases
- Carbonaceous materials with low ash content, low moisture, high fixed carbon content as well as high reactivity should be preferred

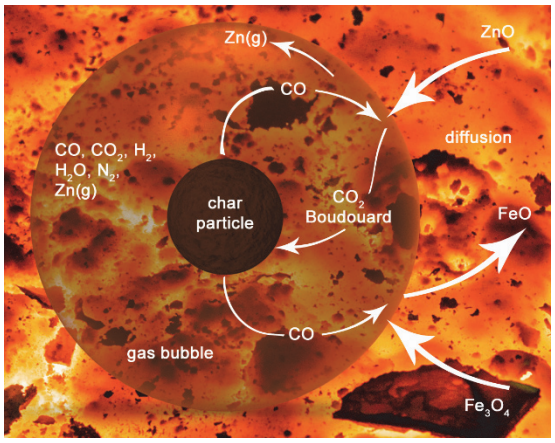

Figure 5-7: Illustration of the reactions occurring in the molten slag, according to [159]

It has to be mentioned that the considerations stated previously were obtained for the slag fuming process. Although these basic thoughts can be used for the “2sDR” process, it is absolutely necessary to perform thermodynamic calculations in advance.

Since the slag consists of a multi-component system, FactSage™ was chosen to model the slag system during the treatment of EAFD. With this, the evolution of the slag formation during the treatment can also be investigated with regard to the melting temperature of the oxidic mixture. As can be seen in Figure 5-8, the evolution of the produced slag out of the EAFD is done in three steps, also using three different ternary systems, starting with the left one. Here, the main components are given, which in the case of a typical EAFD are Zn, Fe and Ca. Minor elements are Si and Mn. Since the partial pressure of oxygen is given, the occurring oxidic phases result based on the thermodynamic equilibrium. Especially wustite is a big problem because there is no fixed stoichiometric composition ($Fe_{1-X}O$). However, the chemical composition of the clinkered material is represented as a pink dot in Figure 5-8. Through the depletion of Zn due to the reduction, the point moves towards the Fe-Ca binary diagram. With this, the concentration moves to the Fe-Ca-Si ternary diagram. Here, similar processes happen, since the iron should also be recovered, leading to the final Ca-Si-Mn system. Attention has to be paid to the final slag composition, since it is very important to avoid areas with high melting temperatures. In the case of EAFD, a silicon oxide addition (sand) should be considered [161].

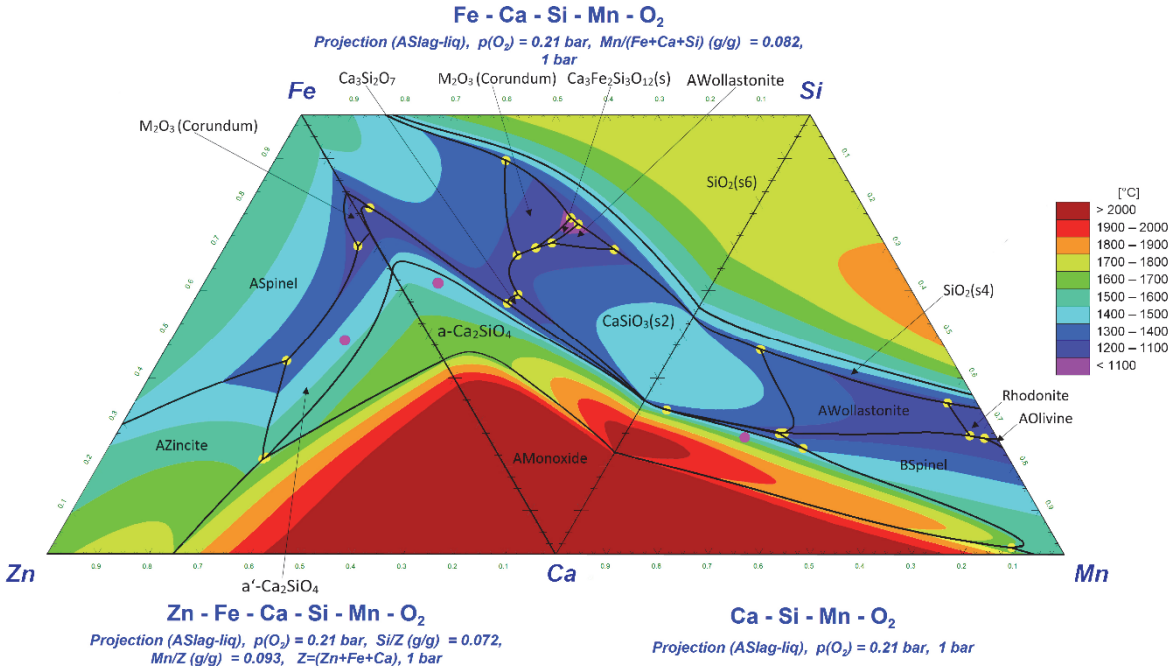

Figure 5-8: Evolution of the slag during the treatment in the 2nd step of the process, starting from the left side. The pink dot represents the slag composition and the melting temperature in each ternary diagram, respectively [161]

Since a main goal of this thesis is the implementation of renewable reducing agents, especially charcoal, it is possible to decrease the CO_2 emission significantly: Due to the fact that all emissions originated from the reduction of oxides cannot – as per definition – be attributed to the other greenhouse gases occurring by using this carbon from a renewable source. Initial experiments and results obtained in the carburization tests, explained in the preceding chapter, show a potential field of the application of charcoal to adjust the carbon content in the iron bath process. In contrast, generated CO_2 from the utilization of fossil petroleum coke, for instance, results in similar quantities of CO_2, but unfortunately, it is not renewable. This leads to increased greenhouse gas emissions from the process. Finally, it has to be mentioned that if there are any gases utilized for heating purposes (e.g. heating up the TBRC), they also have to be added to the overall CO_2 emissions of the recycling process.

A huge benefit of the utilization of charcoal originated from renewable charcoal is the fact that no sulphur is associated with this carbonaceous material. Neither in the obtained iron alloy nor in the off-gas system will sulphur be found, which is definitely an advantage. With respect to the off-gas cleaning system, no attention has to be paid to sulphur, since SO_2 emitters usually need special gas cleaning steps to get rid of sulphur dioxide. Similarities can be seen in the iron alloy where no additional desulphurization has to be performed, owing to the fact that sulphur is well known as a steel parasite.

However, while doing the research for this project, the implementation of charcoal was considered, based on the aforementioned advantages. Therefore, charcoal originated from

residues of the agricultural and forestry industries was used to be converted into an alternative carburization agent. This was employed to adjust the carbon content in the liquid iron bath as well as to feed additional reducing agent simultaneously with the charged clinkered EAFD, to guarantee a remaining carbon content in the metal bath after reduction of around 2 % C, as already explained.

As it is important for the process ramp-up of the procedure, it has to be mentioned that the very first batch is carried out using pig iron granules, given that the liquid metal bath has to be provided in advance. The charged EAFD provides additional iron during its reduction that will increase the quantity of the metal bath, as well as possible chromium and nickel. Therefore, it is necessary to tap a specific amount of metal from time to time and after some batches, respectively, to lower the volume of the iron melt.

In the subsequent chapter, the trial performed will be described with regard to the efficiency of the metal yield as well as the chemical analysis of the dust obtained. The charcoal was produced in the “twin screw reactor” at 850 °C and retention times of 2 h.

5.3 Utilization of charcoal in the iron bath process

The iron bath trial was performed subsequent to the first step of the process in a ~ 50 kg batch scale; however, for the sake of completeness, the data obtained by clinkering the waste material will be represented.

In Table 5-2, the chemical analysis of the feed material, an EAFD from a carbon steel producer, is given as residue which was agglomerated in advance. This material was clinkered in the TBRC at 1,100 °C with an applied retention time of 3 h. This treatment resulted in the expected loss of halides as well as some traces of Zn and Pb, which can be observed in the same table. The weight loss in the clinkering step was 86.8 %, which means the charged batch size of 28.5 kg was reduced to 24.7 kg. The corresponding Sankey diagram is illustrated in Figure 5-9.

Table 5-2: Overview of the chemical analysis [wt-%] of the dust before and after the clinkering step

	Zn	Pb	Fe	Cl	F
EAFD	34.7	3.2	14.9	9.6	0.16
EAFD after clinkering	36.9	0.2	17.2	0.7	0.03

It has to be mentioned that the further processing would be the straight forwarding of the hot material to the iron bath step, to save the heat energy accumulated in the clinkered material. As the scale of the experiments is too small compared to an industrial scale, the two steps of the process had to be performed on two different days.

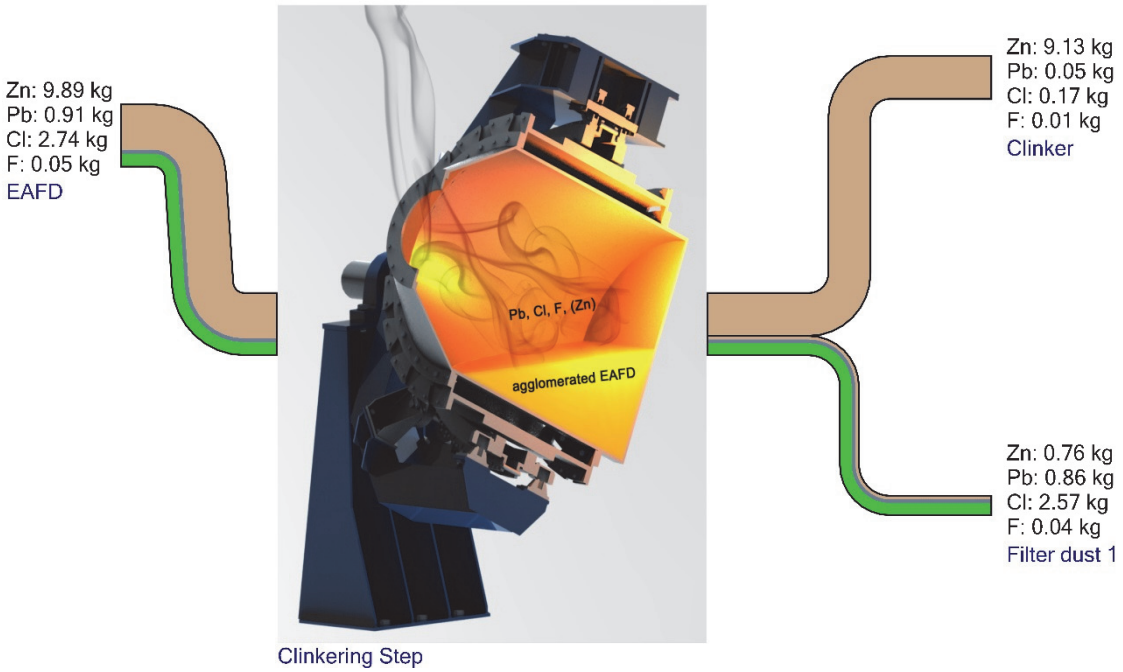

Figure 5-9: Observed mass flow in the clinkering trials using a TBRC

For this trial, an amount of 44.8 kg of pig iron was molten in the TBRC, with a subsequent addition of charcoal to guarantee a carbon content of around 4.3 % in the liquid phase. The basic background of this principle was explained in Chapter 4, but it has to be mentioned that due to the scale of the experiment, only one batch was performed and after this, the liquid phases were tapped. In industrial scale, the slag would be removed and the iron would be re-carburized to be ready for the next batch. With the increase of the metal bath caused by the reduction and further collection of iron, Cr and Ni, it is necessary to tap a small amount of iron. The chemical composition of the material utilized in the second step of the process can be found in Table 5-3; note that 9.98 kg of the clinkered material was also used that is not published in this table.

Table 5-3: Analysis [wt-%] of the material utilized as a basis for the metal bath process

	C	S	Cu	Pb	Zn	Fe
Pig iron granules	3.79	0.024	0.0078	0.002	0.002	93.9
Charcoal “Eucalyptus/Pine No. 4”	95.52					

The waste material was charged onto the liquid and carbon-enriched iron bath, starting immediately with the reduction process. The clinkered material was mixed with additional charcoal to guarantee a final carbon amount in the melt of roughly 2 %. With this, more pre-treated EAFD can be charged in each batch, increasing the size of the treated material per batch as well a better exploitation rate of the iron bath. This leads to a faster increase in elements such as Cr and Ni in the iron alloy, allowing faster tapping and further utilization of the alloy in a steel mill as e. g. master alloy.

The iron bath process was carried out at an average temperature of 1,618 °C and the EAFD was treated for 190 min. It was observed that in general, the density of the charcoal led to a longer charging time of the charcoal/residue mixture in comparison to the powdered pet-coke or relatively high density coke. The highly reactive charcoal caused a high reduction rate of the oxidic residues and further re-oxidation of Zn in the off-gas stream. This caused an enormous increase in the off-gas temperature and with this, a limitation of the process. Usually, this issue can be avoided by applying a spray cooling system in the off-gas pipes. Unfortunately, this type of application is not available at the Chair of Nonferrous Metallurgy. That means the treatment time was extended “artificially” by throttling the power supply of the methane burner that caused a lower metal bath temperature. The corresponding Sankey diagram can be seen in Figure 5-10.

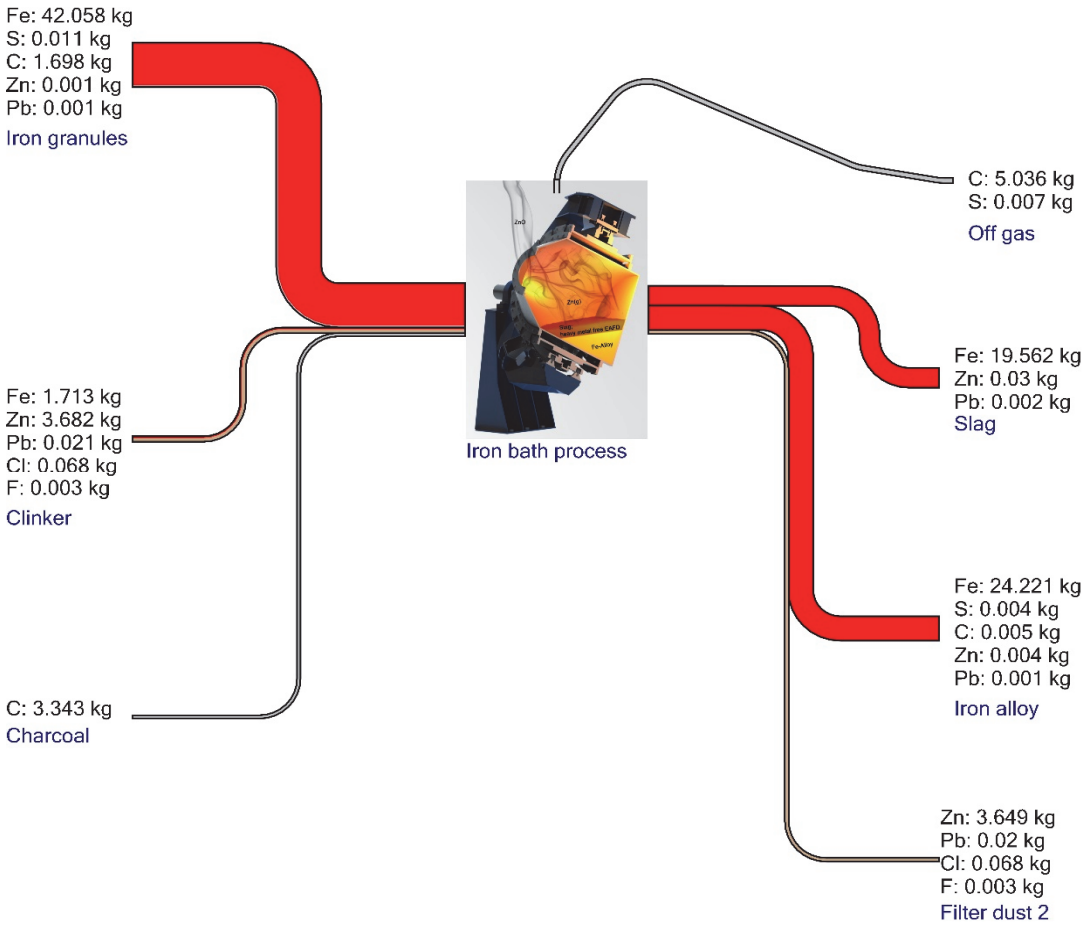

Figure 5-10: Sankey diagram of the second step of the “2sDR” process

In the matter of the achieved quantities of each fraction and its chemical composition, respectively, it can generally be stated that the obtained values are very satisfying. The final chemical composition is represented in Table 5-4.

Table 5-4: Overview of selected elements obtained in the second step of the process, in [wt-%]

	C	Pb	Zn	Fe	Cl	F	S
Regulus	0.02	0.004	0.02	99.59			0.015
Slag		0.005	0.09	58.5			
Dust		0.527	97.58		0.37	0.09	

With respect to the iron alloys obtained, several species in the metal should be discussed. The major element in the metal is of course iron, since the charged pig iron granules are made of this species. Further elements that are necessary for evaluating the success of the treatment are sulphur and zinc. Both originate from the EAFD and in general, it can be stated that the lower the value in the metal, the better the result. As can be seen in Table 5-4, the values are really low, leading to the conclusion that the treatment was successful. Unfortunately, the carbon content in the tapping was lower than calculated since the experimental set-up of the methane burner caused a reduction of the CO, CO_2, H_2 and H_2O produced.

Concerning the slag composition, similar requirements are recommended. Also here, the zinc content should be very low to label the process as successful. According to Table 5-4, the obtained values of Zn could be lowered as well as those of lead, which is also very important regarding the further utilization of the slag. Similar to carbon in the metal phase, iron was oxidized due to some problems with the heat supply using the methane burner. Although the lambda value (air number) was set below one, an incomplete mixture of the burner gases led to inhomogeneous combustion behaviour with a subsequent undesirable but unavoidable partial oxidizing atmosphere.

Theoretically, the dust obtained should consist of mainly ZnO. Of course, a total recovery is impossible due to several reasons (e. g. distribution coefficient, temperature, kinetic effects, etc.) and there is always a significant amount of carry-over material. However, for the dust phase, the results were quite good. A slightly increased lead concentration was recognized, but this would not pose a big problem for direct utilization in the primary zinc industry, since an upstream process prior to the zinc electrolysis is always a Pb/Ag separation.

Only the concentration of the halides is too high, but the results achieved are based on an unavoidable error. Due to the construction of the off-gas pipes attached to the TBRC, an unknown quantity of dust always sticks to the inner wall of the pipes. Since the clinkering experiments were performed using the same experimental set-up, some chlorine and fluorine were settled inside the off-gas system, which was removed later when the second step of the process was performed. Therefore, the realistic Cl and F content would be in the range of 0.37 and 0.09 %, respectively, which would be a very satisfying result since it can be compared with washed Waelz oxide (0.2 % Cl and 0.1 % F).

As a final point, the presented experiment should be compared to ones where fossil carbons were used as carburization and reducing agent, respectively. Basically, the results in the achieved values for each phase were very close, but one important difference could be observed. Due to the fact that renewable resources like charcoal originated from biomass do not carry any sulphur with them, this important factor can be neglected for process modelling. For instance, in the case that sulphur is released to the off-gas stream, an additional gas cleaning unit has to be attached, to remove the SO_2 produced. However, the big advantage of course is the non-existent attribution of the released CO_2 to the greenhouse gas because of the origin of the reducing agent.

Similarities can be stated for the sulphur content in the iron alloy. Because of the negligibly low S amount of biomass-derived charcoal, it was almost not detected in the spark analysis. Since sulphur is known as a steel parasite, it is usually removed prior to the steel production process in the BOF. In the case of charcoal utilization in the “2sDR” process, desulphurization of the generated iron alloy does not have to be performed.

Figure 5-11 illustrates the mass flow of the second step of the “2sDR” process during continuous operation. After tapping the obtained heavy metal-free slag, the iron bath has to be re-carburized again and then, clinkered EAFD can be charged onto the liquid metal bath once more. At this point, the heavy metal recovery starts, similar to the descriptions mentioned earlier. Of course, due to the iron reduction, the quantity of the iron alloy produced increases, so that after several batches, a specific quantity of iron has to be tapped.

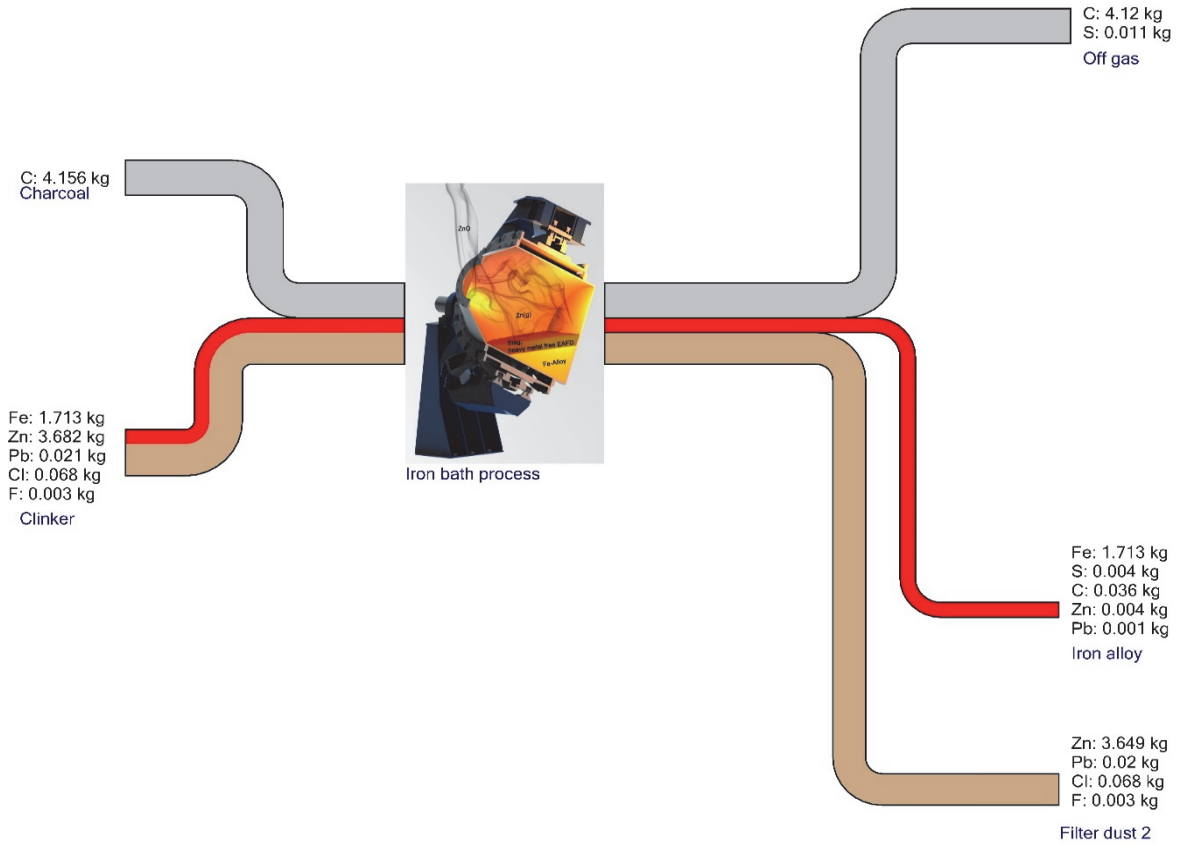

Figure 5-11: Mass flow of the second step during continuous operation of the process

Concluding, it can be stated that a novel process was invented that can treat different types of wastes using a carbon-containing iron bath. Although the process was designed using commercially-available coke, charcoal would be an attractive alternative in the near future. That means the technology is available, but economic considerations have to be performed to identify the appropriate carbonaceous material.

6 Product optimization of the Waelz process

The main product of the Waelz process is the so-called Waelz oxide; its main component is zinc, or rather ZnO. Unfortunately, it is contaminated with halides, which find their way into the gas phase by vaporization or carry-over. The origin, stated earlier, can be found in the input material of the Waelz kiln, mostly EAFDs where chlorine as well as fluorine originates from coatings on steel scrap, the major feed material of the electric arc furnace, where the dust was generated.

However, a detailed description of the generation of the dust as well as its chemical composition can be found in the previous chapter.

Although the Waelz process has some remarkable disadvantages, roughly 80 % of the recycled steel mill dusts are processed using this method. The process set-up of this recycling method is generally very simple. The residues, mostly EAFDs, are mixed with slag, forming additives and reducing agents and agglomerated, resulting in micropellets. The material is forwarded into the upper part of the rotary kiln. Usually, the average length of the kilns is 60 m, with a diameter of 3.6 m. The material moves through the kiln brought about by the rotation as well as the slight decline of the tube, heating up slowly. At the beginning, the charged material is dried and with the increase in temperature, first reactions start. Among others, the thermal decomposition of carbonates and sulphates, the reduction of Fe_2O_3 as well as the starting Boudouard reaction can be named as representative reactions around 900 °C. After passing a little bit more than the first half of the kiln, the main reactions start, since the temperature of the feed material increases up to 1,200 °C. That means that most of the zinc is reduced and volatized and the wustite obtained from the first half of the kiln is converted to iron. Shortly after zinc leaves the bed, it gets immediately re-oxidized to ZnO, and further leaving the kiln in the upper part. The remaining zinc-free slag moves forward toward the discharge head. Nowadays, a huge number of the Waelz kilns use the SDHL technology, which reduces the demand for coke as well as the necessity of the burner unit. Instead of the external heat supply, air is blown on top of the Walz slag that re-oxidizes the iron, thereby releasing heat energy into the kiln with this reaction. Due to its technology, the Waelz process runs without any extra energy supply. Finally, the slag is discharged at the lower part of the kiln and cooled, representing the second product of the process [123; 126; 157].

The obtained products, Waelz oxide (WOX) and Waelz slag, are very difficult to process in further metallurgical operations, since the quality is inferior. As an example, the above-mentioned halides contaminate the WOX, leading to subsequent cleaning steps to be a suitable input material in the primary zinc industry. Therefore, several options are available,

which were pointed out in the previous chapter. In the following sub-chapter, the most common method, the washing of WOX with Na_2CO_3, is described as well as an alternative method, using pyrolysis gas.

In the case of Waelz slag, the major component is iron (as wustite); several other heavy metals, such as Cr, Ni, etc., and the common slag components (SiO_2, Al_2O_3, CaO and MgO). In earlier times, it was possible to use the obtained slag for road construction or other construction purposes. Nowadays, it is used for the building of disposal sites, but it still contains some quantities of heavy metals, which is why this utilization method might be forbidden in the near future, or is actually already prohibited in some countries. Nevertheless, the recovery of these heavy metals as well as the iron is interesting to produce a ferroalloy and a heavy metal-free slag which can be utilized again in road construction, to avoid the cost-intensive disposal. For this, a recycling method will be presented that is able to treat this material by using charcoal and to obtain the aforementioned products according to [162].

Table 6-1: Overview of several possible materials fed into the Waelz kiln, in [wt-%] [126]

	Zn	Pb	Fe	FeO	Cu	Al	Cl	C	SiO2	H2O
Filter cake/ Cupola furnace	31	3	-	10	0.2	-	0.4	11	15	45
Dust from copper and brass industry	43	20	-	0.6	3	-	5	0.6	1	0.3
Dust cupola furnace	31	0.1	-	23	-	-	0.5	5	1.3	0.4
EAF dust	23	0.1	-	35	0.1	-	0.6	2	1	10.6
Lead dust	2	68	-	5	-	-	0.2	2	-	10.4
Zinc-lead oxide	44	15	-	4	0.4	-	4	0.6	1	1.8
Neutral leach Residue	18	7	-	33	1.6	-	-	0.2	3	30
Galvanization dross	92-94	1.0-1.6	1-3	-	-	-	-	-	-	-
HD galvanizing ash	60-75	0.5-2.0	0.2-0.8	-	-		2-5	-	-	-
Cont. galvanizing ash	65-75	0.1-0.5	0.2-0.8	-	-	0.1-0.5	0.5-2	-	-	-
Die-casting dross	90-94	0.1-0.2	low	-	-	1-7	-	-	-	-
Sal skimmings	45-70	0.5-2.0	0.2-0.8	-	-	-	15-20	-	-	-
Brass fume	40-65	0.5-7.0	1-2	-	-	-	2-7	-	-	-
Die-casting ash	55-60	0.1-0.2	low	-	-	3-10	low	-	-	-
Ball mill ash	55-65	0.1-1.0	0.2-0.8	-	-	-	2-5	-	-	-
Zinc dust/overspray	92-95	1-2	0.1-0.5	-	-	-	-	-	-	-

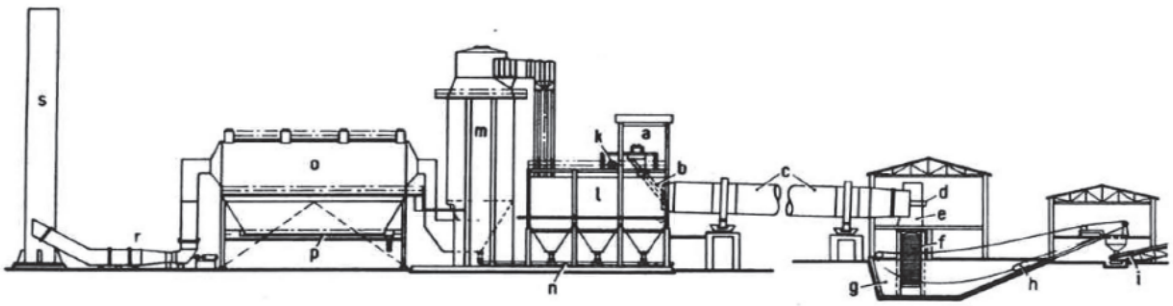

Abb. 4/35. Wälzanlage (N 32, Bd. 3, S. 430)
a = Materialaufgabe, b = Einlaufschurre, c = Wälzofen, d = Zentralgebläse, Brenner, e = Austragskopf, f = Schlackenschurre, g = Schlackengrube, h = Schrapper, i = Schlackenabtransport, k = Sperrluftgebläse, l = Staubkammer, m = Verdampfungskühler, n = Voroxidtransport, o = Elektrofilter, p = Wälzoxid-Transport, r = Abgasgebläse, s = Kamin

Figure 6-1: Waelz kiln for the processing of EAF dust a: Material feeding b: Reel carriers c: Waelz rotary kiln d: Burner e: Discharge Head f: Slag reel carriers g: Slag pit h: Scrapper i: Slag removal k: Sealed air fans l: Dust settling chamber m: Evaporation cooler n: Low grade Waelz oxide transport, o: Electrostatic precipitator, p: Waelz-oxide transport, r: flue gas blower s: stack [157]

Table 6-2: Overview of typical values [wt-%] obtained in the Waelz process [126]

	Zn	Pb	Cd	F	C	FeO	Fe(met)/Fe	Basicity
Waelz slag	0.2-2.0	0.5-2	<0.01	0.1-0.2	3-8	30-50	80-90	
basic								1.5-4.0
acid								0.2-0.5
Waelz oxide	55-58	7-10	0.1-0.2	0.4-0 .7	0.5-1	3-5	-	
Leached waelz oxide	60-68	9-11	0.1-0.3	0.08-0.15	1-1.5	4-7	-	

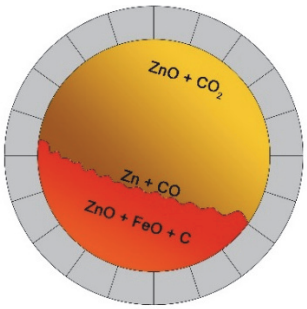

Reactions in gas phase (Oxidising)

$Zn + ½\ O_2 \rightarrow ZnO$

$CO + ½\ O_2 \rightarrow CO_2$

$ZnO + CO + O_2 \rightarrow ZnO + CO_2$

Escaping CO gas and Zn vapour

Reactions in the charge (Reducing)

$ZnO + CO \rightarrow Zn + CO_2$	$FeO + CO \rightarrow Fe + CO_2$
$CO_2 + C \rightarrow 2\ CO$	$CO_2 + C \rightarrow 2\ CO$
$ZnO + C \rightarrow Zn + CO$	$FeO + C \rightarrow Fe + CO$

Figure 6-2: The main reactions in a Waelz kiln [126]

6.1 Clinkering of Waelz oxide

The raw material within this topic is crude Waelz oxide, which is obtained in the off-gas system of the Waelz process. The aim here was to use the top blown rotary converter (TBRC) for an alternative method for clinkering as a subsequent treatment of crude Waelz oxide. Therefore, two different energy carriers for providing the heating energy for the furnace were utilized and compared.

Usually, the most common method for cleaning the WOX is the washing using soda bicarbonate (Na_2CO_3), as described in Chapter 5.1. In the following section, the procedure of the washing step will be described:

At first, the raw material (crude Waelz oxide) is combined with the filtrate of the second leaching step. By adding dissolved sodium bicarbonate at a pH of 9 and temperatures between 60 and 90 °C, the solid material is usually leached for 1.5-2 h. More than 90 % of the alkalis as well as the halides can be removed during this process step. The next part is a second washing step, where the filter cake obtained in the first step is leached. The applied liquid is tap water at a temperature of 40 °C. The retention times of the leaching process are set around 1 h. The remaining chlorides, sulphates and traces of fluorides can be removed using this method. The final solid liquid separation guarantees a relatively pure solid which can be sold as “double leached Waelz oxide” to primary zinc producers. The remaining liquid is returned to the first step, as already stated. This process is often applied by Waelz kiln operators but has a big disadvantage, since the wastewater has to be treated to be allowed to forward it to the sewage discharge. This is the reason why most of the washing facilities are located next to rivers or the sea, because of the fact that here, the permission to proceed the wastewater into the surface water is easier to realize. The disadvantage can therefore be summarized as follows [138; 145]:

- access to the sea
- big washing units
- difficult wastewater treatment, if no sea access is available
- additional washing step

The feed material of the clinkering process is the crude Waelz oxide, similar to the sodium bicarbonate cleaning step. The aim is to perform the heat treatment in a temperature range from 900-1,100 °C. Here, the halides like fluorine and chlorine as well as some heavy metals (lead and cadmium combined to oxides, sulphides, sulphates and chlorides, fluorides) are evaporated while ZnO remains in the solid phase. It is mandatory that for this purpose, the furnace has to be operated in an oxidic mode. The following subchapter will give a more detailed overview of the experimental set-up of the process [117; 138].

6.1.1 Experimental set-up of the clinkering trials

The clinkering experiments to treat crude Waelz oxide were performed in a top blown rotary converter at the Chair of Nonferrous Metallurgy, Montanuniversitaet Leoben. The volume of the TBRC is roughly 80 litres, depending on the thickness of the refractory material. That means an optimum charge of material input is approximately 20-30 litres to guarantee a good

mixing behaviour as well as a satisfying free board to exhaust volatile matter. The rotation speed as well as the angle of the vessel can be adjusted as favoured. A drawing of the furnace can be found on the left-hand side in Figure 6-3. The burner is usually operated by a methane-oxygen mixture with a maximum capacity of 75 kW. The achievable maximum temperature, depending on the investigated process and the refractory material, can be defined as 1,750 °C to 1,800 °C. Furthermore, since the stoichiometric ratio between methane and oxygen can be varied, it is also possible to run the aggregate under oxidizing and reducing conditions.

Since it was the aim to perform a heat treatment of crude Waelz oxide using alternative methods, first trials were carried out with the use of the conventionally applied methane-oxygen burner. Afterwards, a second burner provided the energy by purging pyrolysis gas, produced in the twin screw reactor located along the TBRC, into the vessel, to use a CO_2-neutral source for heating the furnace.

Special focus is laid on differences in the achieved results between the different energy carriers used for heating the clinkering furnace. The amount of clinkered material should be in the range of 20 kg of crude Waelz oxide, where special focus lies on the temperature profile of the kiln as well as possible contaminations in the generated product by the pyrolysis gas.

As a raw material, crude Waelz oxide was used and clinkered under oxidizing atmosphere to selectively vaporize contaminations like halides and lead oxide, as explained before. These first tentative trials should show the reachable temperatures and handling of the combination of TBRC and twin screw reactor as well as the behaviour of Waelz oxide under the atmosphere of burned pyrolysis gas.

To utilize the pyrolysis gas as a burner gas in the TBRC, the fume hood of the metallurgical furnace was slightly modified to guarantee a total combustion of the pyrolysis gas. Therefore, a second burner hole was drilled into the fume hood of the TBRC to utilize the alternative burner gas. The conventional TBRC burner was used as the oxygen supply for the combustion of the pyrolysis gas. A draft of the modified fume hood can be seen on the right side in Figure 6-3.

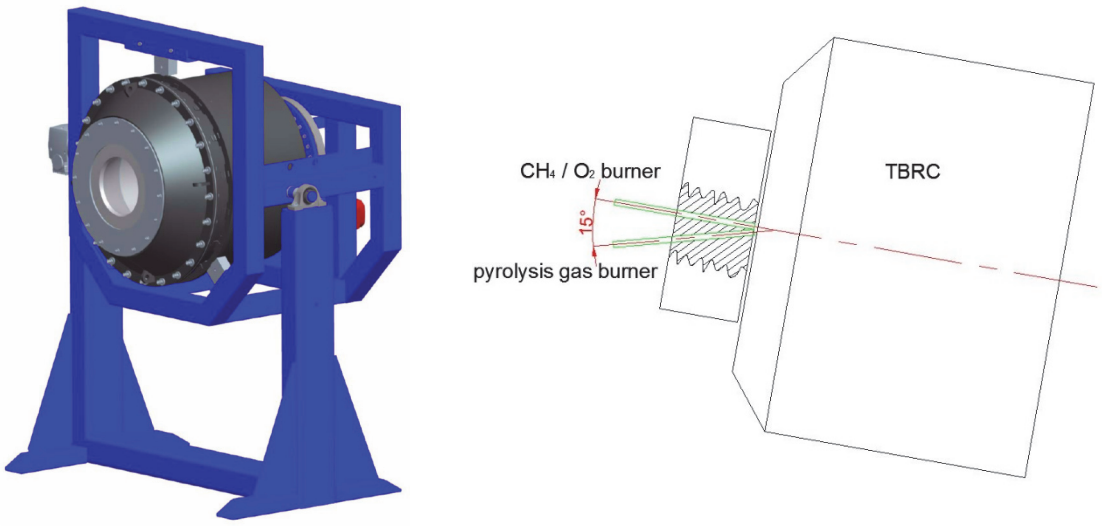

Figure 6-3: Drawing of the TBRC at the Chair of Nonferrous Metallurgy (left) as well as a draft of the optimization of the fume hood (right)

The draft of the experimental set-up can be seen in Figure 6-4 . Furthermore, different burner gases were used and compared regarding their applicability in this furnace and for this purpose, respectively. Therefore, the initial idea was to divide the clinkering experiments into three single trials, as defined below:

- 100 % methane; Lambda (air ratio) = 1.0
- 100 % pyrolysis gas; Lambda = 1.0
- methane/pyrolysis gas mixture; Lambda = 1.0

As described initially, the pyrolysis gas was provided by the twin screw reactor. The carbonized biomass was olive tree cuttings, which were pyrolized at a maximum temperature of 900 °C and retention times around 2 h, since here, the quality of the charcoal allows the maximum quantity of the pyrolysis gas. If the carbonization temperatures were lower, too little gas would be produced and the quality of the charcoal obtained would be too low. Otherwise, decreasing retention times would lead to an enormous amount of gas production, which would lead to a blow out of the charged material inside the TBRC. To guarantee the total combustion of the pyrolysis gas, the occurred off-gas at the fume hood of the furnace was monitored by applying an additional gas analyser to the off-gas hood of the TBRC, since the production of CO would cause under stoichiometric conditions.

At the very beginning, the TBRC was slowly heated up to 1,200 °C. After reaching this temperature, the crude Waelz oxide was charged into the furnace, whereby the clinkering process started shortly after the heat-up of the input material. During the treatment time, samples were taken every 30 min. to verify the success of the clinkering step. Lastly, the treated Waelz oxide was tapped and cooled after 2 h. The charged material itself was

forwarded to the furnace, without any agglomeration like a pelletizing step. However, during the process of crude Waelz oxide, the material was agglomerated to pellets anyway.

The previously described experimental procedure was performed in each of the trials except for the second one with 100 % pyrolysis gas; in this case, just one sample was taken during the tapping.

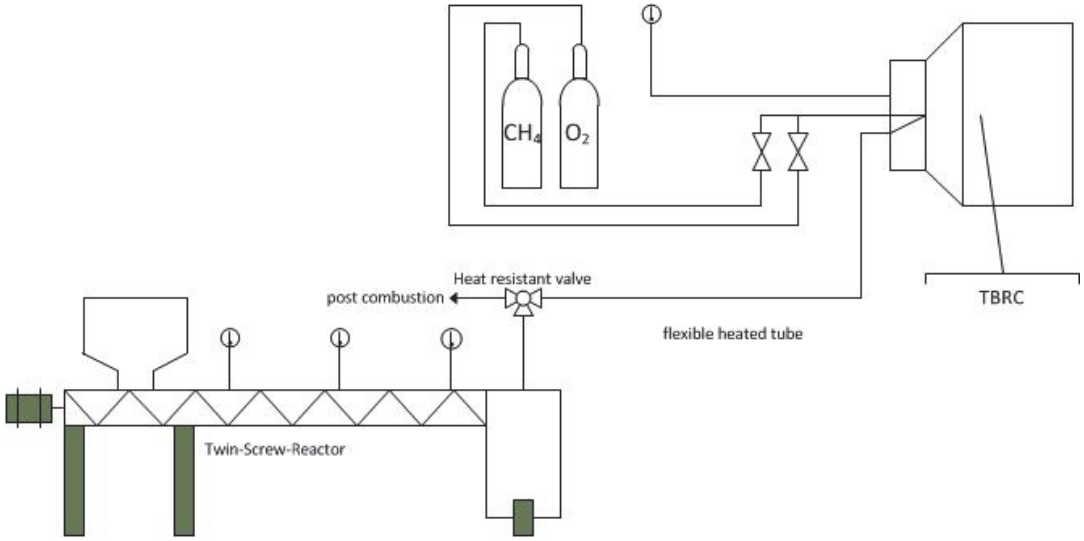

Figure 6-4: Draft of the experimental set-up with the twin screw reactor, the heated flexible tube and the TBRC

6.1.2 Results of the alternative cleaning step

In this chapter, the results of the clinkering experiments carried out at the Chair of Nonferrous Metallurgy are described.

6.1.2.1 First trial; 100 % CH_4

As stated earlier, the first clinkering experiment was performed with CH_4 as a burner gas at 1200 °C and a retention time of the crude Waelz oxide of 2 h. Actually, the trial could be carried out without any problems. Since it was the first experiment in this test series, there were some decreases in temperature when taking a sample, as pictured in Figure 6-5. The results of the chemical analysis of the clinkered material can be seen in Table 6-3 and Figure 6-6. In comparison to previous projects performed with a synthetic mixture of a common Waelz oxide, the results of the first study show good efficiency in the removal of volatiles [151]. The treatment time in this case seems to be at least 60 min., as can be seen in Table 6-3. Longer clinkering times still have a small impact on the removal of alkalis as well as on lead.

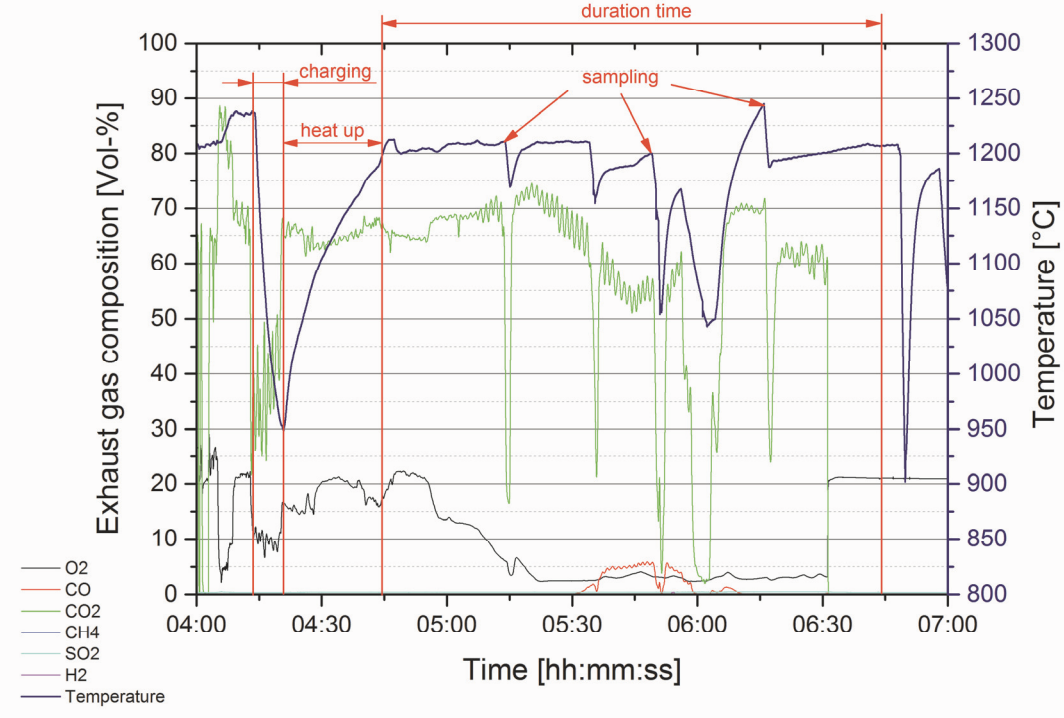

Figure 6-5: Recording of the temperature profile as well as the evolution of the gas composition during the first experiment

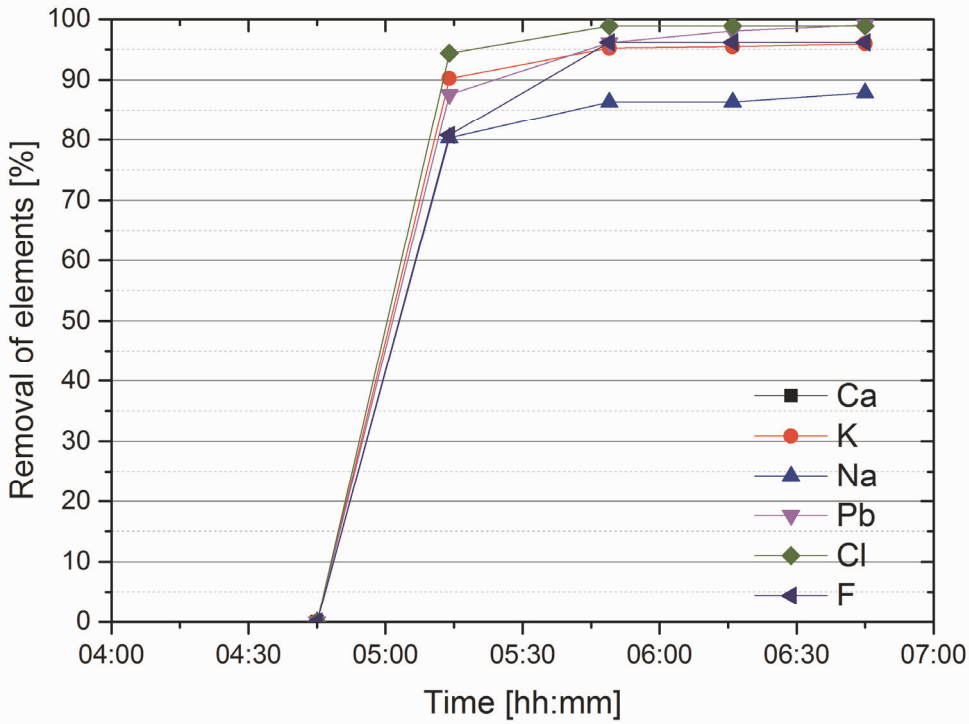

Figure 6-6: Illustration of the removal of the disturbing elements in the first trial

In Table 6-3, the success of the removal of disturbing elements in the first experimental procedure is given.

Table 6-3: Results of the chemical analysis from the samples taken during the first experiment

		Removal of Elements [%]				
Sample No	Time [min]	K	Na	Pb	Cl	F
1	30	90.24	80.30	87.57	94.40	80.77
2	60	95.24	86.36	96.12	> 98.90	> 96.15
3	90	95.48	86.36	98.06	> 98.90	> 96.15
4	120	> 95.95	> 87.88	> 99.03	> 98.90	> 96.15

6.1.2.2 Second trial; 100 % pyrolysis gas

The second trial was performed with the pyrolysis gas originated from the carbonization of olive tree cuttings. The gas was collected at the exhaust pipe of the carbonization unit and redirected by a heated flexible tube into a heat-resistant steel pipe, which served as the burner. This steel pipe was fixed to the second burner hole (Figure 6-3). The carbonization unit was started 1.5 h in advance to fill the carbonization reactor with biomass/charcoal to achieve constant (steady-state) pyrolysis gas for the clinkering step.

As can be seen in the resulting temperature graph in Figure 6-7, it is hardly possible to use the pyrolysis gas only in connection with oxygen for heating purposes, since the gas consists of mainly H_2 and CO (cf. Table 6-4). This is the reason for the reactivation of the methane burner after approx. 45 minutes (Figure 6-7) to guarantee 1,200 °C treatment temperature of the crude Waelz oxide. By activating the CH_4, the temperature increased very fast, since the combustion energy of methane is very high. As shown in Figure 6-7, shortly after starting the methane input, the furnace achieved the required 1,200 °C and the clinkering process could be finished.

Table 6-4: Specific combustion enthalpy of selected gas species at 900 °C

Gas species	Specific Combustion Enthalpy [MJ/m³]
CH_4	35.7
CO	2.2
H_2	2.3
Pyrolysis gas [1]	12.3

[1] Details are given in Chapter 3.2

Furthermore, clogging resulting from the incomplete combustion of the pyrolysis gas shortly after fixing the gas analysing system could be recognized. This is the reason why the graph of the exhaust gas composition is incomplete, as illustrated in Figure 6-7. Moreover, due to the high amount of soot which is in the pyrolysis gas, there was a significant increase in the dust load in the off-gas cleaning system (Figure 6-8). In the second trial, a single sample was taken

at the end. The aim was to have no influencing factors - like taking samples - on the result of the clinkering process with pyrolysis gas.

In Table 6-5, the results of the thermal treatment are listed. Although the experimental procedure was not satisfying, the obtained results are the same as in the first trial. The reason for this behaviour is that the halides, which are in the crude Waelz oxide, are very volatile even at lower temperatures. Moreover, the high amount of water originated from the combustion of the pyrolysis gas was responsible for the good removal efficiency, allowing a kind of hydrolysis. By comparing these results with the ones from the theoretical Waelz oxide mixture, a good removal of disturbing elements could be observed.

Table 6-5: Result of the chemical analysis obtained in the second trial

		Removal of Elements [%]				
Sample No	Time [min]	K	Na	Pb	Cl	F
1	120	> 95.95	> 87.88	> 99.03	> 98.90	> 96.15

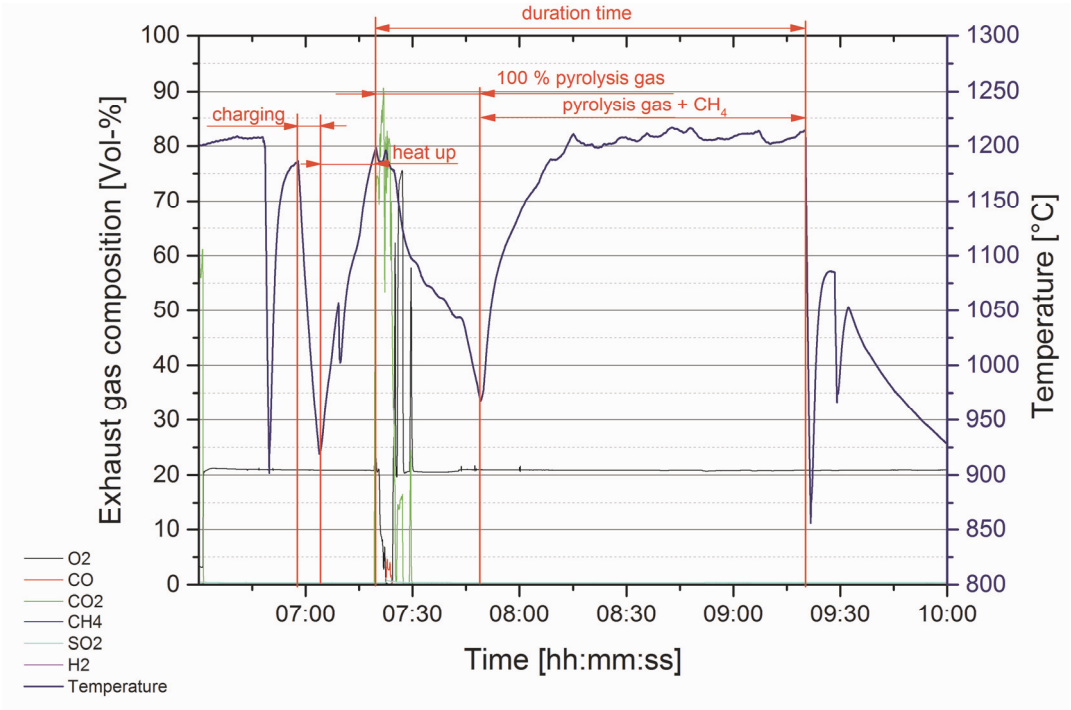

Figure 6-7: Temperature distribution and exhaust gas composition in the second experiment

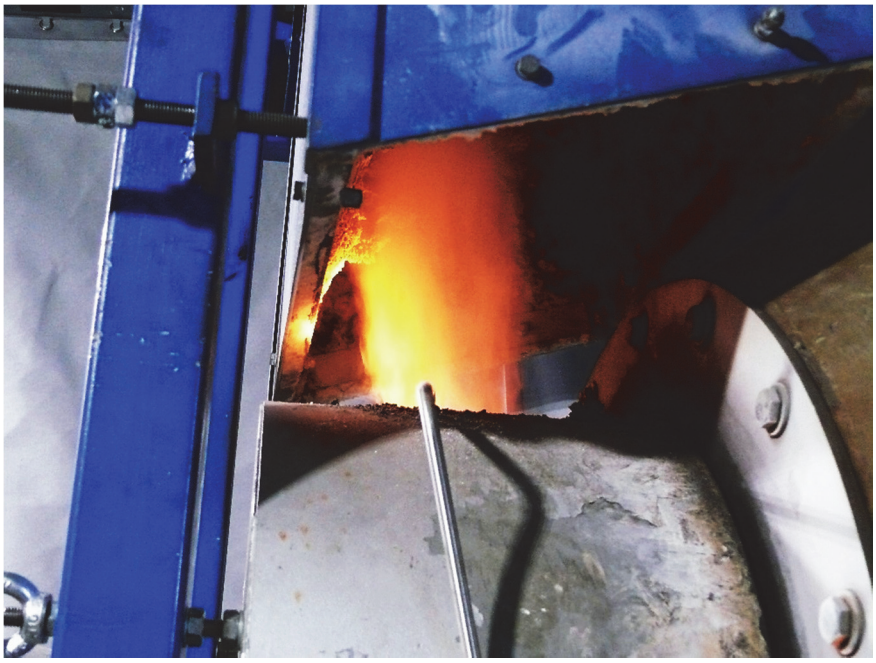

Figure 6-8: Representative picture of the increasing dust load of the off-gas when using pyrolysis gas

6.1.2.3 Third trial; pyrolysis gas / CH_4 gas mixture

The third experiment was performed using a pyrolysis gas/CH_4 gas mixture from the beginning of the trial as the burner gas. The experimental procedure concerning sampling was the same as in the 1st trial. Furthermore, the gas analysis worked more efficiently, seeing as more spare parts were prepared in advance for fast maintenance during the trial, due to the fact that the knowledge obtained from the second trial led to this action. With this, a total combustion of the gas mixture could be ensured, which means that no CO, H_2 or any other hydrocarbons were exhausted, since the gas analysis always showed actual data, as is described in Figure 6-9.

In Figure 6-10 and Table 6-6, the results of the chemical analysis are shown. Because there was an undesirable reduction step shortly after the 2nd sample taking, the chemical analysis showed worse results than in the first clinkering trials. Nevertheless, compared to typical clinkering processes, which were performed in the first two experiments, the achieved results were satisfying.

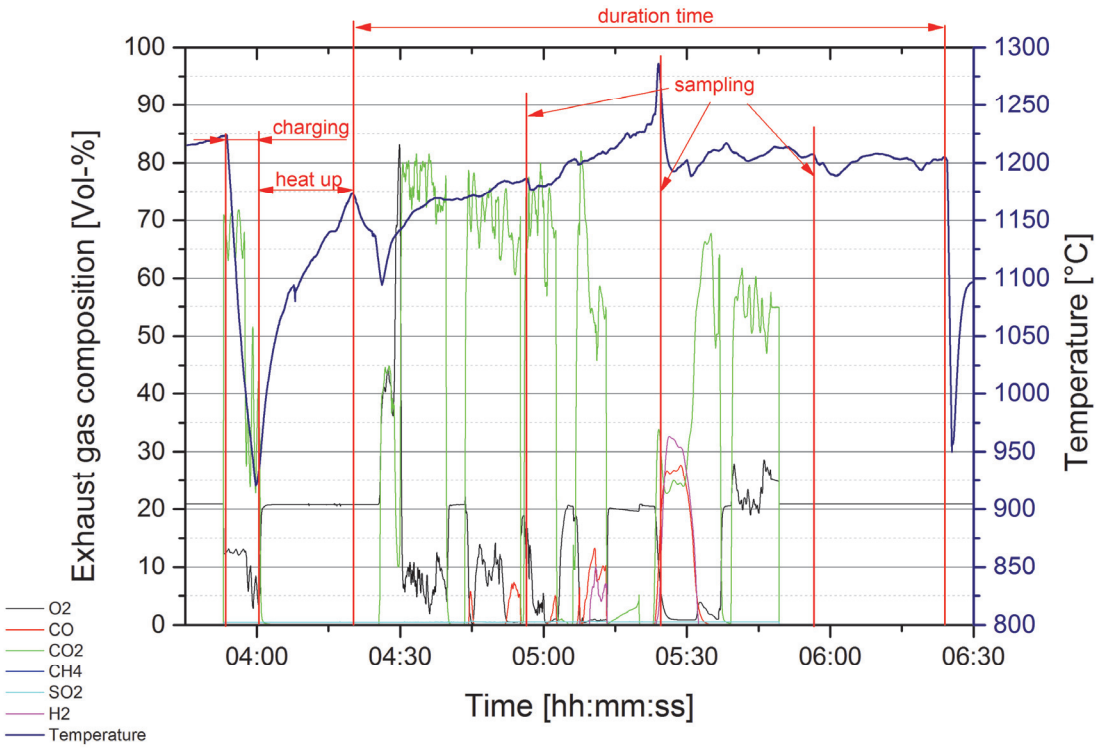

Figure 6-9: Plot of the temperature distribution as well as the exhaust gas composition in the 3rd experiment

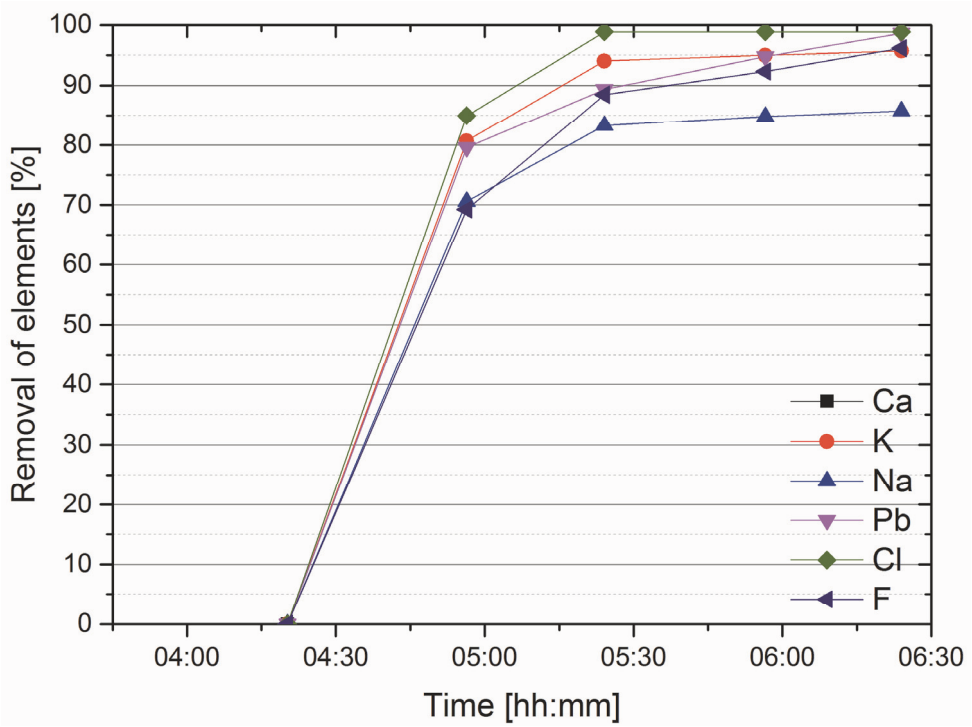

Figure 6-10: Development of the elements during the removal of the halides in the last trial

In Table 6-6, the removal of the elements during the clinkering process is listed.

Table 6-6: Tabulation of the removal of the elements during the 3rd experiment

		Removal of Elements [%]				
Sample No	Time [min]	K	Na	Pb	Cl	F
1	30	80.71	70.61	79.61	84.95	69.23
2	60	94.05	83.33	89.32	98.90	88.46
3	90	95.00	84.85	94.76	98.90	92.31
4	120	95.71	85.76	98.64	> 98.90	> 96.15

In this part of the chapter, a short conclusion of the experiments is given and the removal of disturbing elements such as chlorine, fluorine, as well as lead, sodium and potassium in a top blown rotary converter are described. In Figure 6-11, a picture of the tapping after the treatment is shown. The material itself was pelletized during the clinkering step, which was the desired process, as expressed in a previous section.

Figure 6-11: Tapping of clinkered material from the TBRC

The first trial was carried out with 100 % CH_4 as the burner gas for two hours of clinkering time at 1,200 °C. The results show a good yield of the desired elements. Even with low clinkering times (1 hour), there was a significant decrease in the halides, alkalis and lead. Therefore, the percentage of these elements went down with increasing treatment time.

The second trial was done by using pyrolysis gas from the twin screw reactor. For that reason, the pyrolysis unit was charged with 15 kg of olive tree cuttings. To achieve high amounts of pyrolysis gas, high carbonization temperatures were chosen. The gas was redirected by a flexible heated tube and passed into the TBRC using a steel pipe. In doing so, the main burner

of the TBRC served as a source for the oxygen. As already mentioned, there was a temperature loss due to the high amount of hydrogen in the pyrolysis gas and therefore, the main burner system was switched on again. Nevertheless, the clinkering process itself was a success if the results of the first and second trial are compared.

The combination of both experiments resulted in the last trial, where both gases were used in combination. In principle – because of the problems which occurred in the 2nd experiment – the last trial was similar to the previous one, but more attention was paid to the gas composition and the temperature inside the TBRC. However, there were some troubles with the total combustion of the gas mixture, which were fixed very fast. The results regarding the chemical composition of the clinkered material were good, comparable to the first two tests. It should be mentioned that the experimental procedure in this case was very hard to control, due to the parallel operation of facilities. This considerable effort in installation engineering (e.g. pyrolysis gas delivery just in time) seems to be disadvantageous in the case of an up-scaled industrial process.

Finally, Figure 6-12 shows a picture taken shortly after the tapping. The agglomerated treated Waelz oxide is available in a particle size between 1 and 10 cm.

Figure 6-12: Hot clinkered material soon after tapping

Altogether it could be seen that the top blowing rotary converter is a possible furnace for clinkering. It should be mentioned that for this kind of process, an upstream agglomeration step is required to prevent blowouts of the crude Waelz oxide during the charging process. However, the utilization of pyrolysis gas for heating purposes is not very reasonable; the use of a combined methane/pyrolysis gas burner may be considered, although the dust load in the

alternative heating agent is very high. For the moment, it seems that the best utilization possibility of pyrolysis gas is its use as a reducing agent or the combustion for producing electrical energy or process heat.

6.2 Treatment of Waelz slag

The aim of this study is the recovery of Fe, Cr, Ni as well as other heavy metals in an iron alloy and to obtain ZnO and PbO in the off-gas in the reduction of Waelz slag. Therefore, charcoal was utilized to serve as a reducing agent to save CO_2 emissions, to minimize the contribution to the global climate change by using a novel recycling process.

It was already mentioned that the Waelz slag is usually used in Europe in the field of landfill building, in earlier times even for road construction. Since the legal requirements will change in the near future, new developments for cleaning the slag form remaining heavy metals have to be found. At the moment, there is general research in the field of slag utilization as well as recycling being conducted; details are published in [162]. For this, a short summary will serve as a basis to reflect the key facts for this kind of treatment. According to this research, four different possibilities are available as to how to deal with this topic. There might be other ones like leaching, SX, etc., but since this chapter will show the application of charcoal, they are not taken into account in the following section.

The first method presented treats the residue in a furnace at temperatures around 1,050 °C, which means in the solid state. Carbon is added to the slag granules and according to thermodynamics, carbon is converted by means of the Boudouard reaction to CO by the CO_2 originated from the combustion of the methane burner. The CO/H_2 mixture (the H_2O is reduced, as well) acts as a reducing agent to recover mainly Zn and Pb. Unfortunately, this theory does not take into account the bad kinetics, and the resulting yields of this process are very low.

Further possibilities are the utilization of pyrolysis gas, like it was already used here [21]. Since the gas contains a huge amount of reducing agents, it might act as a reducing gas for the recovery of heavy metals, in this case Zn, Fe and Pb. The Waelz slag was charged into a retort and heated to temperatures between 1,000 and 1,150 °C. The hot pyrolysis gas was forwarded from the twin screw reactor into the bottom of the retort. The gas was flushed form the bottom to the top of the furnace. Zinc should be reduced and vaporized and also be exhausted at the top. First tentative trials showed a good Zn removal efficiency, higher than 90 %. Since these experiments were very satisfying, large-scale experiments were performed which are mentioned in the following reference [162].

The previous methods illustrate a “solid (Waelz slag)-solid (carbon)” and “solid-gas pyrolysis gas)” reaction system, where the Waelz slag stays in the solid state. Another possibility is to use the iron bath process presented in the previous chapter for the recycling. The difference is that the first clinkering step is not necessary, since the volatile matter like chlorine and fluorine compounds was already removed in the Waelz kiln. However, the basics are similar, since the residue is charged onto a carbon-containing iron bath. That leads to a very high Zn removal in the slag as well as a total recovery of iron, which can be found in the liquid phase of the process. The high yields as well as the process set-up lead to the conclusion that this type of “liquid-solid” process is a potential solution for the subsequent treatment of Waelz slag [162].

Finally, the last option should be mentioned, which also belongs to the group of “liquid-solid” process types, performed with a small but significant difference. Instead of an initial molten iron bath, an iron alloy is produced batch-wise during the process. In particular, the goal was to produce an iron alloy with the implementation of a submerged arc furnace, where a representative drawing is pictured in Figure 6-13. The remaining zinc oxide is reduced and volatized as well, obtained and collected in the bag house filters of the site. Hence, the treated Waelz slag is free from heavy metals afterwards and can be forwarded for further utilization, such as for road construction purposes. This way of treatment was chosen to be operated with charcoal as a reducing agent, so the experimental set-up as well as the obtained results will be presented in the following sub-chapters.

Figure 6-13: Schematic drawing of the applied submerged arc furnace [163]

6.2.1 Experimental procedure

The trial was performed in a submerged arc furnace, with a capacity of 50 kg and maximum power of 45 kW. The furnace was lined with Ankermix from RHI AG and with a graphite containing ramming mix, respectively, since the operation mode of the furnace was with direct current. Table 6-7 shows the initial composition of the Waelz slag, which was treated in this novel recycling process. As can be seen from the table, the residue contains a relatively high and untypical amount of ZnO as well PbO at well-optimized operations, but according to the literature [123], these values are still realistic. Because of the fact that the residual feed material was grainy, agglomeration did not have to take place. If an upscaling of the process is considered, a briquetting or pelletizing step might be necessary since a certain amount of gas permeability is required if more Zn is contained in the Waelz slag.

Table 6-7: Chemical composition of the applied Waelz slag

Species	ZnO	PbO	Cu_2O	FeO	MnO	CaO	MgO	Al_2O_3
wt-%	10.3	1.2	0.3	38.2	4.5	21.1	4	2.7
Species	SiO_2	S	Sn	C	Cr_2O_3	NiO	Sum	
wt-%	6.2	1.6	0.1	3.2	0.6	0.1	94.0	

Based on the fact that a specific basicity of the final recycled slag is recommended, some quartz was added, also to influence the slag smelting temperature in a positive way. Since the CaO content in the Waelz slag is relatively high, the main constituent of the additives was quartzite. This leads to a decrease in the slag smelting behaviour, if the total recovery of Zn, Pb, Cu, Fe as well as Sn, Cr and Ni is considered. The slag consists of mainly CaO and traces of MgO, Al_2O_3 and SiO_2. The quaternary diagram CaO-MgO-SiO_2-Al_2O_3 can be observed in Figure 6-14. It is shown that the SiO_2 addition caused lower melting temperatures. The chemical composition of the additive quartz sand is represented in Table 6-8, where it can be seen that it contains basically silicon oxide and traces of alumina and iron oxide.

Table 6-8: Composition of the additive, which was charged for slag forming purposes

Species	Fe_2O_3	Al_2O_3	SiO_2	Sum
wt-%	0.6	4.5	94.9	100

Finally, the proximate analysis (dry base) of the carbonaceous material is shown in Table 6-9. Instead of the usually mentioned ash content, the chemical composition of the material is given to get in formation of the ash constitution. However, since the amount of ash is relatively low, it can be neglected for the mass and energy balance. Basically, it can be stated that the fixed carbon content is very high, which underlines the utilization of charcoal in metallurgical furnaces. Since the original biomass is relatively free from ash (found in the bark), this type of carbon carrier is definitely suited for this purpose.

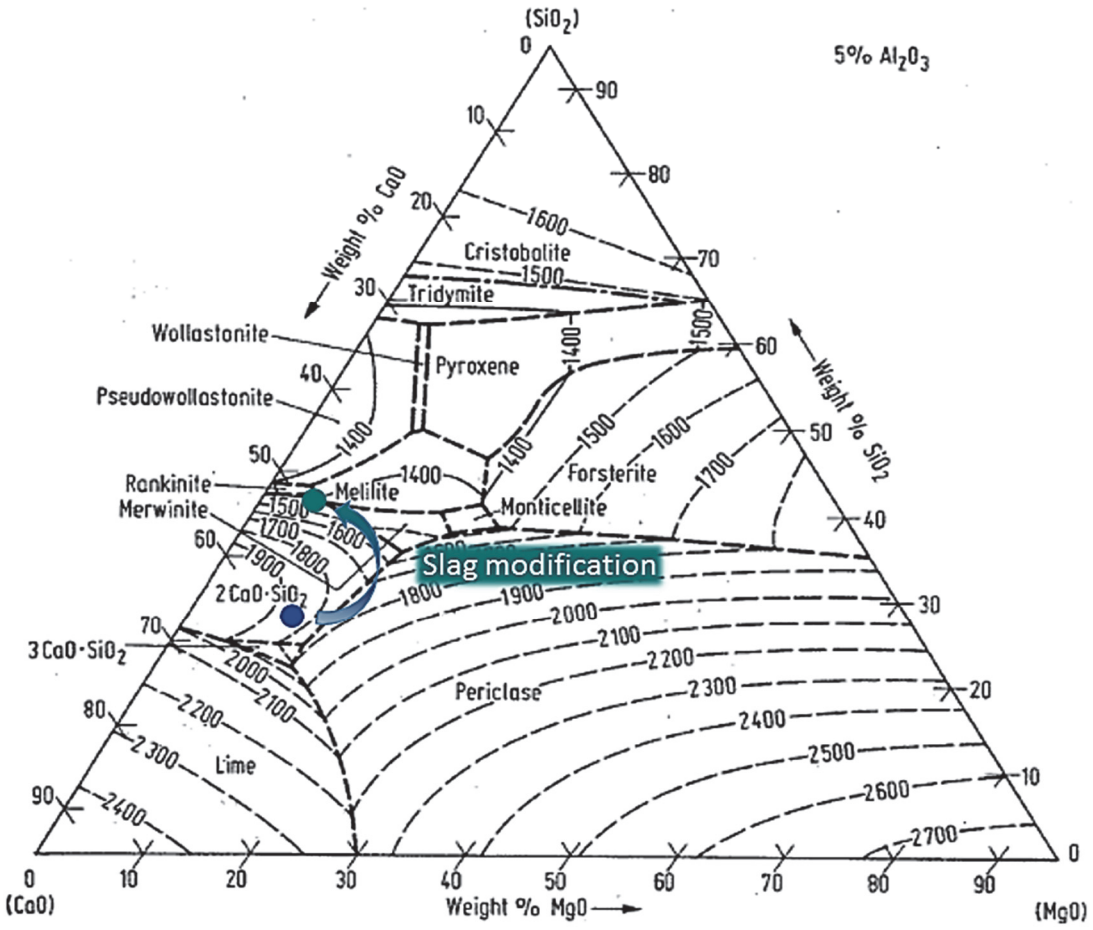

Figure 6-14: Evolution of the slag composition by adding quartzite [164]

Table 6-9: Proximate analysis as well as ash analysis of the charcoal originated from eucalyptus cuttings

Species	C_{Fix}	vol.*	SiO_2	CaO	MgO	Al_2O_3	Fe_2O_3	Na_2O	K_2O	SO_3	P_2O_5	Sum
wt-%	95.5	2.3	0.07	1.75	0.09	0.02	0.06	0.02	0.03	0.01	0.07	99.9

* volatiles

The feed material was weighted and mixed and charged into the furnace little by little, which was started with melting down a blast furnace slag, since it is known for its relatively neutral basicity and good melting behaviour. It was possible to produce a liquid base where the waste material can be molten down. To put it simply, the carbon reduces the oxidic metals which form a metal bath at the bottom together with the molten slag, floating on the metal. The basic principle as well as thermodynamics and kinetics have already been described in a previous chapter. In the case of Zn and Pb, they are volatized and leave the furnace as ZnO and PbO, respectively. Finally, the liquid phases are tapped and cooled down. Table 6-10 gives an overview of the charged materials.

Table 6-10: Overview of the materials charged into the SAF

Material	kg
Waelz slag	60
Quartzite	8
Charcoal	5
Sum	73

After solidification and cooling down, the slag can be separated from the metal and weighted. Regrettably, it was not possible to get the quantity of the dust generated during the process. The chemical composition and the amount can be estimated by recalculation via comparison of the feed material and the obtained products.

6.2.2 Results

Basically, it can be stated that the results obtained using this experimental set-up were very promising regarding the yields of the single elements, as can be seen in the Sankey diagram in Figure 6-15. Especially the recycling of iron was very successful. Only 0.32 % of the Fe input was left in the slag.

Furthermore, zinc could be reduced as well, whereby the fraction was forwarded to the gas phase where it was re-oxidized to ZnO, similar to lead, which partly evaporates as oxide during heat up.

In the case of chromium, there is a slight quantity of it in the remaining slag, but this could be avoided by upscaling the experiment. Since the reducing potential increases at higher temperatures (that can be guaranteed at bigger furnace sizes), the residual 17.75 % Cr of the overall Cr input can be reduced as well and found in the Fe alloy.

The carbon charged in the submerged arc furnace has two purposes; first, to reduce the oxides and second, to increase the carbon content in the iron melt. Here, the huge benefit of renewable carbons is underlined, because of the fact that the whole evolved C (as CO) is, according to the definition, CO_2-neutral.

With regard to the distribution of sulphur, it can be seen that it was mostly collected in the slag as well as combusted. That means for an industrial implementation of the present process, attention has to be paid to the removal of sulphuric components in the off-gas by applying a subsequent flue gas treatment, mostly based on calcium hydroxide (slaked lime).

Finally, the elemental distribution of copper should be mentioned. Since copper is one of the noblest elements within the Waelz slag, it will be collected in the metal phase. Usually, there

might be some concern when copper is found in iron alloys, as it is known to induce surface cracks in the hot rolling process. Therefore, in the field of construction steel production, the limit is set to < 0.15 % Cu in the iron alloy. As the Cu content in the iron alloy equals 0.85 %, it is far too high for simple steel processing. To utilize the produced ferroalloy for construction steel, it has to be diluted with other iron-containing resources like steel scrap in the steel plant. Furthermore, it is known that there are some steel grades which allow higher amounts of copper. It is known that contents of > 0.3 % Cu lead to a significant increase in the hardness (especially in extra low carbon steels, alloyed with titanium) as well as a higher resistance to weathering.

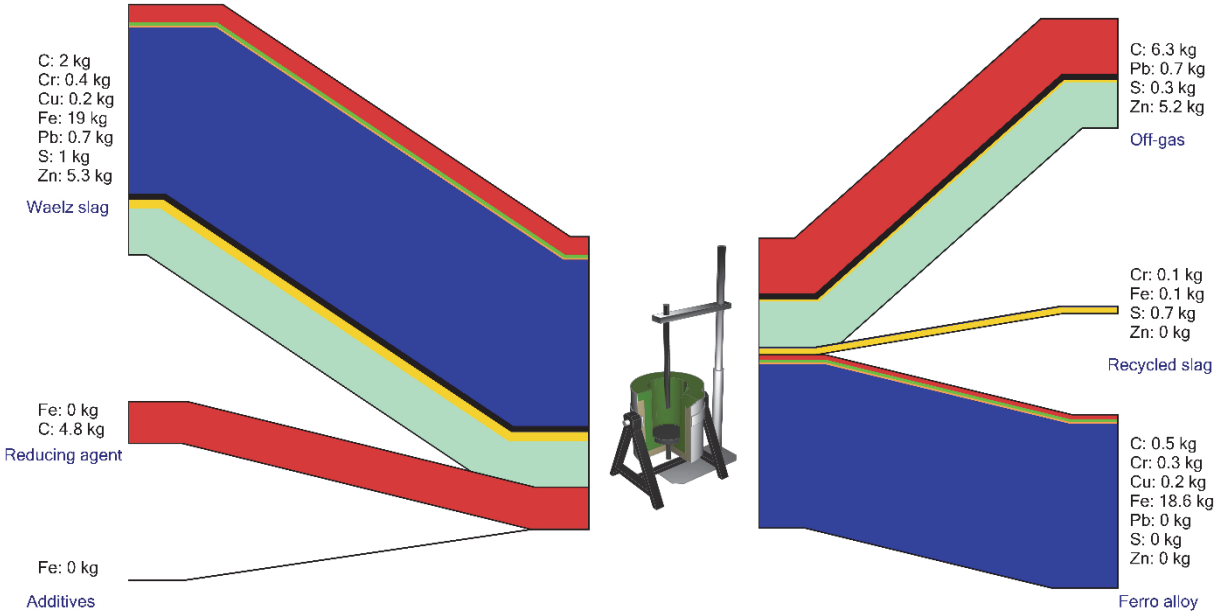

Figure 6-15: Sankey diagram of the applied Waelz slag recycling process

Concluding, it can be stated that a possible solution to get rid of the Waelz slag was presented, where future studies may lead to further implementation in industrial facilities. Nevertheless, it was shown that charcoal would be a suitable reducing agent, especially when low CO_2 emissions are required. Finally, it should be mentioned that the detailed studies in this field which also lead to this type of Waelz slag treatment can be found in the doctoral thesis of [162].

The big advantage of charcoal could also be pointed out in this case. No sulphur was added during the charging of carbonaceous material, since charcoal is free from sulphur. This means a possibly occurring sulphur in the off-gas system can be attributed to the fossil carbon fed in the Waelz kiln process. However, previous studies showed a definite utilization possibility for charcoal in the Waelz process that would finally lead to a sulphur-free process, if a submerged arc furnace is attached to a charcoal-operated Waelz kiln.

Table 6-11: Mass balance of selected elements obtained during the Waelz slag treatment in the SAF

		Zn		Pb		Cu		Fe		Mn		Si	
		kg	%	kg	%	kg	%	kg	%	kg	%	kg	%
Input	WS	5.26	100.00	0.71	100.00	0.19	100.00	18.95	99.81	2.21	100.00	3.41	49.01
	Q	0.00	0.00	0.00	0.00	0.00	0.00	0.03	0.18	0.00	0.00	3.54	50.97
	C	0.00	0.00	0.00	0.00	0.00	0.00	0.00	0.01	0.00	0.00	0.00	0.02
Output	Fe	0.03	0.50	0.01	1.34	0.20	100.00	18.62	99.68	0.95	56.85	1.17	17.32
	Slag	0.03	0.57	0.00	0.00	0.00	0.00	0.06	0.32	0.72	43.15	5.61	82.68
	Gas	5.21	98.93	0.70	98.66	0.00	0.00	0.00	0.00	0.00	0.00	0.00	0.00

		C		S		Sn		Cr		Ni	
		kg	%	kg	%	kg	%	kg	%	kg	%
Input	WS	2.04	29.88	1.03	99.99	0.05	100.00	0.39	100.00	0.07	100.00
	Q	0.00	0.00	0.00	0.00	0.00	0.00	0.00	0.00	0.00	0.00
	C	4.78	70.12	0.00	0.01	0.00	0.00	0.00	0.00	0.00	0.00
Output	Fe	0.54	7.98	0.04	4.30	0.06	100.00	0.32	82.25	0.03	36.34
	Slag	0.00	0.00	0.71	69.12	0.00	0.00	0.07	17.75	0.04	63.66
	Gas	6.27	92.02	0.27	26.58	0.00	0.00	0.00	0.00	0.00	0.00

6.3 Conclusion of the optimization possibilities

In this chapter, two possibilities for product upgrade were presented, both of which are based on products obtained in the Waelz process. Furthermore, in these trials, the implementation of an alternative resource such as charcoal or pyrolysis gas was carried out with respect to the resulting CO_2 emissions, which are zero, according to the definition of CO_2 neutrality.

The first example presented dealt with the utilization of the pyrolysis gas that is usually a by-product of the carbonization of biomass. Due to the fact that several options are available how to proceed with the gaseous fraction, as it was presented in Chapter 3.3.2, the present application should serve as a demonstration that the pyrolysis gas can be used for clinkering purposes. The chemical analysis of the gas analysis pointed out a high amount of hydrogen as well as carbon monoxide, which leads to a low heating value. Nevertheless, as the gas amount at the selected temperatures is relatively high, there would be the opportunity that the huge quantity of pyrolysis gas would be able to manage the heat supply. Unfortunately, the amount of gas available was too low, which leads to an extreme decrease in the temperature shortly after switching the heat supply to pyrolysis gas. That means it was necessary to switch the methane burner on again to keep the furnace at the desired temperature. Surprisingly, the chemical analysis of the treated material was relatively good in comparison to the trial where

a methane/oxygen burner was used solely. The reason was that the moisture led to an increasing volatilization behaviour of the undesirable components. A major disadvantage was the agglomeration of the Waelz oxide, which would lead to a subsequent grinding afterwards. A subsequent utilization of treated Waelz oxide in the primary zinc (hydro) metallurgy requires fine powder, since a leaching step in sulphuric acid is performed prior to the winning electrolysis.

With regard to the Waelz slag treatment in the submerged arc furnace using alternative reducing agents, the trial showed good results. Although the fundamental principle of the experiment was based on the “in-bed” principle, good iron recovery, according to the definition, could be achieved. Further, the removal of the remaining heavy metals was very successful, since the chemical analysis of the recycled slag exposed only slight quantities in the chromium content. With a necessary process optimization, it is definitely possible to solve this issue, because of the fact that otherwise, the slag would have to be classified as hazardous waste [162], since the maximum content of 70 ppm in case of landfilling could be exceeded in future. However, zinc and lead were able to be totally recovered, similar to the iron, which has a recovery rate of nearly 99.7 % in the metal. In summary, this type of treatment is definitely a promising technology, if the legal requirements force Waelz slag operators to treat their obtained Waelz slag to recover the remaining quantities of heavy metals.

7 Conclusions

In this thesis, several possibilities of employing alternative reducing agents such as charcoal or pyrolysis gas in metallurgical recycling processes with a special focus on EAFD recycling were presented. Usually, these types of processes are fossil carbon-based, which leads to unavoidable CO_2 taxes. Therefore, the aim was to find alternatives to avoid these expenses.

The initial tasks within this scientific work were the production and characterization of charcoal and the corresponding pyrolysis gas under various parameters like the maximum treatment temperature and the retention time. This is necessary since raw biomass cannot be used inside a metallurgical furnace without any change in the process set-up and without any conversion of the biomass into a proper solid, respectively. Therefore, a special carbonization reactor was used which is able to treat waste biomass at untypically high temperatures and at various retention times inside the reaction chamber. A valuable result of these studies was that by applying these relatively high temperatures, the initial requirements for utilization in a metallurgical process are fulfilled.

Regarding the second product obtained by carburization, the pyrolysis gas, several significant observations were made; the higher the pyrolysis temperature, the higher the amount of gas. Furthermore, high temperatures lead to an increased formation hydrogen and carbon monoxide. Since a total utilization of both products – the solid and the gaseous – is mandatory, utilization possibilities should be considered in this case, as well.

Charcoal can be found in metallurgical furnaces especially in Brazil, where so-called “mini blast furnaces” are operated. Due to the relatively low compressive strength of charcoal compared to fossil coke, the height, and with this the output, are limited. Especially the concerns about the possible climate change also led researchers associated with metallurgy to focus on the renewal reducing agent. The blending of coke and utilization at sintering plants and at PCIs can be named in the case of iron and steel production and several trials for the use of charcoal in Waelz kilns can be mentioned for the recycling of EAFDs.

The present thesis focuses on an alternative process to treat EAFDs, the so-called “2sDR” process. The big advantage of this treatment method is a recovery of heavy metals without any generation of new wastes. Aside from very good zinc oxide quality (no additional cleaning necessary), a heavy metal-free slag and a heavy metal-enriched iron alloy are an encouraging result, which should definitely lead to an upscaling into a pilot plant-size. Moreover, with the very successful use of charcoal, the CO_2 generation could be decreased dramatically, since the CO_2 originated due to reduction purposes cannot be contributed to the overall greenhouse gas emissions.

Further implementation was carried out in the recycling of Waelz slag. It was stated earlier that future changes in the legislative requirements, which have already come into effect in some countries, will forbid the usage of the residue as underground material in construction. Therefore, alternative ways have to be found to minimize the amount of waste or to recover the remaining heavy metals. Since the second option is much more environmentally friendly, post treatment in a submerged arc furnace was performed. Analogous to the “2sDR” process, a heavy metal-free slag remains that can be used without any problems as raw material in the construction industry. Furthermore, an iron alloy is produced which can be applied as a master alloy in the iron and steel industry.

An option for the utilization of the pyrolysis gas is – beside some applications to generate heat and energy – to use it as an alternative burner gas in a metallurgical furnace. Especially the clinkering of Waelz oxide using the combustion heat of the alternative burner gas is a very sophisticated way to remove undesirable elements from zinc oxide. Although the achieved results show that the heat energy is not enough to keep the temperature inside the kiln at the desired temperature, the results were very satisfying, seeing that the combustion gases also force the cleaning at lower temperatures.

Finally, it can be stated that the research carried out within this thesis showed a definite possibility to use alternative reducing agents such as charcoal and pyrolysis gas in metallurgical furnaces without any deterioration of the achieved product.

8 Outlook

Since the utilization of charcoal in metallurgical furnaces could be proven, the present chapter will focus on the future development of possible biomass-operated metallurgical plants. Several factors have to be taken into account, which will definitely have an important influence on the future implementation of charcoal and pyrolysis gas-based processes in the field of metallurgy:

It is mandatory that every process should run continuously and without any interruption. Therefore, it is absolutely essential that the biomass potential is high enough to deliver an appropriate amount of raw biomass per time period to the carbonization facility. Especially waste wood or agricultural and forestry residues are available in high amounts. Moreover, it is known that a huge amount of these wastes is not being used at the moment, which could be accessed easily and low in price.

Of course, since the usage of biomass is generally a very important topic regarding the development of the climate due to the anthropogenic CO_2 evolution, several other technologies are under development which implement biomass in their processes. Among others, biomass cogeneration plants and the bio-fuels industry can be named as examples, which might lead to an increase in the biomass price.

A high influencing factor would also be the price development of the fossil carbonaceous materials, such as crude oil, natural gas and coal. Only increasing prices will lead to a rethinking to change the type of carbon carriers to renewable ones.

Similar to that is the aforementioned CO_2 tax, which depends on the supply and demand of companies. However, due to the fact that the emission trading system entered the third phase in 2013, a decrease in certificates each year will increase the price for one tonne of CO_2. This will obviously lead to a higher CO_2 price and with this, a utilization of biomass is becoming more and more interesting for the European industry. Because the implementation of biomass-derived products requires some investment costs, the higher CO_2 taxes will lead to several projects that deal with the utilization of biomass as an alternative reducing agent in metallurgical facilities.

9 Bibliography

[1] Cubasch, U., D. Wuebbles, D. Chen, et al.: Introduction. in: Stocker, T., Qin, D., G.-K. Plattner, et al.: Climate change 2013, Cambridge University Press, Cambridge, New York, 2013.

[2] European Commission: The EU emissions trading scheme system (EU ETS). Publications Office, Luxembourg, 2013.

[3] Linares, P., F. Javier Santos, M. Ventosa and L. Lapiedra: Incorporating oligopoly, CO2 emissions trading and green certificates into a power generation expansion model. Automatica 44 (2008), 6, p. 1608–1620.

[4] Sookun, A., R. Boojhawon and S.D. Rughooputh: Mapping drivers of climate change: Carbon budget index for Mauritius. Ecological Indicators 46 (2014), p. 340–350.

[5] Hammoudeh, S., D.K. Nguyen and R.M. Sousa: What explain the short-term dynamics of the prices of CO2 emissions? Energy Economics 46 (2014), p. 122–135.

[6] Fagiani, R. and R. Hakvoort: The role of regulatory uncertainty in certificate markets: A case study of the Swedish/Norwegian market. Energy Policy 65 (2014), p. 608–618.

[7] Kunsch, P.L., J. Springael and J.-P. Brans: The zero-emission certificates: A novel CO2-pollution reduction instrument applied to the electricity market. European Journal of Operational Research 153 (2004), 2, p. 386–399.

[8] European Energy Exchange AG: Emissions Auctions. https://www.eex.com/en/products/emission-allowances/emissions-auctions, 10.02.2015.

[9] UNFCCC: Kyoto protocol to the United Nations framework. http://unfccc.int/resource/docs/convkp/kpeng.pdf, 10.02.2015.

[10] IEA - International Energy Agency: CO2 Emissions from fuel combustion - Highlights. http://www.iea.org/publications/freepublications/publication/CO2EmissionsFromFuelCombustionHighlights2014.pdf, 10.02.2015.

[11] Europan Parliament: Directive 2003/87/EC of the European Parliament and of the Council of 13 October 2003 establishing a scheme for greenhouse gas emission allowance trading within the Community and amending Council Directive 96/61/EC. http://eur-lex.europa.eu/legal-content/EN/TXT/PDF/?uri=CELEX:32003L0087&from=DE, 10.02.2015.

[12] Europan Parliament: Directive 2009/29/EC of the European Parliament and of the council of 23 April 2009 amending Directive 2003/87/EC so as to improve and extend the greenhouse gas emission allowance trading scheme of the Community. http://eur-lex.europa.eu/legal-content/EN/TXT/PDF/?uri=CELEX:32009L0029&from=DE, 10.02.2015.

[13] UNFCCC: Clarifications on definition of biomass and consideration of changes in carbon pools due to a CDM project activity. https://cdm.unfccc.int/EB/020/eb20repan08.pdf, 10.02.2015.

[14] Antrekowitsch, J., T. Griessacher, D. Offenthaler and H. Schnideritsch: Charakterisierung und Verhalten von Zink-, Blei- und Halogenverbindungen beim Recycling von Elektrolichtbogenofenstäuben. BHM Berg- und Hüttenmännische Monatshefte 153 (2008), 5, p. 182–188.

[15] Ecofys, Fraunhofer Institute for Systems and Innovation Res and Öko-Institut: Methodology for the free allocation of emission allowances in the EU ETS post 2012 - Sector report for the aluminium industry. http://www.ecofys.com/files/files/091102_aluminium.pdf, 10.02.2015.

[16] Ecofys, Fraunhofer Institute for Systems and Innovation Res and Öko-Institut: Methodology for the free allocation of emission allowances in the EU ETS post 2012 - Report on the project approach and general issues. http://www.ecofys.com/files/files/091102_projectapproach_andgeneralissues_000.pdf, 10.02.2015.

[17] IEA Clean Coal Centre: CO2 abatement in the iron and steel industry. http://www.iea-coal.org.uk/documents/82861/8363/CO2-abatement-in-the-iron-and-steel-industry,-CCC/193, 10.02.2015.

[18] Republik Österreich: Deponieverordnung. https://www.ris.bka.gv.at/Dokumente/BgblAuth/BGBLA_2008_II_39/BGBLA_2008_II_39.pdf, 10.02.2015.

[19] Europan Parliament: Council Decision of 19 December 2002 establishing criteria and procedures for the acceptance of waste at landfills pursuant to Article 16 of and Annex II to Directive 1999/31/EC. http://eur-lex.europa.eu/legal-content/EN/TXT/PDF/?uri=CELEX:32003D0033&from=DE, 10.02.2015.

[20] Environmental protection agency: Identification and Listing of Hazardous Waste 40 CFR §261.4(b): Exclusions: Solid Wastes which are Not Hazardous Wastes. http://www.epa.gov/epawaste/hazard/wastetypes/wasteid/pdfs/rcra2614b-ref.pdf, 10.02.2015.

[21] Griessacher, T.M.: Einsatzmöglichkeiten von Biomasse als Reduktionsmittel in metallurgischen Recyclingprozessen. Montanuniversitaet Leoben. Doctoral Thesis, 2012.

[22] Gudenau, H.W.: Materialsammlung zur Vorlesung "Aufbereitung und Reduktion II" - Fossile Energieträger und deren Veredelung für metallurgische Prozesse. Institut für Eisenhüttenkunde der Rheinisch-Westfälischen Technischen Hochschule Aachen, Aachen, 1995.

[23] Strauß, K.: Kraftwerkstechnik. Springer-Verlag Berlin Heidelberg, Berlin, Heidelberg, 2009.

[24] Li, K., R. Khanna, J. Zhang, et al.: The evolution of structural order, microstructure and mineral matter of metallurgical coke in a blast furnace: A review. Fuel 133 (2014), p. 194–215.

[25] Basu, P.: Biomass gasification and pyrolysis. Academic Press, Burlington, MA, 2010.

[26] ASTM International: ASTM D3174 Test Method for Ash in the Analysis Sample of Coal and Coke from Coal. ASTM International, West Conshohocken, PA.

[27] ASTM International: ASTM D3175 Test Method for Volatile Matter in the Analysis Sample of Coal and Coke. ASTM International, West Conshohocken, PA.

[28] ASTM International: ASTM E1755 Test Method for Ash in Biomass. ASTM International, West Conshohocken, PA.

[29] Deutsches Institut für Normung: DIN ISO 11465. Beuth Verlag, Berlin, 1996.

[30] Deutsches Institut für Normung: DIN 51719. Beuth Verlag, Berlin, 1997.

[31] Deutsches Institut für Normung: DIN 51720. Beuth Verlag, Berlin, 2001.

[32] Deutsches Institut für Normung: DIN 51732. Beuth Verlag, Berlin, 2007.

[33] Deutsches Institut für Normung: DIN EN ISO 15350. Beuth Verlag, Berlin, 2010.

[34] Brunauer, S., P.H. Emmett and E. Teller: Adsorption of Gases in Multimolecular Layers. Journal of the American Chemical Society 60 (1938), 2, p. 309–319.

[35] Lowell, S.: Characterization of porous solids and powders. Kluwer Academic Publishers, Dordrecht, Boston, 2004.

[36] Atkins, P.W. and J. de Paula: Physikalische Chemie. Wiley-VCH, Weinheim, 2010.

[37] Lozano-Castelló, D., D. Cazorla-Amorós and A. Linares-Solano: Usefulness of CO2 adsorption at 273 K for the characterization of porous carbons. Carbon 42 (2004), 7, p. 1233–1242.

[38] ASTM International: D5341 Test Method for Measuring Coke Reactivity Index (CRI) and Coke Strength After Reaction (CSR). ASTM International, West Conshohocken, PA.

[39] Koppers, H. and A. Jenkner: Reaktionsfähigkeit, Graphitierung und elektrische Leitfähigkeit von Koks. Archiv für das Eisenhüttenwesen 5 (1932), 11, p. 543–547.

[40] Bhattacharya, S., K.B. Kabir and K. Hein: Dimethyl ether synthesis from Victorian brown coal through gasification – Current status, and research and development needs. Progress in Energy and Combustion Science 39 (2013), 6, p. 577–605.

[41] Umar, D.F., H. Usui and B. Daulay: Change of combustion characteristics of Indonesian low rank coal due to upgraded brown coal process. Fuel Processing Technology 87 (2006), 11, p. 1007–1011.

[42] Kou, J., Z. Bai, W. Li, J. Bai and Z. Guo: Effects of mineral matters and hydrogen bonding on rheological behaviors of brown coal–oil slurries. Fuel 132 (2014), p. 187–193.

[43] Commission of the European Communities: Synthesis gas production in the blast furnace: feasablilty study. http://bookshop.europa.eu/da/synthesis-gas-production-in-the-blast-furnace-pbCDNA11128/downloads/CD-NA-11-128-2A-C/CDNA111282AC_001.pdf%3Bpgid=y8dIS7GUWMdSR0EAlMEUUsWb00006GhK_oHg%3Bsid=_5IQnZFYzgcQjsJa3tWOOvN9svEO7zObg8I=?FileName=CDNA111282AC_001.pdf&SKU=CDNA111282AC_PDF&CatalogueNumber=CD-NA-11-128-2A-C, 10.02.2015.

[44] Feliciano-Bruzual, C.: Charcoal injection in blast furnaces (Bio-PCI): CO2 reduction potential and economic prospects. Journal of Materials Research and Technology 3 (2014), 3, p. 233–243.

[45] Shi, L., Q. Liu, X. Guo, W. Wu and Z. Liu: Pyrolysis behavior and bonding information of coal — A TGA study. Fuel Processing Technology 108 (2013), p. 125–132.

[46] O'Keefe, J.M., A. Bechtel, K. Christanis, et al.: On the fundamental difference between coal rank and coal type. International Journal of Coal Geology 118 (2013), p. 58–87.

[47] Farrenkopf, M. and E. Karsten: Koks. Selbstverlag des Deutschen Bergbau-Museums, Bochum, 2003.

[48] Chen, W.-H., S.-W. Du and T.-H. Yang: Volatile release and particle formation characteristics of injected pulverized coal in blast furnaces. Energy Conversion and Management 48 (2007), 7, p. 2025–2033.

[49] Nieto-Delgado, C., F.S. Cannon, P.D. Paulsen, et al.: Bindered anthracite briquettes as fuel alternative to metallurgical coke: Full scale performance in cupola furnaces. Fuel 121 (2014), p. 39–47.

[50] Bosy, B.: Brennstoffe. http://www.bosy-online.de/Brennstoffe.htm#Anthrazit, 14.01.2015.

[51] Neumann, F.: Gußeisen: Schmetztechnik, Metallurgie, Schmeizbehandlung. Expert, Reningen-Malmsheim, 1994.

[52] Ouyang, Z., J. Zhu and Q. Lu: Experimental study on preheating and combustion characteristics of pulverized anthracite coal. Fuel 113 (2013), p. 122–127.

[53] Benk, A. and A. Coban: Investigation of resole, novalac and coal tar pitch blended binder for the production of metallurgical quality formed coke briquettes from coke breeze and anthracite. Fuel Processing Technology 92 (2011), 3, p. 631–638.

[54] Benk, A. and A. Coban: Molasses and air blown coal tar pitch binders for the production of metallurgical quality formed coke from anthracite fines or coke breeze. Fuel Processing Technology 92 (2011), 5, p. 1078–1086.

[55] Buschmann, W.: Koks, Gas, Kohlechemie. Klartext, Essen, 1993.

[56] Scaroni, A.W., M.R. Khan, S. Eser and L.R. Radovic: Coal Pyrolysis. in: Elvers, B., G. Bellussi: Ullmann's encyclopedia of industrial chemistry, Wiley-VCH, Weinheim, 2011.

[57] Hoffman, E.J.: Coal conversion. Energon Co., Laramie, Wyo., 1978.

[58] Machado, André da S., A.S. Mexias, A.C. Vilela and E. Osorio: Study of coal, char and coke fines structures and their proportions in the off-gas blast furnace samples by X-ray diffraction. Fuel 114 (2013), p. 224–228.

[59] GUPTA, S., D. FRENCH, R. SAKUROVS, et al.: Minerals and iron-making reactions in blast furnaces. Progress in Energy and Combustion Science 34 (2008), 2, p. 155–197.

[60] Exxonmobile: Mineralölverarbeitung. http://www.exxonmobil.com/Germany-German/PA/Files/news_broschueren_mineraloelverarbeitung.pdf, 10.02.2015.

[61] Al-Haj-Ibrahim, H. and B.I. Morsi: Desulfurization of petroleum coke: a review. Industrial & Engineering Chemistry Research 31 (1992), 8, p. 1835–1840.

[62] Predel, H.: Petroleum Coke. in: Elvers, B., G. Bellussi: Ullmann's encyclopedia of industrial chemistry, Wiley-VCH, Weinheim, 2011.

[63] Gary, J.H. and G.E. Handwerk: Petroleum refining. M. Dekker, New York, 2001.

[64] Superior Graphite: Desulco. http://www.superiorgraphite.com/pdf/Desulco-English-05.pdf, 10.02.2015.

[65] Markel, R.F.: Apparatus for high-temperature treatment of petroleum coke, US3807961 A, 1974.

[66] Kaltschmitt, M., H. Hartmann and H. Hofbauer: Energie aus Biomasse. Springer, Berlin, New York, 2009.

[67] Lehmann, J. and S. Joseph: Biochar for environmental management. Earthscan, London, Sterling, VA, 2009.

[68] Strezov, V., T. Evans and P. Nelson: Carbonization of Biomass Fuels. in: Brenes, M.D.: Biomass and bioenergy, Nova Science Publishers, New York, 2006.

[69] Antal, M.J. and M. Gronli: The Art, Science, and Technology of Charcoal Production. Industrial & Engineering Chemistry Research 42 (2003), p. 1619–1640.

[70] Alonso, D.M., S.G. Wettstein and J.A. Dumesic: Bimetallic catalysts for upgrading of biomass to fuels and chemicals. Chemical Society reviews 41 (2012), 24, p. 8075–8098.

[71] Osteroth, D.: Biomasse. Springer-Verlag, Berlin, New York, 1992.

[72] Rösler, G.: Holzkohleherstellung sowie deren Charakterisierung hinsichtlich Ersatzreduktionsmittel in metallurgischen Prozessen. Montanuniversitaet Leoben. Masters Thesis, 2011.

[73] Campbell, N.A.: Biology. Benjamin/Cummings, Menlo Park, CA, 1996.

[74] Fengel, D. and G. Wegener: Wood. Walter de Gruyter, Berlin, New York, 1989.

[75] Krevelen, D. W. van and J. Schuyer: Coal science. Elsevier, Amsterdam u.a., 1957.

[76] Karaosmanoğlu, F., A. Işığıgür-Ergüdenler and A. Sever: Biochar from the Straw-Stalk of Rapeseed Plant. Energy & Fuels 14 (2000), 2, p. 336–339.

[77] Lua, A.C., T. Yang and J. Guo: Effects of pyrolysis conditions on the properties of activated carbons prepared from pistachio-nut shells. Journal of Analytical and Applied Pyrolysis 72 (2004), 2, p. 279–287.

[78] Lee, D.H., H. Yang, R. Yan and D.T. Liang: Prediction of gaseous products from biomass pyrolysis through combined kinetic and thermodynamic simulations. Fuel 86 (2007), 3, p. 410–417.

[79] Herrmann, A., R. Neuenfeldt and M. Klemm: Durchführung von Teermessungen an einer Versuchsanlage. Deutsches Biomasseforschungszentrum gemeinnützige GmbH, Leipzig, Germany, 2013.

[80] Midrex Technologies, Inc.: The MIXREX process. http://www.midrex.com/assets/user/media/MIDREX_Process-Brochure.pdf, 10.02.2015.

[81] Duarte, P., J. Becerra, C. Lizcano and A. Martinis: Energiron Direct Reduction Technology - Economical, Flexible, Environmentally Friendly. http://www.tenovagroup.com/pdf/technical/128-AceroLatinoAmerNov2008.pdf, 10.02.2015.

[82] Plaul, F., C. Böhm and J. Schenk: Fluidized-bed technology for the production of iron products for steelmaking. The Journal of The Southern African Institute of Mining and Metallurgy (2009), 108, p. 121–128.

[83] Nuber, D.: Circored fine ore direct reduction. Millennium Steel (2006), p. 37–40.

[84] CEN TF 143: TarWeb.Net - The international standard for tar and particle measurement in biomass producergas. http://www.eeci.net/index.html, 10.02.2015.

[85] Lerda, D.: Polycyclic Aromatic Hadrocarbons (PAHs) Factsheet. European Commission - Joint Research Centre - IRMM, Geel. Belgium, 2010.

[86] Uçar, S. and S. Karagöz: The slow pyrolysis of pomegranate seeds: The effect of temperature on the product yields and bio-oil properties. Journal of Analytical and Applied Pyrolysis 84 (2009), 2, p. 151–156.

[87] A. D. McNaught, A. Wilkinson: IUPAC Compendium of Chemical Terminology. Blackwell Scientific Publications, Oxford, 1997.

[88] Williams, A., J.M. Jones, L. Ma and M. Pourkashanian: Pollutants from the combustion of solid biomass fuels. Progress in Energy and Combustion Science 38 (2012), 2, p. 113–137.

[89] Michel, R., S. Rapagnà, P. Burg, et al.: Steam gasification of Miscanthus X Giganteus with olivine as catalyst production of syngas and analysis of tars (IR, NMR and GC/MS). Biomass and Bioenergy 35 (2011), 7, p. 2650–2658.

[90] Font Palma, C.: Modelling of tar formation and evolution for biomass gasification: A review. Applied Energy 111 (2013), p. 129–141.

[91] Baumhakl, C. and S. Karellas: Tar analysis from biomass gasification by means of online fluorescence spectroscopy. Optics and Lasers in Engineering 49 (2011), 7, p. 885–891.

[92] Kienberger Thomas, Karl Jürgen, Mair Stephan: Fixed-Bed Methanation of biogeneous SynGas, Ideas for the decentralized approach. 18th European Biomass Conference and Exhibition, Lyon (France), 2010.

[93] T.A. Milne, R.J. Evans: Biomass Gasifier “Tars”: Their Nature, Formation, and Conversion, Golden, Colorado (USA), 1998.

[94] Han, J. and H. Kim: The reduction and control technology of tar during biomass gasification/pyrolysis: An overview. Renewable and Sustainable Energy Reviews 12 (2008), 2, p. 397–416.

[95] Emmerich, F.G. and C.A. Luengo: Babassu charcoal: A sulfurless renewable thermo-reducing feedstock for steelmaking. Biomass and Bioenergy 10 (1996), 1, p. 41–44.

[96] Suopajärvi, H., E. Pongrácz and T. Fabritius: The potential of using biomass-based reducing agents in the blast furnace: A review of thermochemical conversion technologies and assessments related to sustainability. Renewable and Sustainable Energy Reviews 25 (2013), p. 511–528.

[97] Suopajärvi, H. and T. Fabritius: Towards More Sustainable Ironmaking—An Analysis of Energy Wood Availability in Finland and the Economics of Charcoal Production. Sustainability 5 (2013), 3, p. 1188–1207.

[98] Vaish, A., S. Singh, M. Humane and N. Goswami: Woodchar - A sustainable reductant and renewable source of thermal energy for tribal iron making. Journal of Metallurgy and Materials Science 48 (2006), 1, p. 51–58.

[99] Krzesińska, M., S. Pusz and Ł. Smędowski: Characterization of the porous structure of cokes produced from the blends of three Polish bituminous coking coals. International Journal of Coal Geology 78 (2009), 2, p. 169–176.

[100] Zandi, M., M. Martinez-Pacheco and T.A. Fray: Biomass for iron ore sintering. Minerals Engineering 23 (2010), 14, p. 1139–1145.

[101] Lovel, R., K. Vining and M. Dell'Amico: Iron ore sintering with charcoal. Mineral Processing and Extractive Metallurgy 116 (2007), 2, p. 85–92.

[102] Ooi, T.C., D. Thompson, D.R. Anderson, et al.: The effect of charcoal combustion on iron-ore sintering performance and emission of persistent organic pollutants. Combustion and Flame 158 (2011), 5, p. 979–987.

[103] Babich, A., D. Senk and M. Fernandez: Charcoal Behaviour by Its Injection into the Modern Blast Furnace. ISIJ International 50 (2010), 1, p. 81–88.

[104] Suopajärvi, H., E. Pongrácz and T. Fabritius: Bioreducer use in Finnish blast furnace ironmaking – Analysis of CO2 emission reduction potential and mitigation cost. Applied Energy 124 (2014), p. 82–93.

[105] Mathieson, J.G., H. Rogers, M.A. Somerville and S. Jahanshahi: Reducing Net CO2 Emissions Using Charcoal as a Blast Furnace Tuyere Injectant. ISIJ International 52 (2012), 8, p. 1489–1496.

[106] LeValley, T.L., A.R. Richard and M. Fan: The progress in water gas shift and steam reforming hydrogen production technologies – A review. International Journal of Hydrogen Energy 39 (2014), 30, p. 16983–17000.

[107] Weitkamp, J.: FUELS – HYDROGEN STORAGE | Zeolites: Encyclopedia of Electrochemical Power Sources, Elsevier, 2009.

[108] Fassinou, W.F., Van de Steene, Laurent, S. Toure, G. Volle and P. Girard: Pyrolysis of Pinus pinaster in a two-stage gasifier: Influence of processing parameters and thermal cracking of tar. Fuel Processing Technology 90 (2009), 1, p. 75–90.

[109] Fagbemi, L., L. Khezami and R. Capart: Pyrolysis products from different biomasses. Applied Energy 69 (2001), 4, p. 293–306.

[110] Encinar, J.M., F.J. Beltrán, A. Bernalte, A. Ramiro and J.F. González: Pyrolysis of two agricultural residues: Olive and grape bagasse. Influence of particle size and temperature. Biomass and Bioenergy 11 (1996), 5, p. 397–409.

[111] Encinar, J., J. González and J. González: Fixed-bed pyrolysis of Cynara cardunculus L. Product yields and compositions. Fuel Processing Technology 68 (2000), 3, p. 209–222.

[112] Predel, B.: C-Fe (Carbon-Iron). in: Madelung, O.: B-Ba – C-Zr; Landolt-Börnstein - Group IV Physical Chemistry, Springer-Verlag, Berlin/Heidelberg, 1992.

[113] Berns, H. and W. Theisen: Eisenwerkstoffe - Stahl und Gusseisen. Springer Berlin Heidelberg, Berlin, Heidelberg, 2008.

[114] Brokmeier, K.-H.: Induktives Schmelzen. W. Girardet, Essen, 1966.

[115] Neumann, F.: Gusseisen. Expert-Verl., Renningen-Malmsheim, 1994.

[116] Guézennec, A.-G., J.-C. Huber, F. Patisson, et al.: Dust formation in Electric Arc Furnace: Birth of the particles. Powder Technology 157 (2005), 1-3, p. 2–11.

[117] Ye, G., J. White and L.Y. Wei: Association of halogens in electric arc furnace dust and zinc oxide fume before and after leaching. in: Gaballah, I., Hager, J., R. Solozabel: Global Symposium on Recycling Waste Treatment and Clean Technology, REWAS'99, Minerals, Metals & Materials Society, Warrendale, PA, 1999.

[118] Zunkel, A.: EAF dust as an electrolytic zinc resource. in: Queneau, P.B., R.D. Peterson: Third International Symposium, Recycling of Metals and Engineered Materials, Minerals, Metals & Materials Society, Warrendale, Pa, 1995.

[119] Rüttern, J.: Various concepts for the recycling of EAFD. in: Harre, J.: 3. Seminar Networking between Zinc and Steel, GDMB, Clausthal-Zellerfeld, 2011.

[120] Badger, S. and W. Kneller: The characterization and formation of electric arc furnace (EAF) dusts. in: Iron and Steel Society of AIME: 55th Electric furnace conference, Iron and Steel Society, Warrendale, PA, 1998.

[121] Remus, R., S. Roudier, M.A. Aguado-Monsonet and L. Delgado Sancho: Best available techniques (BAT) reference document for iron and steel production. Publications Office, Luxembourg, 2013.

[122] Worldsteel Association: Steel Statistical Yearbook 2013, Brussels, 2013.

[123] Kozlov, P.A.: The Waelz Process 2003. Ore and metals publishing house, Moscow, 2003.

[124] Berlow, J. and J. Keenan: U.S. EPA: Best Demonstrated Available Technology (BDAT), Washington, D.C., 1988.

[125] Ruh, A. and T. Krause: The Waelz Process in Europe. in: Harre, J.: 3. Seminar Networking between Zinc and Steel, GDMB, Clausthal-Zellerfeld, 2011.

[126] Antrekowitsch, J., S. Steinlechner, A. Unger, et al.: Zinc and Residue Recycling. in: Worrell, E., M.A. Reuter: Handbook of recycling, Elsevier, Amsterdam, 2014.

[127] Xue, T., W.C. Cooper, R. Pascual and S. Saimoto: Effect of fluoride ions on the corrosion of aluminium in sulphuric acid and zinc electrolyte. Journal of Applied Electrochemistry 21 (1991), 3, p. 238–246.

[128] Bartusch, H., Fernández Alcalde, Ana María and M. Fröhling: Erhöhung der Energie- und Ressourceneffizienz und Reduzierung der Treibhausgasemissionen in der Eisen-, Stahl- und Zinkindustrie (ERESTRE). Erhöhung der Energie- und Ressourceneffizienz und Reduzierung der Treibhausgasemissionen in der Eisen-, Stahl- und Zinkindustrie (ERESTRE) 2 (2013).

[129] Olper, M. and M. Maccagni: From C.Z.O. to zinc cathode without any pre-treatment. The EZINEX process: Lead & zinc 2008, The Southern African Institute of Mining and Metallurgy, Durban, 2008.

[130] Martin, D., G. Diaz, M.A. Garcia and F. Sanchez: Extending zunc production possibilities through solvent extraction. The Journal of The Southern African Institute of Mining and Metallurgy (2002), p. 463–468.

[131] Díaz, G. and D. Martín: Modified Zincex process: the clean, safe and profitable solution to the zinc secondaries treatment. Resources, Conservation and Recycling 10 (1994), 1-2, p. 43–57.

[132] Havlík, T., Vidor e Souza, Bruna, A.M. Bernardes, Schneider, Ivo André Homrich and A. Miskufová: Hydrometallurgical processing of carbon steel EAF dust. Journal of hazardous materials 135 (2006), 1-3, p. 311–318.

[133] Jha, M., V. Kumar and R. Singh: Review of hydrometallurgical recovery of zinc from industrial wastes. Resources, Conservation and Recycling 33 (2001), 1, p. 1–22.

[134] Steinlechner, S. and J. Antrekowitsch: Options for Halogen Removal from Secondary Zinc Oxides. in: Harre, J.: 3. Seminar Networking between Zinc and Steel, GDMB, Clausthal-Zellerfeld, 2011.

[135] Shawabkeh, R.A.: Hydrometallurgical extraction of zinc from Jordanian electric arc furnace dust. Hydrometallurgy 104 (2010), 1, p. 61–65.

[136] Antrekowitsch, J. and H. Antrekowitsch: Hydrometallurgically recovering zinc from electric arc furnace dusts. JOM 53 (2001), 12, p. 26–28.

[137] Dutra, A., P. Paiva and L.M. Tavares: Alkaline leaching of zinc from electric arc furnace steel dust. Minerals Engineering 19 (2006), 5, p. 478–485.

[138] Antrekowitsch, J. and D. Offenthaler: Die Halogenproblematik in der Aufarbeitung zinkhältiger Reststoffe. BHM Berg- und Hüttenmännische Monatshefte 155 (2010), 1, p. 31–39.

[139] Youcai, Z. and R. Stanforth: Integrated hydrometallurgical process for production of zinc from electric arc furnace dust in alkaline medium. Journal of hazardous materials 80 (2000), 1-3, p. 223–240.

[140] Orhan, G.: Leaching and cementation of heavy metals from electric arc furnace dust in alkaline medium. Hydrometallurgy 78 (2005), 3-4, p. 236–245.

[141] Bayat, O., E. Sever, B. Bayat, V. Arslan and C. Poole: Bioleaching of zinc and iron from steel plant waste using Acidithiobacillus ferrooxidans. Applied biochemistry and biotechnology 152 (2009), 1, p. 117–126.

[142] Montenegro, V., P. Oustadakis, P.E. Tsakiridis and S. Agatzini-Leonardou: Hydrometallurgical Treatment of Steelmaking Electric Arc Furnace Dusts (EAFD). Metallurgical and Materials Transactions B 44 (2013), 5, p. 1058–1069.

[143] Chen, W.-S., Y.-H. Shen, M.-S. Tsai and F.-C. Chang: Removal of chloride from electric arc furnace dust. Journal of hazardous materials 190 (2011), 1-3, p. 639–644.

[144] Bruckard, W.J., K.J. Davey, T. Rodopoulos, J.T. Woodcock and J. Italiano: Water leaching and magnetic separation for decreasing the chloride level and upgrading the zinc content of EAF steelmaking baghouse dusts. International Journal of Mineral Processing 75 (2005), 1-2, p. 1–20.

[145] Menad, N., J. Ayala, F. Garcia-Carcedo, E. Ruiz-Ayúcar and A. Hernández: Study of the presence of fluorine in the recycled fractions during carbothermal treatment of EAF dust. Waste Management 23 (2003), 6, p. 483–491.

[146] Haiki, K., H. Hata and M. Sakata: The new removal technology of halogen from leaching solution of secondary zinc oxide. in: METSOC: 51st Annual Conference of Metallurgists (COM 2012), 2012.

[147] Southwick, L.M.: From Dust to Iron: New directions in EAF dust processing. in: AIST: 2008 Scrap Substitutes & Alternative Ironmaking V, 2008.

[148] Southwick, L.M.: Red herrings on the path of technology development: Capital destruction in the pursuit of a bad idea. in: METSOC: 51st Annual Conference of Metallurgists (COM 2012), 2012.

[149] Schneeberger, G.: Verfahrensentwicklung und Anlagenoptimierung beim Recycling von Filterstäuben aus der Eisen- und Stahlindustrie. Montanuniversitaet Leoben. Doctoral Thesis, 2013.

[150] Southwick, L.M.: Processing EAF Dust with Confidence: a Comparision of Utilising a Waelz Kiln versus Using a Rotary Hearth Furnace. Steel Tech 6 (2012), 2, p. 61–68.

[151] Steinlechner, S.: Amelioration and market strategies for zinc oxide with focus on secondary sources. Montanuniversitaet Leoben. Doctoral Thesis, 2013.

[152] Fleischanderl, A. and U. Gennari: Verfahren zum Verwerten von Schlacke, EP1627084 A1, 2004.

[153] Edlinger, A.: Verfahren zum Behandeln von Schlacken oder Schlackengemischen auf einem Eisenbad, EP1252343 A1, 2002.

[154] Mocker, M., F. Stenzel and M. Franke: Potenzial der Metalle in Stäuben. in: Thomé-Kozmiensky, K.J.: Aschen, Schlacken, Stäube aus Abfallverbrennung und Metallurgie, TK, Neuruppin, 2013.

[155] Edlinger, A. and A. Gössnitzer: Verfahren zur Herstellung von hydraulischen Bindemitteln und/oder Legierungen wie z.B. Eisenchrom oder Eisenvanadium, EP0770149 A1, 1996.

[156] Thaler, C. and W. Kepplinger: Wertmetallgewinnung aus Abfällen mit einem neuentwickelten Kupferbadreaktor. in: Lorber, K.E.: Abfallwirtschaft, Abfalltechnik, Deponietechnik und Altlasten, VGE-Verl, Essen, 2008.

[157] Pawlek, F.: Metallhüttenkunde. De Gruyter, Berlin, New York, 1983.

[158] Richards, G.G. and J.K. Brimacombe: Kinetics of the zinc slag-fuming process: Part II. Mathematical model. Metallurgical and Materials Transactions B 16 (1985), 3, p. 529–540.

[159] Richards, G.G. and J.K. Brimacombe: Kinetics of the zinc slag-fuming process: Part III. Model predictions and analysis of process kinetics. Metallurgical and Materials Transactions B 16 (1985), 3, p. 541–549.

[160] Koch, K. and D. Janke: Schlacken in der Metallurgie. Stahleisen, Düsseldorf, 1984.

[161] Pichler, C.A.M. and J. Antrekowitsch: Innovative recyclingslag-treatment. in: Castro, F., Vilarinho, C., J. Carvalho, et al.: 2nd International Conference: WASTES:Solutions, Treatments and Opportunities - Book of proceedings, Guimares, Portugal, 2013.

[162] Pichler, C.A.: Verwertungsstrategien von Wälzschlacke. Montanuniversitaet Leoben. Doctoral Thesis, 2014.

[163] Unger, A.: Entwicklung eines Recyclingprozesses zur simultanen Rückgewinnung von Wertmetallen aus Reststoffen der Blei- und Zinkindustrie. Montanuniversitaet Leoben. Doctoral Thesis, 2015.

[164] Allibert, M.: Slag atlas. Verlag Stahleisen, Düsseldorf, 1995.

10 List of Figures

Figure 1-1: Schematic drawing of the basic principle of the greenhouse effect and the influencing parameters [1] 2
Figure 1-2: Price development of the CO_2 taxes over the last years according to the EEX [8]....4
Figure 2-1: Schematic drawing of the evolution of coal, a process that needs several million years [23] 9
Figure 2-2: Illustration of graphitizing (a) and non-graphitizing carbons (b) [24] 10
Figure 2-3: Basis for the characterization of solid carbon carriers [25] 10
Figure 2-4: Differences in the fixed carbon content (water free base) of seven charcoal samples according to the analysis standard (DIN/ISO. or ASTM)....12
Figure 2-5: Extract from an adsorption isotherm with the calculated B.E.T. line [34; 35]....15
Figure 2-6: “Quantachrome Instruments NOVA 2000e” for the measurement of the specific surface area and pore size distribution....17
Figure 2-7: Test equipment for the measurement of the reactivity from charcoals 18
Figure 2-8: Standardized furnace with attached N_2/CO_2 purging and thermocouples according to ASTM D 5341 [38]....19
Figure 2-9: Comparison of the standardized CRI value with those from the set-up available at the Chair of Nonferrous Metallurgy....20
Figure 2-10: Comparison of the obtained CRI values from the ASTM with the R-value from the NEM testing unit 20
Figure 2-11: Experimental set-up for the determination of the coke reactivity according to Koppers; 1: CO_2 bottle; 2: gas bubble counter; 3: pressure valve; 4: pressure balance bottle; 5: drying tower; 6: pressure gauge; 7: quartz tube; 8: Ubbelode-furnace; 9: gas receiver bottle; 10: gas extraction; 11: thermometer; a: coke sample; b: quartz sieve; c: asbestos; d: fireclay [39] ..21
Figure 2-12: Principal set-up of a coke oven chamber [47]....23
Figure 2-13: Sectional drawing of the bottom part of a blast furnace equipped with a powder coal injection [48] 23
Figure 2-14: Koppers Becker underjet coke oven furnace [57]....25
Figure 2-15: Process overview of the origination of crude oil-derived products [63]....27
Figure 2-16: Drawing of a production unit for desulphurized coke [65] 29
Figure 3-1: Visualization of the organic components in biomass [70] 30
Figure 3-2: Products obtained from the thermochemical treatment of biomass [68]....31
Figure 3-3: Semi-continuous “twin screw reactor” for the production of high quality charcoal....32

Figure 3-4: Ternary diagram “C-H-O” (in at-%) of several biomasses as well as a second layer representing several biomass conversion processes according to [25]; F = fast pyrolysis; H = hydrogen; S= steam; O = oxygen; P = slow pyrolysis.....34
Figure 3-5: Thermal decomposition of a biomass particle under pyrolysis conditions [25] 34
Figure 3-6: Development of the charcoal yield subject to the maximum carbonization temperature; own data and from [21; 72].....35
Figure 3-7: Banana-shaped evolution of the fixed carbon content dependent on the obtained charcoal yield; own data and from [21; 72] 36
Figure 3-8: Evolution of the charcoal yield at varying retention times in the “twin screw reactor” 37
Figure 3-9: Decrease of the analysed volatile matter at increasing retention times.....38
Figure 3-10: Overview of the results obtained in the carburization experiments in the “twin screw reactor” as well as comparable fossil carbons from Chapter 2, according to [25], data from [21; 72] and own experiments.....38
Figure 3-11: van Krevelen diagram with own used biomass/charcoals as well as carbonaceous material from literature provided in Chapter 2, from [21; 72] and own literature, diagram according to [25; 75].....39
Figure 3-12: Evolution of the specific surface area subject to the pyrolysis temperature as well as the retention time of the biomass/charcoal [72] 40
Figure 3-13: Influence of the raw material (biomass) on the average gas composition at a pyrolysis at 850 °C maximum temperature and retention time 2 h 42
Figure 3-14: Evolution of the gas composition at varying retention times at the pyrolysis of olive tree cuttings, 850° C.....43
Figure 3-15: Overview of the obtained syn-gas content (H_2 and CO) at varying pyrolysis temperatures.....44
Figure 3-16: Experimental set-up of the tar protocol according to the research group of the European Union [84].....45
Figure 3-17: Possibilities for gas and tar formation depending on the pyrolysis parameters [93].....49
Figure 3-18: Change in the gas evolution during the heating up of biomass with absence of air [93].....50
Figure 3-19: Tar, gas and fly ash evolution in incomplete combustion, which can be compared with a pyrolysis process [88].....51
Figure 3-20: Schematic drawing of a steam reforming process of CH_4 with a subsequent water gas shift reaction for increasing the H_2 amount, using a metal catalyst (M) [106] 58
Figure 3-21: Overview on the utilization possibilities of charcoal at the recycling of EAFDs .60

Figure 4-1: “Iron –Carbon” binary diagram [112] 62
Figure 4-2: More detailed and technical binary diagram “Iron-Carbon” under standard conditions 63
Figure 4-3: Schematic overview of the experimental procedure of the carburization experiments; in this case, the carbon content was increased to 4.0 % using an induction furnace; diagram from [113] 65
Figure 4-4: Carbonization of steel melts at 1,550 °C with different carbon carriers, a…carbon content of the melt; PK...petroleum coke; GK...gas-coal; hcc...high carbon coke; EK....electrode coal; HK… char carbonized at low temperatures; A...anthracite; GE...graphite electrodes; KG...coal granules [114] 66
Figure 4-5: Drawing of the hot stage microscope available at the Chair of Nonferrous Metallurgy; the main parts are the light source (left), the furnace (middle) and the camera (right) 67
Figure 4-6: Cross-sectional view of the experimental set-up of the sample and the sample holder inside the hot stage microscope 68
Figure 4-7: Calculated ternary systems using FactSage™. The green dot represents the ash analysis of the carbonaceous material: top left: charcoal “Eucalyptus/Pine No.2”; top right: charcoal “Eucalyptus/Pine No.6”; middle left: charcoal “Olive tree cuttings”; middle right: charcoal “Vines”; bottom: “Petroleum coke” ... 69
Figure 4-8: High-temperature heat resistance furnace “Heraeus K 1750” 70
Figure 4-9: Photo of the inside of the applied furnace 71
Figure 4-10: Net diagram showing the results of the increase in the carbon content to max. 4.3 % C 72
Figure 4-11: Obtained results of the carburization diagrams up to 4.5 % C represented in a net diagram 73
Figure 4-12: Picture of the tilted induction furnace produced by “ITG-Induktionsanlagen” 74
Figure 4-13: Simplified draft of the experimental set-up 74
Figure 4-14: Vacuum sample taker (top) and temperature measurement lance (bottom), both with single use attachment for sampling and temperature measurement, respectively 75
Figure 4-15: Water basin optimized for the granulation of liquid iron 77
Figure 4-16: Carburization and burn-off behaviour of charcoal “Eucalyptus No.4” 78
Figure 4-17: Dissolution as well as burn-off behaviour of charcoal made from eucalyptus trees (species No.6) 79
Figure 4-18: Carburization diagram of charcoal made from olive tree cuttings 80

Figure 4-19: Results of the carburization behaviour of the fossil reference "petroleum coke" 81
Figure 5-1: Scheme of the clinkering step using a TBRC 89
Figure 5-2: Vaporization pressure of selected chlorides at changing temperatures. The interception of the turquoise lines represents the working conditions for the clinkering step 90
Figure 5-3: Thermodynamic calculation of several fluorides to determine their vaporization temperature depending on the pressure 91
Figure 5-4: Experimental set-up of the second step of the 2sDR process in the TBRC 92
Figure 5-5: Slag fuming furnace for the producing of zinc out of the slag obtained in the lead shaft furnace 1: slag feed; 2: fuming furnace; 3: post combustion chamber; 6: cooling water discharge; 7: cooling water collector; 8: pyrite injection unit; 9: oil injection unit; 10: hot blast bustle pipe; 11: cold blast bustle pipe [157] 93
Figure 5-6: Gibbs energy of selcted components depending on temperature 95
Figure 5-7: Illustration of the reactions occurring in the molten slag, according to [159] 96
Figure 5-8: Evolution of the slag during the treatment in the 2nd step of the process, starting from the left side. The pink dot represents the slag composition and the melting temperature in each ternary diagram, respectively [161] 97
Figure 5-9: Observed mass flow in the clinkering trials using a TBRC 99
Figure 5-10: Sankey diagram of the second step of the "2sDR" process 100
Figure 5-11: Mass flow of the second step during continuous operation of the process 103
Figure 6-1: Waelz kiln for the processing of EAF dust a: Material feeding b: Reel carriers c: Waelz rotary kiln d: Burner e: Discharge Head f: Slag reel carriers g: Slag pit h: Scrapper i: Slag removal k: Sealed air fans l: Dust settling chamber m: Evaporation cooler n: Low grade Waelz oxide transport, o: Electrostatic precipitator, p: Waelz-oxide transport, r: flue gas blower s: stack [157] 106
Figure 6-2: The main reactions in a Waelz kiln [126] 106
Figure 6-3: Drawing of the TBRC at the Chair of Nonferrous Metallurgy (left) as well as a draft of the optimization of the fume hood (right) 109
Figure 6-4: Draft of the experimental set-up with the twin screw reactor, the heated flexible tube and the TBRC 110
Figure 6-5: Recording of the temperature profile as well as the evolution of the gas composition during the first experiment 111
Figure 6-6: Illustration of the removal of the disturbing elements in the first trial 111
Figure 6-7: Temperature distribution and exhaust gas composition in the second experiment 113

Figure 6-8: Representative picture of the increasing dust load of the off-gas when using pyrolysis gas 114
Figure 6-9: Plot of the temperature distribution as well as the exhaust gas composition in the 3rd experiment 115
Figure 6-10: Development of the elements during the removal of the halides in the last trial 115
Figure 6-11: Tapping of clinkered material from the TBRC 116
Figure 6-12: Hot clinkered material soon after tapping 117
Figure 6-13: Schematic drawing of the applied submerged arc furnace [163] 119
Figure 6-14: Evolution of the slag composition by adding quartzite [164] 121
Figure 6-15: Sankey diagram of the applied Waelz slag recycling process 123

11 List of Tables

Table 1-1: Tabulation of selected metals in connection with their production ways and produced emissions [15–17] 6
Table 1-2: Limiting values of heavy metals in landfills in selected countries and communities [18–20] 6
Table 2-1: Max. / Min. values of mineral matter (wt-%) in different coke samples according to [24] 11
Table 2-2: Test parameters for the determination of moisture, volatiles as well as the ash content of solid fuels [26–28] for ASTM; [29–31] for DIN 12
Table 2-3: Comparison of the different characterization methods and the applied reactivity measurement [38, 39] 19
Table 2-4: Proximate analysis [wt-%] of selected brown coals from Indonesia (col. 1-3) [41] and China (col. 4 and 5) [42] 22
Table 2-5: Range of the proximate analysis [wt-%] of 34 selected stone coals [45] 22
Table 2-6: Proximate analysis [wt-%] of three different anthracite coals 24
Table 2-7: Overview of the proximate analysis [wt-%] of eighteen different coke samples [59] 26
Table 2-8: Typical ranges of the proximate analysis of green petroleum coke (values are on dry base) [61] 27
Table 2-9: Typical chemical analysis of Desulco® coke [64] 28
Table 3-1: Overview of the benzene derivates obtained in the pyrolysis of pomegranate seeds [86] 46
Table 3-2: Phenolic compounds found in the condensable gases during pyrolysis of pomegranate seed [86] 47
Table 3-3: Results of the GCMS analysis of acids and esters in the tar fraction [86] 47
Table 3-4: Summary of alkanes of pomegranate seeds obtained at the GCMS [86] 47
Table 3-5: List of N-containing compounds detected in the tar in a GCMS [86] 48
Table 3-6: Overview of Polycyclic aromatic hydrocarbons in the condensable pyrolysis gas [86] 48
Table 3-7: Average values from the permanent gas measurement [79] 52
Table 3-8: Results of the tar measurement with the maximum and minimum values obtained during the experiments [79] 53
Table 3-9: Part of the combustion calculation of the permanent gas fraction 54
Table 3-10: Calculation of the heat energy of the tar fraction obtained during the pyrolysis of biomass in the “twin screw reactor” 54
Table 4-1: Additional description of the binary diagram “Fe-C” in Figure 4-2 [113] 64

Table 4-2: Chemical composition of the applied iron 67
Table 4-3: Results of the hot stage microscope measurement as well as the major ash components as well as the theoretical melting point according to FactSage™ ... 68
Table 4-4: Proximate analysis [wt-%] of the used carbons 71
Table 4-5: Chemical analysis of the pure iron used in the trials 75
Table 4-6: Proximate analysis [wt-%] and the sulphur content in different carbonaceous material used in the trials 76
Table 5-1: Typical values [wt-%] of the feed material of the Waelz kiln as well as its products [125; 126] 85
Table 5-2: Overview of the chemical analysis [wt-%] of the dust before and after the clinkering step 98
Table 5-3: Analysis [wt-%] of the material utilized as a basis for the metal bath process 99
Table 5-4: Overview of selected elements obtained in the second step of the process, in [wt-%] 101
Table 6-1: Overview of several possible materials fed into the Waelz kiln, in [wt-%] [126] .. 105
Table 6-2: Overview of typical values [wt-%] obtained in the Waelz process [126] 106
Table 6-3: Results of the chemical analysis from the samples taken during the first experiment 112
Table 6-4: Specific combustion enthalpy of selected gas species at 900 °C 112
Table 6-5: Result of the chemical analysis obtained in the second trial 113
Table 6-6: Tabulation of the removal of the elements during the 3rd experiment 116
Table 6-7: Chemical composition of the applied Waelz slag 120
Table 6-8: Composition of the additive, which was charged for slag forming purposes 120
Table 6-9: Proximate analysis as well as ash analysis of the charcoal originated from eucalyptus cuttings 121
Table 6-10: Overview of the materials charged into the SAF 122
Table 6-11: Mass balance of selected elements obtained during the Waelz slag treatment in the SAF 124